Summer 7-12-2015

AIRBORNE INFECTION IN HEALTHCARE ENVIRONMENTS: IMPLICATIONS TO HOSPITAL CORRIDOR DESIGN

Ehsan Mousavi
University of Nebraska - Lincoln, ehsan.mousavirizi@gmail.com

AIRBORNE INFECTION IN HEALTHCARE ENVIRONMENTS: IMPLICATIONS TO HOSPITAL CORRIDOR DESIGN

by

Seyed Ehsan Mousavi Rizi

A DISSERTATION

Presented to the Faculty of

The Graduate College at the University of Nebraska

In Partial Fulfillment of Requirements

For the Degree of Doctor of Philosophy

Major: Engineering

(Construction Engineering and Management)

Under the Supervision of Professor Kevin R. Grosskopf

Lincoln, Nebraska

July, 2015

AIRBORNE INFECTION IN HEALTHCARE ENVIRONMENTS: IMPLICATIONS TO HOSPITAL CORRIDOR DESIGN

Seyed Ehsan Mousavi Rizi, Ph.D.

University of Nebraska, 2015

Advisor: Kevin R. Grosskopf

Several studies have linked nosocomial transmission airborne diseases to airflow in healthcare settings. Quasi-experimental methods are developed to observe the aerodynamic transport behavior of synthetic respiratory particles in corridors of a hospital. Computational models, validated by experimental results, are then developed to explore the spatial relationships of supply-exhaust air ventilation in patient corridors. The aim of this study is to determine optimal HVAC design strategies to contain and remove airborne contaminants in healthcare environments.

In addition to occupant comfort, hospital HVAC systems are designed to provide ventilation and directional airflow to contain, dilute and remove contaminants including airborne disease. Of 183 epidemiological studies published worldwide from 1960-2005, however, only 10 studies were deemed by a panel of international experts as having conclusively demonstrated the effectiveness of ventilation to control the spread of airborne disease in healthcare settings.

Two experimental tests were conducted; one placing patient corridors under directional airflow and the second placing the corridors under non-directional airflow. The purpose

of these tests was to observe the spatial-temporal movement of artificially-generated aerosols with respect to particle size and ventilation mode and to assess the probability of contamination from infectious sources inside and outside of the patient area. Next, computational fluid dynamic (CFD) models were developed and validated by experimental results to test several ventilation rates with modified supply-exhaust air system configurations in patient corridors.

Results suggest that dissemination of bio-aerosols in hospital corridors could be exacerbated by directional airflow caused by either the spatial arrangement of supply-exhaust air ventilation, or, the pressure relationship between the corridor and surroundings spaces. Within the non-directional or 'neutral' airflow regime, modified supply-exhaust air system configurations reduced average particle concentration 30% and transport distance more than 60% without increasing air change rate. Aerosols $\leq 0.5 \mu m$, however, were observed more than 30m from the source with comparatively less regard to airflow mode or supply-exhaust air system configuration. Ventilation arrangements can potentially reduce concentrations and improve distributions of particles. And, higher ventilation rates do not necessarily culminate in better results.

To

Whom I wish to come soon

ACKNOWLEDGEMENT

I would like to express my sincere thanks and gratitude to my committee chair Professor Kevin Grosskopf for his advice, precious time and constant support throughout my career at the University of Nebraska-Lincoln. Not only has he been an outstanding advisor, he has also been my best friend throughout my PhD studies at UNL. He continually conveyed the spirit of adventure in regard to research and scholarship, and excitement in the process to becoming a better human being.

I truly appreciate the valuable input and comments made by my committee members Professor Terry Stentz, Professor Josephine Lau, and Professor David Yuill without which my efforts would not have been complete and fruitful. My deep appreciation to Professor Timothy Wentz for his kind and supporting behavior towards me during my stay at Nebraska, and for being a spectacular teacher from which all students have benefitted over a course of many years. I would like to acknowledge the many other professors and instructors at the University of Nebraska who dedicate their lives to the teaching and service of others.

To my wife, Negin, who has patiently endured many days of my impatience, petulance, and short-temperedness. She convinced me to pursue this education, supported me to complete it, and certainly will be on my side as I develop the next level of my career.

Finally, I would like to express the deepest appreciation to my parents for their unconditional love, financial and moral support.

TABLE OF CONTENTS

LIST OF FIGURES

LIST OF TABLES

LIST OF SYMBOLS

Latin Symbols

c = contaminant concentration (kg/s)

c_0 = Supply air contaminant concentration (kg/s)

c_i = initial contaminant concentration (kg/s)

c_e = ending contaminant concentration (kg/s)

C_c = Cunningham slip correction factor (-)

C_D = Drag coefficient (-)

C_p = Heat capacity at constant pressure (J/kg.^{o}K)

D = Number of disease cases

dp = Particle diameter (m)

$d_{i,j}$ = Rate of deformation tensor (-)

$\vec{\boldsymbol{g}}$ = Gravitational acceleration vector (m/s^2)

g = Skewness (-)

I = Number of infectors (-)

K = Turbulence Kinetic Energy (m^2/s^2)

n = air change rate (hour^{-1})

$n(t)$ = Brownian force (N)

p = Breathing rate per person (-); Pressure (Pa)

$\bar{p}$ = Time averaged pressure (Pa)

p' = Pressure fluctuation (Pa)

q = quantum generation rate (-)

Q = Ventilation Rate (m^3/s)

P_T = Probability of transport (-)

R^2 = Determination correlation (-)

Re = Reynolds number (-)

S = Number of susceptible (-)

$\vec{\boldsymbol{u}}$ = Velocity field vector (m/s)

$\vec{\boldsymbol{u}}_p$ = Particle velocity field vector (m/s)

t = Time (s)

$u_x;\ u_y;\ u_z$ = Velocity components in x, y, z directions (m/s)

$u'_x;\ u'_y;\ u'_z$ = Fluctuating velocity components in x, y, z directions (m/s)

$\bar{u}_x;\ \bar{u}_y;\ \bar{u}_z$ = Time averaged velocity components in x, y, z directions (m/s)

V = Volume (m^3)

$\dot{V}_{pol}$ = Contaminant generation rate (kg/s)

$x;\ y;\ z$ = Cartesian coordinates (m)

Greek Symbols

β = Kurtosis of sample

σ = Stefan-Boltzmann constant (W/m^2K^4); Standard Deviation of sample

μ = Dynamic viscosity (Pa.s)

ξ = Gaussian random number (-)

π = Constant equal to 3.1415 (-)

ρ = Density of air (kg/m^3)

ρ_p = Density of particle (kg/m^3)

LIST OF ACRONYMS

ACH	= Air Change per Hour
AHU	= Air Handling Unit
AIIR	= Airborne Infectious Isolation Room
ARD	= Acute Respiratory Disease
BC	= Boundary Condition
CFD	= Computational Fluid Dynamics
DNS	= Direct Numerical Simulation
DRW	= Discrete Random Walk
HAI	= Healthcare Associated Infection
HCW	= Health Care Worker
HVAC	= Heating, Ventilation, and Air Conditioning
LES	= Large Eddy Simulation
MeSH	= Medical Subject Heading
NS	= Navier- Stokes
RANS	= Reynolds-Averaged Navier-Stokes
SARS	= Severe Acute Respiratory Syndrome
VFD	= Variable Frequency Drive
VZV	= Varicella Zoster Virus

CHAPTER 1: INTRODUCTION

1.1 Introduction

Certain pathogens are transmitted through air by respiratory droplets that desiccate shortly after emission and form *droplet nuclei* [1]. Droplet nuclei are sufficiently small (<5.0µm) to remain suspended in air indefinitely, and thus, create a pathway between an infected and susceptible person [2]. This process is called 'airborne transmission'. Airborne transmission from a source to a susceptible deals with numerous factors. Some engage biological and epidemiological parameters in the transmission mechanism. While others focus on physical phenomena causing pathogens to spread within a particular function space (e.g. corridors of a hospital). In a sense, the latter are the engineering parameters and include geometry of the space, ventilation strategies, and pressure relationship with adjacent spaces. Regardless of the route, transmission is proportional to the number of infectious agents, or quantum rate [3,4]. Thus, engineering endeavors are invariably focused on finding strategies to remove, disinfect, and contain infectious quanta. This of course, is of utmost importance in healthcare environments where infectious agents are rife and diverse. Particularly, patient corridors host human traffic of a vast variety of individuals including patients, visitors, and healthcare workers (HCW's). The source in corridors is neither sedentary nor microbiologically identical which demands an astute use of engineering tools to design a healthier environment.

1.2 Context of the Problem

1.2.1 Healthcare Associated Infection (HAI)

Approximately one in every ten hospitalized patients deals with healthcare associated infection (HAI) after admission. The evident result of this is prolonged stay in hospitals and more therapeutic intervention [5]. Such interventions entail a direct cost of providing care in addition to indirect costs that are also incurred to patients due to workplace absenteeism and intangible costs attributed to pain caused by the infection. In 2002, the annual number of HAI in U.S. hospitals was approximately 1.7 million of which 98,987 deaths were associated with the infection. This indeed, has ranked HAI's as the fifth leading cause of death in the United States. A deeper look reveals that airborne infection is a prominent route of disease transmission in healthcare environments. Maggil et al. [6] reported pneumonia and surgical-site infection as the most common types of HAI (21.8%). Accordingly, *S. aureus* and *Klebsiella Pneumoniae,* both known to disseminate via airborne route [7,8], are amongst the top three agents causing infection in healthcare environments. Moreover, Weber et al. [9] showed that only 21% of pneumonia is due to unsterile ventilator (device-related) which leaves about four-fifth of it attributable to the airborne route.

Such tragic data has compelled the Department of Health and Human Services to target the elimination of HAI's as a priority. In fact, not only the governmental authorities are anxious to mitigate this problem, healthcare manager are also keen to address it in a systematic, and perhaps, less costly manner.

1.2.2 Energy Consumption

High energy consumption is a serious issue in healthcare facilities that, indeed, ensues from the prevention of healthcare associated infection. Unlike residential and office buildings, hospital heating, ventilation and air conditioning (HVAC) system is generally not 'load' driven, but is predicated on providing adequate ventilation air to maintain a wide range of directional airflow relationships and air change rates to contain, dilute and remove hazards such as volatile medical gases, particulates and *airborne disease*. For example, patient corridors are typically an interior space with low density occupancy for which a comfort-based design produces less than one air change per hour (ACH). Despite this, ASHRAE Standard 170-2008 recommends 4ACH for patient corridors. The average healthcare facility has 3-5 times the energy use intensity of a typical office building [10]. Although hours of operation and equipment 'plug' loads contribute to disproportionately high energy consumption in hospitals, HVAC systems account for more than two-thirds of all energy use (Figure 1-1).

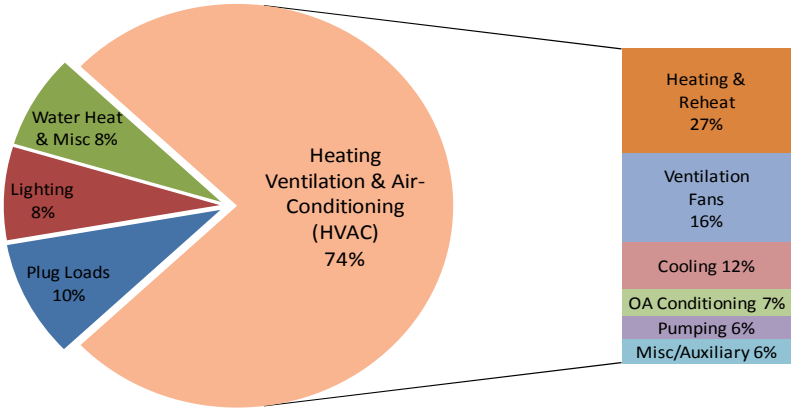

Figure 1-1 Hospital Energy Use by Source[11]

1.3 Research Question Development

Several codes and standards have been developed to legislate a set of minimum requirements for ventilation systems in healthcare environments. For example, the American Society of Heating, Ventilation, Refrigeration, and Air-Conditioning Engineers (ASHRAE) issues a specific standard pertaining to ventilation of healthcare facilities [12]. Other organizations such as World Health Organization (WHO), and the American Institute of Architects (AIA) have also set forward recommendations in this regard [13,14]. In specific, ASHRAE Standard 170-2013 provides a Table containing requirements on pressure relationship with adjacent spaces, minimum ventilation rates, air recirculation, and thermal comfort parameters (Figure 1-2). The Purpose of this standard is to define ventilation system design requirements that provide *environmental control* for comfort, *asepsis*, and odor in health care facilities.

TABLE 7.1 Design Parameters (*Continued*)

Function of Space	Pressure Relationship to Adjacent Areas (n)	Minimum Outdoor ach	Minimum Total ach	All Room Air Exhausted Directly to Outdoors (j)	Air Recirculated by Means of Room Units (a)	Design Relative Humidity (k) %	Design Temperature (l) °F/ °C
Combination AII/PE anteroom	(e)	NR	10	Yes	No	NR	NR
Labor/delivery/recovery/postpartum (LDRP) (s)	NR	2	6	NR	NR	Max 60	70-75/21-24
Labor/delivery/recovery (LDR) (s)	NR	2	6	NR	NR	Max 60	70-75/21-24
Patient Corridor	NR	NR	2	NR	NR	NR	NR

Figure 1-2 ASHRAE Standard 170, Design Parameters

As can be seen, aside from the thermal comfort parameters (e.g. Temperature and Relative Humidity), there are major requirements pertaining to the space hygiene and infection control. Engineering parameters such as ventilation rates and space pressurization are deemed to affect the spread of viable pathogens [15]. Regulating these requirements, however, has been the most eminent pragmatic step toward the research

problem, if not the only one. As a result, ventilation rates and pressure relationships with adjacent spaces have been regulated with respect to space function. These numbers seem to be consensus based meaning that they have been derived from the experience of scholars in the field [16,17].

Furthermore, there seems to be a paucity of research-based evidence to quantify engineering parameters (e.g. ventilation rate, etc.) relative to occupants' health and well-being. Of 183 epidemiological studies published worldwide from 1960-2005, only 10 studies were deemed by a panel of international experts as having conclusively demonstrated an association between airflow and the transmission of airborne disease. Collectively, data was insufficient to specify minimum ventilation standards to control the spread of airborne disease in any setting [18]. In another multidisciplinary review, Sundell et al. revealed an uncertainty as to the form of the ventilation-health relationship [19]. Although many studies observed a *trend* between ventilation rate and health, the real relation and the attributed mechanisms have still remained ambiguous.

In particular, studies of this nature do not exist for patient corridors. In spite of this, the ventilation rates have recently been changed from 4 ACH to 2 ACH in the latest version of ASHRAE Standard 170-2013 [12]. Moreover, pressure relationship with adjacent spaces is not required (NR) for patient corridors by ASHRAE which can possibly turn into an infinite number of legitimate design strategies. Also, unlike airborne infection isolation rooms (AIIRS), no recommendations have been put in place for the exhaust air grille and/or supply diffuser placements.

Therefore, this dissertation aims at testing the authenticity and reliability of recommendations made by current codes relative to airborne particle dissemination within patient corridors. Specifically, the following questions will be addressed:

1. What pressure relationship must be maintained in patient corridors relative to adjoining spaces in order to mitigate airborne particle spread?
2. What is the impact of ventilation arrangements on airborne particle dissemination for a given ventilation rate? In other words, how could engineers control the motion of airborne particles by means of altering inlet/outlet arrangements as opposed to increasing ventilation rate (i.e. more energy)?
3. How does ventilation rate influence the concentrations and distributions of airborne particles within patient corridors?

1.4 Research Design

Both quasi-experimental and computational procedures were employed to address the research questions. In fact, a series of tests were conducted in an actual hospital's corridors, which was decommissioned at the time, to explore the aerodynamic behavior of surrogate particles. Next, CFD models were developed, and validated by experimental results, to further study cases specifically on various ventilation rates.

1.5 Dissertation Organization

In the following contribution, in Chapter 2, a review of the selected literature is presented with respect to airborne infection, theoretical background of indoor air motion, and particle tracking techniques. In Chapter 3, the experimental setup and equipment used are

presented and ample information about the patient ward geometry and mechanical system is provided. Next, the CFD development procedures and nuances of computational modeling are elaborated, and the CFD model validation is discussed. In Chapter 4, experimental results of two conducted tests are discussed. Subsequently and in Chapter 5, computational results are presented as a threefold: 1) preliminary results, 2) results pertaining to space pressurization, and 3) results pertaining to ventilation rates. In Chapter 6, this dissertation concludes by discussing how the findings support (impugn) current codes. Specifically, ASHRAE Standard 170 recommendations on pressurization and minimum ventilation requirement will be questioned. Based on the evidence, the non-directional flow strategy is suitable for corridors. Moreover, increasing the ventilation rate does not *proportionally* lower particle concentrations, and therefore, is not necessarily *the solution.*

CHAPTER 2: LITERATURE REVIEW

In this chapter, early works on airborne infection in healthcare settings are reported and summarized. Particularly, studies focusing on infection transmission as well as indoor air and particle motion are of interest and will be discussed separately.

2.1 Infection in Hospitals

Acute respiratory disease (ARD) is the leading cause of infectious disease morbidity and mortality in the world, resulting in nearly four million deaths each year [20]. ARDs that constitute a public health emergency of international concern include severe acute respiratory syndrome (SARS), pandemic influenza, pneumonic plague and human episodes of avian influenza. Although many other agents are capable of producing contagious respiratory disease, (e.g. rubella, varicella, etc.), large-scale outbreaks with high morbidity and mortality are comparatively rare. Tuberculosis seldom presents as an ARD, but its infectivity, particularly within the public transportation and healthcare environment, is also cause for international concern [21]. Pneumonias account for <15% hospital acquired infections (HAIs) but result in more than one-third of all HAI deaths [22].

Establishment of infection control procedures, including environmental controls, is critical for containment and removal of pathogens that may otherwise constitute a major public health threat, particularly in clinical settings. Environmental controls are based on the known transmission routes of the disease and include methods to reduce the concentration of infectious agents in the air and on surfaces. *Contact transmission* of microorganisms can occur by direct body contact between an infected person and

susceptible host, or, by indirect contact with a contaminated object. *Droplet transmission* occurs when respiratory droplets, usually >5μm in size, are propelled a short distance (<1m) from an infected person and deposited on the conjunctivae, mouth, nasal, throat or pharynx mucosa of another person [15]. *Airborne transmission* of disease is caused by desiccated respiratory droplets (e.g. droplet nuclei), usually <5μm in size, that remain suspended in the air over long distances and time.

A patient with an airborne infectious disease requires airborne precautions, including placement into an airborne infectious isolation room. Infectious isolation rooms are prioritized for patients with obligate or preferential airborne infections, and, for patients infected with novel ARDs with no information on possible routes of transmission. An infectious isolation room is a room with ≥12 air changes per hour (ACH) and *inward* directional airflow designed to contain, dilute and remove airborne contaminants. An ACH is a volume of air equal to the volume of the room that will be replaced in one hour.

Inward directional airflow prevents contaminated air from leaking out into corridors and other adjacent spaces and is achieved by creating negative air pressure within the isolation room. For isolation rooms with 0.05m^2 or less air leakage area, ≥2.5Pa negative air pressure can be achieved by exhausting ≥55L/s more air than is supplied to the room [13,14,23]. A patient requiring only standard, contact or droplet precautions may be placed into a general patient room where source controls and personal protective equipment (PPE), not special ventilation procedures, may be required to prevent disease transmission.

The rationale for determining minimum ventilation rates is based on two main factors; the effect of ventilation on the concentration of airborne contaminants, and, the effect of ventilation on the infection probability for known airborne diseases [21]. To determine the time necessary to reduce an initial concentration of contaminant to a desired or ending concentration of contaminant, the following *concentration decay* or 'purge' *equation* can be used [24];

$$t = \frac{V}{Q}\ln\left(\frac{c_i}{c_d}\right) \quad \textbf{1}$$

Where;

t = time (s)

V = volume of the space (m^3)

Q = ventilation rate (m^3/s)

c_i = contaminant concentration, initial (g/m^3)

c_d = contaminant concentration, ending (g/m^3).

In the above equation, the ratio of ventilation to room volume can be expressed as an ACH (Air Change per Hour). Similarly, the ratio of initial contaminant concentration to ending concentration can be expressed as a percentage of removal, usually 90%, 99% or 99.9%. Using this simple equation, the time necessary to achieve a desired removal efficiency can be determined relative to ACH. For an isolation room with 12 ACH, the initial contaminant load can be reduced by 90% in 12 minutes, 99% in 23 minutes, and,

99.9% in 35 minutes. This calculation, however, assumes an initial contaminant concentration, pure ventilation air and perfect mixing, not a continuous release of contagion from an infectious patient under less ideal airflow conditions.

To determine the concentration from a constant contaminant source within a room, the following *dilution ventilation equation* can be used;

$$V\frac{dc}{dt} = Q(c_o - c) + \dot{V}_{pol} \quad \textbf{2}$$

Where;

∂c = change in concentration

∂t = change in time

c_o = contaminant concentration, supply air (g/m^3)

c = contaminant concentration, room (g/m^3)

$\dot{V}_{pol}$ = contaminant generation rate (g/s)

Solving for room contaminant concentration (c) at any point in time,

$$c = (c_o + \frac{\dot{V}_{pol}}{Q})(1 - e^{-nt}) + c_i e^{-nt} \quad \textbf{3}$$

Where;

n = air change rate.

For the purpose of determining long-term exposure where time (t) is very large, the initial room concentration (c_i) becomes less significant, while the contaminant generation rate ($\dot{V}_{pol}$) and ventilation rate (Q) approaches the following simplified, steady-state solution;

$$c = (c_o + \frac{\dot{V}_{pol}}{Q}) \quad \textbf{4}$$

Again, these computational methods indicate that higher ventilation rates reduce the time necessary to remove airborne contaminants, suggesting that the exposure time and infective dose may be reduced. These mathematical models assume perfect mixing where the contaminant concentration is the same everywhere in the room, such as a gaseous pollutant. Airborne disease, however, consists of pathogenic microorganisms aerosolized on small particles or in droplets. Unlike a gas, the concentration of particles in the air is not uniform, but is determined by particle size, settling velocity, particle-particle interactions, surface deposition and airflow. The length of time particles remain suspended in the air is largely governed by particle size, which is determined by the fluid containing the organism(s), the force at emission, the initial size of the droplet, temperature, humidity and the size of the organism(s) within a droplet[25].

Several studies found that respiratory activities such as coughing and sneezing can produce between 500-40,000 expiratory droplets per event with mean aerodynamic diameters (d_a) between 1-15µm [1,26,27]. More than 70% of these droplets were found to be in the respirable range of 10µm or less [28,29], each capable of supporting a poly-microbial composition of viruses (0.02-0.3µm) and bacteria (0.3-5.0µm). Device-generated aerosols can produce droplets in even greater concentrations and much smaller in size,

which are more able to cause infection with a smaller dose [30–36]. Of cough-generated aerosols containing viable *Mycobacterium tuberculosis*, 90% were found in particles <5.0µm [37]. With deposition velocities between 10^{-5} and 10^{-6} m/s, particles <5.0µm can remain suspended in airflow almost indefinitely [25]. Even particles >5.0µm can remain airborne by the movement of ventilation air, people and medical equipment [38].

Given the complexities of quantifying airborne particle concentration and behavior, the *Wells–Riley equation* was developed to approximate the effect of ventilation on the infection probability for known airborne diseases. Specifically, the Wells-Riley equation considers not only the concentration and length of time pathogenic particles are present in the air, but also other epidemiological and environmental factors such as the infectivity of the pathogen (q) and survival of the pathogen (I) [39]. The parameters used in the Wells–Riley equation (below) include ventilation rate, generation of infectious droplet nuclei (e.g. 'quanta') and duration of exposure;

$$P = \left(\frac{D}{S}\right) = 1 - e^{\left(-\frac{Ipqt}{Q}\right)} \quad (5)$$

Where;

P = probability of infection for susceptible

D = number of disease cases

S = number of susceptible

I = number of infectors

p = breathing rate per person (m^3/s)

q = quantum generation rate by an infected person (quanta/s)

t = total exposure time (s)

Q = outdoor air supply rate (m^3/s).

According to the Wells–Riley equation, the probability of infection through infectious droplet nuclei is inversely related to the ventilation rate. For a patient producing 1 quanta/min in a $110m^3$ isolation room with 12 ACH, the estimated risk of infection for 15 minutes of exposure is approximately 0.37%. For the same patient producing 6 quanta/min during a bronchoscopy, the estimated risk of infection for 15 minutes of exposure increases to 2.25% for susceptible, unprotected cohort patients or healthcare workers (HCWs).

Although the Wells-Riley equation has become the most widely accepted model for airborne disease transmission in indoor environments, it also assumes steady-state airflow conditions and ignores the proximity of susceptible people to an infectious source and the random, stochastic transmission behavior of small populations in a clinical setting [40]. Invariably, computational methods may be unable to specify minimum ventilation standards without supporting epidemiological evidence. Yet, of 183 epidemiological studies published worldwide from 1960-2005 with keywords or medical subject headings (MeSH) pertaining to airborne transmission of communicable respiratory diseases, only 40 studies provided data on ventilation. Of these, only 10 studies were deemed by an

international panel of experts as having conclusively demonstrated an association between airflow and the transmission of airborne disease [18].

Only one study of 1,289 HCWs in 17 Canadian hospitals found a conclusive association between and ventilation and airborne disease transmission in a clinical setting. In this study, tuberculin conversion was 3.4 times higher in patient rooms with <2.0 ACH when compared to patient rooms ≥2.0 ACH [41]. Results, however, were insufficient to recommend a minimum ventilation rate for infection control, or, a maximum ventilation rate above which there was no further reduction of infection risk.

Five other studies, however, were able to demonstrate a conclusive association between directional airflow and the transmission of airborne disease. In one such study, a pediatric patient receiving respirator-assisted ventilation with varicella zoster virus (VZV) pneumonia was implicated in the transmission of secondary infections to 13 of 24 susceptible cohort patients. Retrospective studies found that the index patient's room had no exhaust, resulting in a positive (outward) airflow-pressure relationship with respect to the corridor and adjacent spaces. Analysis of a nearby patient room having a 90% attack rate found the supply air system inoperable, resulting in a negative (inward) airflow-pressure relationship with respect to the index patient's room and corridor [42].

In a similar study, secondary VZV infection occurred in eight out of 36 susceptible patients despite isolation procedures. Tracer gas (SF_6) released in the index patient's room following the outbreak reached concentrations in the corridor as high as 10% of those inside the patient room. Concentrations of SF_6 then 'halved' every 4.9-7.3m in the

adjacent corridor. Correspondingly, attack rates declined at roughly the same rate as the decline in SF_6 concentration. All infections occurred in rooms less than 30.5m from the index case where SF_6 was detected in the adjacent corridor [43].

A later study found that secondary VZV infection occurred in seven out of 41 susceptible pediatric patients who were in the same ward as two index patients isolated in rooms without negative pressure ventilation. The pediatric staff later moved to another facility equipped with negative air pressure isolation units. Over a period of one year following the relocation, six index cases were admitted with cutaneous VZV into the care of the same pediatric staff utilizing the same isolation procedures used in the previous facility. Of 110 susceptible cohort patients, none developed nosocomial chickenpox [44].

In a rural U.S. hospital, nine secondary cases of tuberculosis and 59 tuberculin skin test conversions occurred after exposure to a patient with large tuberculous abscesses. Tuberculin reactivity among patients in rooms adjacent to the index case was 2.9 times greater than those located on the other end of the corridor. Results of retrospective air flow studies found that the exhaust air was partially obstructed, causing the index patient's room to pressurize with respect to the corridor and adjacent spaces [45].

More recently, evidence has shown that airborne transmission of SARS is possible, especially for the epidemics that occurred in Hong Kong and Toronto [46,47]. In both events, there was a clear association between the temporal-spatial infection pattern between the index case and secondary cases that could not be explained by the known limitations of either contact or droplet transmission. Again, retrospective airflow analyses found the

supply air rate (20.2m^3/min) to be nearly 4 times the exhaust rate (5.2m^3/min) in the index patient room, resulting in a strong outflow of contaminated air to the corridor and adjacent rooms. Again, a direct correlation was observed between attack rates and aerosol concentrations simulated by tracer gas (CO_2) and computational models.

Although these and several other studies clearly support the use of negative airflow-pressure for airborne isolation, several underlying factors, including door position, door motion, and personnel movement likely contributed to the success (or failure) of these 'air barriers'. As Leclair [42] indicates, "activities" associated with the index patient's critical care "necessitated frequent and prolonged opening of the door to the room." Gustafson [43] noted that tracer gas concentrations near the patients' beds averaged 50% of those in the immediate corridor with entry door fully open despite 0.3-1.1m^3/min outward airflow from rooms to the corridor.

Another retrospective study of nosocomial transmission of VZV to 3 HCWs found tracer gas (NO_2) concentrations in a nursing station equal to (or greater) than concentrations of NO_2 released through an open door from a nearby isolation room under 0.7m^3/min negative air pressure [48]. In a subsequent study, a nurse was reported to have passed equipment through a doorway to other hospital staff attending to a VZV patient in isolation. Despite 3.0Pa negative air-flow-pressure, the nurse developed the same genotype of VZV, even though he did not enter the room [49].

In each of these studies, the position of the door, the door-opening motion and the movement of HCWs and equipment likely resulted in a breakdown of otherwise properly

maintained isolation conditions. An analysis of the door-opening motion indicates that the negative airflow-pressure relationship between an isolation room and adjacent spaces can be transiently reversed if the door-opening motion is too rapid. Specifically, when the a door is opened, a dipolar vortex of air wraps around the leading edge of the door, allowing temporary spillage of potentially infectious air into the anteroom or corridor. The exchange volume of air produced by the door-opening motion is comparable to the swept volume of the door, or approximately $3m^3$.

An added exchange volume of air can be produced by a person entering the room. A typical person with a forward projected area of $0.8m^2$ walking at 1m/s can generate a 'body wake' of approximately $4m^3$ [49]. Together, a HCW opening a door and quickly exiting an AIIR can transport as much as 5-10 percent of the room volume to the corridor despite a 2.5Pa pressure difference [50]. If a temperature difference exists between the isolation room and corridor, colder (denser) air from the corridor may force warmer air from the isolation room upward into the breathing zone of unprotected HCWs entering the anteroom (vestibule), or, to persons nearby in the corridor [49]. Supporting this premise, a cluster sample of 346 patients with acquired immunodeficiency syndrome (AIDS) found that 21 nosocomial multidrug-resistant tuberculosis infections occurred in a total of 16 patient rooms that were located two rooms or less away from index cases. In four of these rooms, inward airflow from the corridor to the patient room was observed at the bottom of the doorway while outward airflow from the patient room to the corridor was observed at the top of the doorway [51].

2.2 Theoretical Background and Considerations

2.2.1 Viscous Fluid flow Formulation

In general, for air as a fluid with constant properties in the ambient temperature and pressure range, the Navier-Stokes (NS) equations have the following form:

$$\nabla.\vec{\boldsymbol{u}} = 0 \quad \textbf{6}$$

$$\rho\frac{D\vec{\boldsymbol{u}}}{Dt} = \rho\vec{g} - \boldsymbol{\nabla}p + \mu\boldsymbol{\nabla}^2\vec{\boldsymbol{u}} \quad \textbf{7}$$

Where u is the velocity vector, p is the pressure and air properties (ρ and μ) are constant. However, several works [52–56] have shown that air motion within enclosed environments have a strong turbulent characteristic which is not negligible. Based on the Reynolds decomposition concept, velocity and pressure can be decomposed into a mean and a fluctuating component [57] which are listed through Eqs. 8 to 11:

$$u_x(x,y,z,t) = \bar{u}_x(x,y,z,t) + u'_x(x,y,z,t) \quad \textbf{8}$$

$$u_y(x,y,z,t) = \bar{u}_y(x,y,z,t) + u'_y(x,y,z,t) \quad \textbf{9}$$

$$u_z(x,y,z,t) = \bar{u}_z(x,y,z,t) + u'_z(x,y,z,t) \quad \textbf{10}$$

$$p(x,y,z,t) = \bar{p}(x,y,z,t) + p'(x,y,z,t) \quad \textbf{11}$$

where u'_x, u'_y and u'_z are fluctuating velocity components; $\bar{u}_x$, $\bar{u}_y$ and $\bar{u}_z$ are time averaged velocity components; p' is the fluctuating pressure and $\bar{p}$ is the time averaged pressure.

In a turbulent flow, the fluctuation values (u_i') become comparable to the mean values, and thus, significant. The fluctuations are in general random, and time-dependent. Although the conservation equations still hold under turbulence, they become extremely difficult and computationally intensive to solve. Therefore, a principled practice is to create models which approximate the turbulence. Various attempts have been invested in exploring turbulence in flows and it can be generally divided into three major categories:

2.2.1.1 Reynolds Average Navier Stokes (RANS) Model

The idea for this method is to use the time-average velocity and create a model to incorporate the fluctuation values into the solution. Experiments on turbulent flow show that the velocity of particles varies with respect to both time and space [58]. Although turbulence is proved to be random, some aspects of it can be studied through the averaging process. Statistical averaging of an arbitrary function related to turbulence (f) with respect to time in a time period (T) longer than that of a typical fluctuation period (Eq. 12) reveals consistent characteristics [59].

$$\overline{\boldsymbol{u}} = \frac{1}{\mathrm{T}}\int_{t}^{t+\mathrm{T}} \boldsymbol{u}(x,y,z,t)dt \qquad \textbf{12}$$

Besides, the instantaneous velocity distribution may not be of interest from practical point of view in real-world problems. By definition, the time average of u' is zero, however, one half of the sum of the time-average of the fluctuations squared is referred to as the turbulence kinetic energy.

$$\boldsymbol{u}' = [u_x', u_y', u_z'] \qquad \textbf{13}$$

$$K = \frac{1}{2}(\overline{u_x'}^2 + \overline{u_y'}^2 + \overline{u_z'}^2) \quad \textbf{14}$$

In fact, if turbulence is to be described by only one velocity scale, it would be $K^{1/2}$. Using the time-average notion, turbulence is simulated under the premise that the conservation equations are solved for the time-averaged velocity and the turbulence parameters such as the turbulent kinetic energy, in the form of partial differential equations, are employed to approximate the turbulence. In this sense, the final solution loses the details pertaining to turbulence. The RANS equations are mathematically analogous with the Navier-Stokes equations except for the turbulence fluctuating terms which are treated as additional shear stresses appearing in only turbulent flow. The prominent advantage of using this group of modeling is its simplicity. A disadvantage however, is that using this method's outcome to track particle movements will end in about 10% error since the particle movement is extremely related to the intermittent component of velocity.

2.2.1.2 Large Eddy Simulation (LES)

This approach carries out a full unsteady Navier-Stokes calculation and the approximations take place to model small eddies and relate them to large eddies. In a turbulent flow, eddies are formed due shear stress between two layer of the fluid which make the fluid swirl and create a reverse current flow. Eddies generally are seen when the fluid flow near an obstacle. The obstacle could be a solid surface or even the body of fluid with a lower velocity. Therefore, the velocity gradient can cause eddies to happen. Eddies can have a size as big as largest length scale in the system or as small as the molecular level [60,61]. The lower limit of the eddy size depends on the Reynolds number, the larger the Reynolds number is the smaller the eddy size will become. Eddies of any

size transfer momentum and energy, thus even the smallest scales must be considered. Since the numerical calculations are performed in an unsteady manner, those eddies smaller than the grid size will resolve into the system. The approximation is brought in to model the small eddied momentum and energy transfer and somehow related that to those of the larger eddy sizes. This method is very computationally intensive limited to moderate Reynold numbers which makes it hardly achievable with our existing computational facilities. On the other hand, the flow details are maintained and is determinant of the particle motion within the fluid. The general procedure of LES consists of the following steps [62]:

- Decompose the flow variables into large-scale and small-scale by utilizing a filter function.
- Filter the governing equations and constitute the filter-averaged Navier Stokes equations. Similar to the RANS method, we observe the appearance of small eddies' contribution. This part needs to be somehow modeled.
- Model the unresolved (filtered) scaled stresses.
- Solve the equations for the large-scale contribution by incorporating the small-scale role.

2.2.1.3 Direct Numerical Simulation (DNS)

This method solve the full unsteady conservation equations of the flow and requires no simulation for turbulence. This method is highly constrained by the Reynolds number magnitude. Thus far, using the most advanced supercomputers, this method can perform for flows with Reynolds number of the order of 10^4. Therefore, the DNS is not applicable

to real-life problems. However, a very important application of DNS is to provide details and evidence for improving turbulence models. It can perfectly work as a form of validation for other methods.

2.2.2 Particle Track Formulation

In general, two accepted approaches are used to model the motion of a second species in a carrier domain: the Eulerian and Lagrangian methods. The Eulerian method treats particles as continuum within the carrier domain, solves the fundamental equations for the new species and considers the interaction between species. This method, however, is established for environments in which the second species' concentration is sufficiently large to create a continuum [63,64]. Alternatively, the Lagrangian method treats particles as solid, non-deformable entities whose motion is determined by the forces exerted on them [65]. The Lagrangian method track particle by solving the following equation

$$\frac{d\boldsymbol{u}_p}{dt} = F_D\left(\boldsymbol{u} - \boldsymbol{u}_p\right) + \frac{\boldsymbol{g}\left(\rho_p - \rho\right)}{\rho_p} + \boldsymbol{n}(t) + \boldsymbol{F}_L + \boldsymbol{F} \qquad \textbf{15}$$

Above is an ordinary differential equation where the only unknown is particle velocities. $\vec{u}$ and $\vec{u}_p$ are air and particle velocity respectively. The first term in the right hand side of the equation is the drag force, F_D is

$$F_D = \frac{18\mu}{\rho_p d_p^2}\frac{C_D Re}{24} \qquad \textbf{16}$$

Where ρ_p and d_p are the particle density and diameter respectively, Re is the Reynolds number and C_D is the drag coefficient that is calculated by (Figure 2-1) [66]

$$C_D = \begin{cases} \dfrac{24}{Re} & Re < 1 \\ \dfrac{24}{Re}\left(1 + \dfrac{Re^{\frac{2}{3}}}{6}\right) & 1 < Re < 1000 \\ 0.44 & Re > 1000 \end{cases} \quad (17)$$

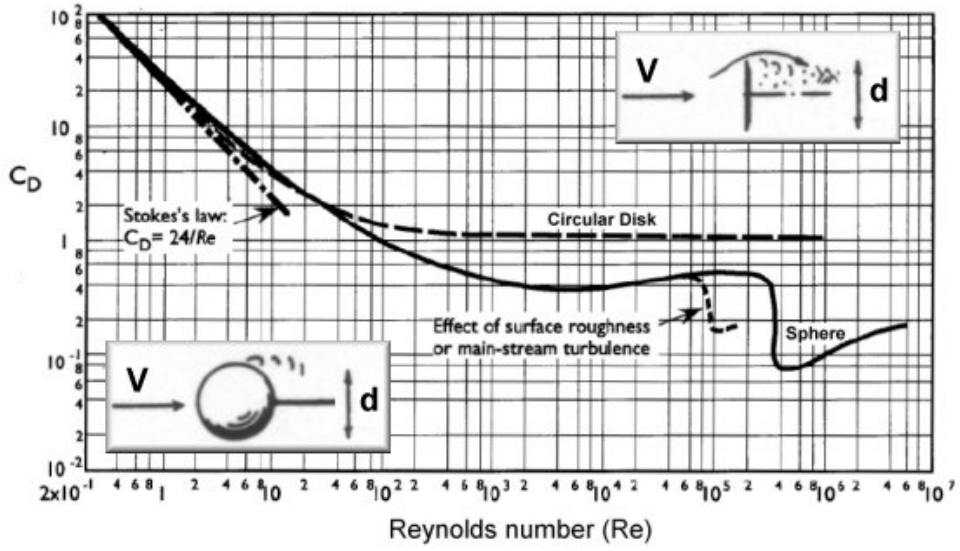

Figure 2-1 Drag Coefficient versus Reynold Number

The second term is associated with the gravity and buoyancy. n(t) and F_L are the Brownian and Saffman's lift force [65] respectively and the last term represents other forces such as the Virtual mass and pressure gradient forces.

$$\boldsymbol{n}(t) = \zeta_i \sqrt{\frac{216\mu\sigma T}{\pi {\rho_p}^2 C_c \Delta t}} . d_p^{-2.5} \quad (18)$$

$$F_{L,i} = 5.188 \frac{\nu^{1/2} \rho d_{ij} \left(u_i - u_{p,i}\right)}{\rho_p (d_{lk} d_{kl})^{1/4}} . d_p^{-1} \quad 19$$

Where ζ is a Gaussian random number with zero mean and unit variance, dij is the rate of deformation tensor σ is the Boltzmann constant. ρp and dp are particle density and diameter respectively. And Cc is the Cunningham slip correction factor.

Particle velocity is the only unknown in Eq. 15 to be found. Particle trajectories are computed with the following equations

$$\boldsymbol{u}_p = \frac{d\boldsymbol{x}_p}{dt} \quad \mathbf{20}$$

Where $\mathbf{x}_p$ is the particle position vector in the domain.

In summary, As stated in the WHO Guideline [21], *"There is little evidence that ventilation directly reduces the risk of disease transmission, but many studies suggest that insufficient ventilation increases disease transmission."* Specifically, in patient corridors, not enough research has been conducted to correlate ventilation to the risk of disease transmission.

The existing literature suggests that the Realizable k-ε model is suitable for modeling indoor air motion and the Eulerian-Lagrangian method is vastly used for simulating discrete phase (e.g. particles) behavior within a given domain.

CHAPTER 3: METHODOLOGY

3.1 Experimental Location and Description

A 37,510m^2 hospital, vacated in November 2009, was used to simulate the aerodynamic behavior of surrogate respiratory aerosols under various ventilation alignments in various function spaces. A total of two tests were conducted in the ward corridors on the 5th floor of an eight (8) story 'bed' tower (Figure 3-1, Figure 3-2, Figure 3-3). The ward consisted of twenty-eight (28) general patient rooms and two (2) airborne infectious isolation rooms (AIIRs) as well as ancillary function spaces. The ward was supplied 168.8m^3/min of 100% outside air (as verified by duct traverse measurements) from a single air handling unit (AHU) providing conditioned air directly to the corridor, ancillary spaces and isolation rooms (Figure 3-4). The corridor was supplied 89.2 m^3/min (53%) of the total supply air. Exhaust air within the ward was removed by two (2) exhaust air risers serving other zones on other floors. Pressure measurements indicated that the 5th floor ward was positive in relation to the 4th floor (7.5Pa) and neutral in relation to the 6th floor. Grille type diffusers were used in this hospital and the supply air temperature was 15.8°C. Since a controlled lab condition was not met, quasi-experimental tests were conducted where parameters such as ventilation rate, supply temperature, geometry of the space were under control. Other parameters such as outside temperature and humidity, wind speed and direction, radiation through windows, and indoor temperature distribution were not under control.

Figure 3-1 Exterior View of Hospital

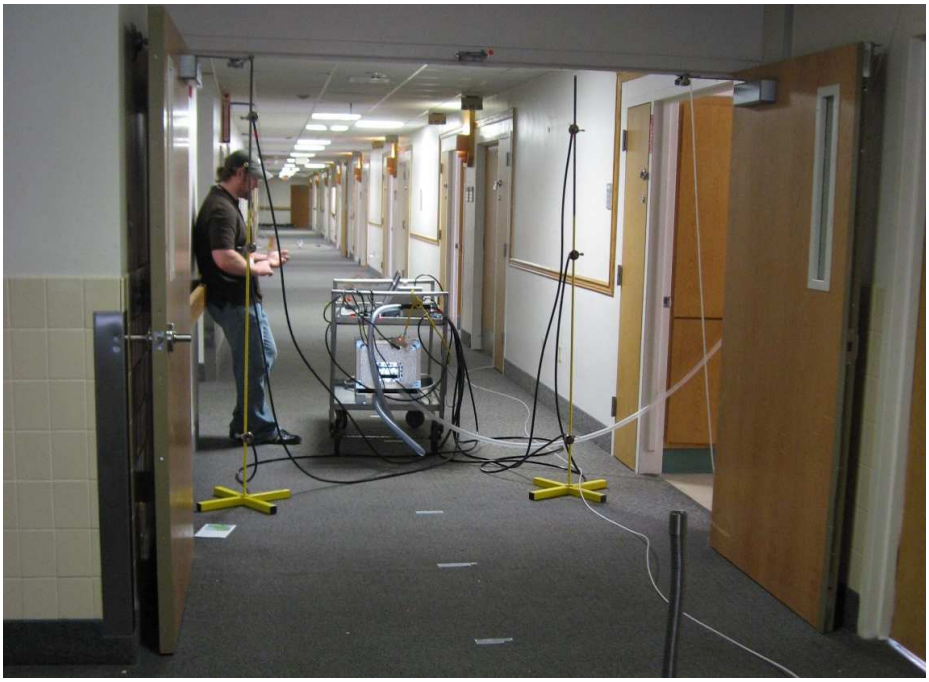

Figure 3-2 General Patient Ward Corridors, NUCON F-1000-DD Aerosol Detector and Aerosol Sampling Equipment

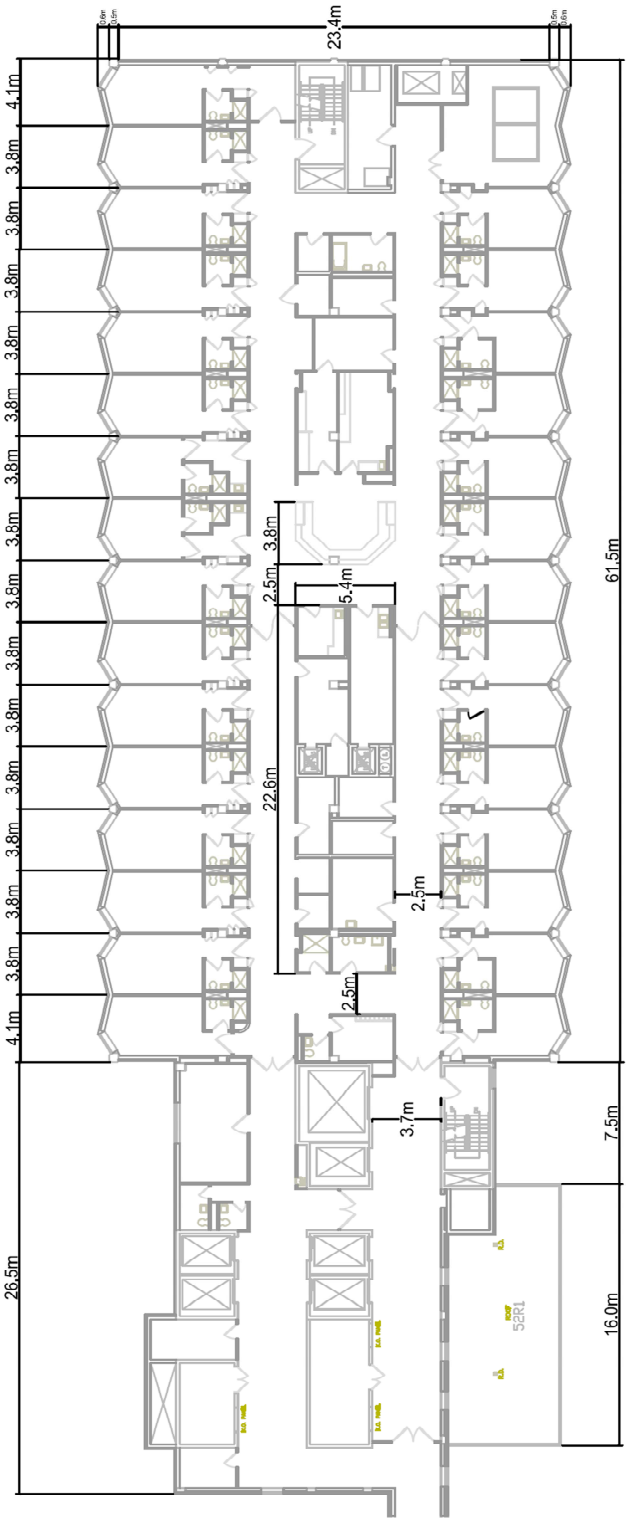

Figure 3-3 General Patient Ward Plan, the 'Bed Tower'

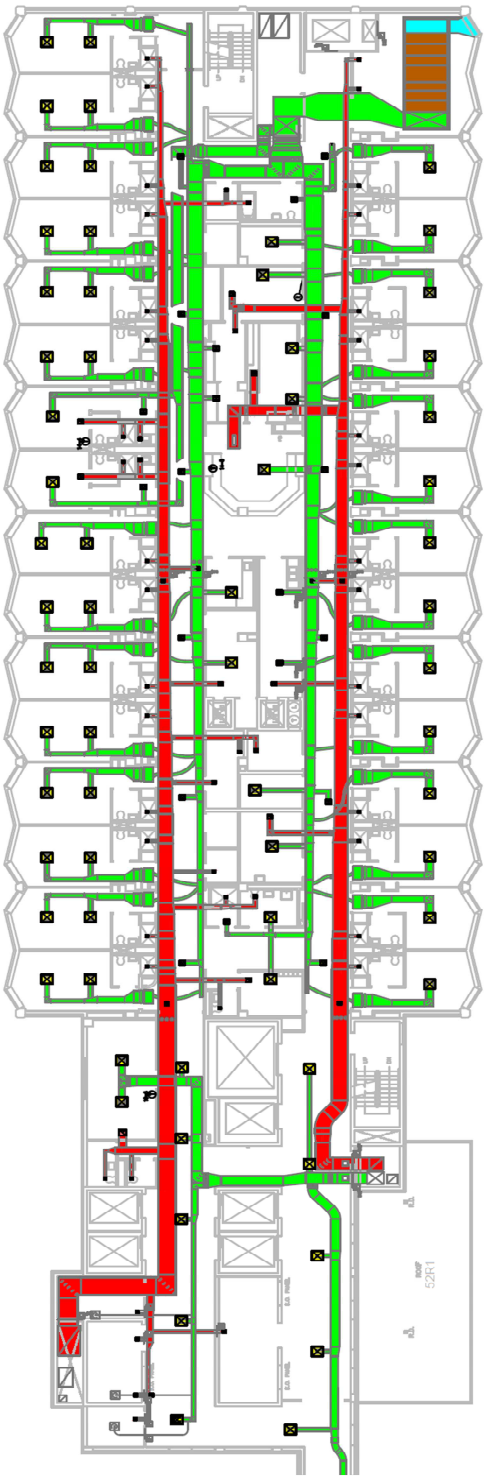

Figure 3-4 General Patient Ward Mechanical Plan

3.2 Quasi-Experimental Method

To simulate a respiratory aerosol, a synthetic aliphatic hydrocarbon (polyaliphaticolefin) approximately 84.7% of the density of water (at 20°C) was aerosolized at a rate of approximately 1.0g/min at 0.4L/s airflow rate [52,67] to generate a 0.5µm-3.0µm poly-disperse liquid aerosol. The aerosolization rate was intended to represent the respiratory volume of two human subjects at rest. The particle size distribution (Figure 3-5) was consistent with two studies [28,29] which found that a human cough generates ~10^4 particles with a size distribution of 0.5-15.0µm (71% <10.0µm) which desiccate by half immediately after release.

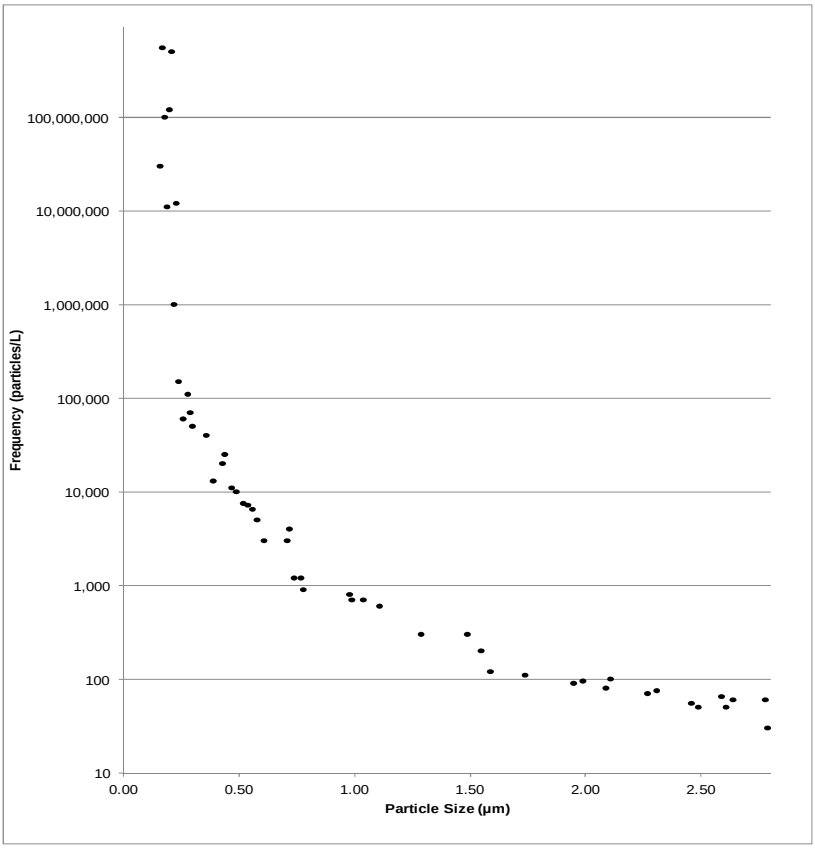

Figure 3-5 Particle Size Distribution of NUCON SN-10 Pneumatic Aerosol Generator

The aerosol was continuously injected in the main corridor between an elevator lobby and the entrance to the patient area (Figure 3-6) to simulate the exposure of patients to other potentially infectious patients, healthcare workers and visitors transiting the bed tower elevators. The aerosol was released at the approximate location of a non-ambulatory patient's nose-mouth at rest (0.8m) using a NUCON SN-10 pneumatic aerosol generator.

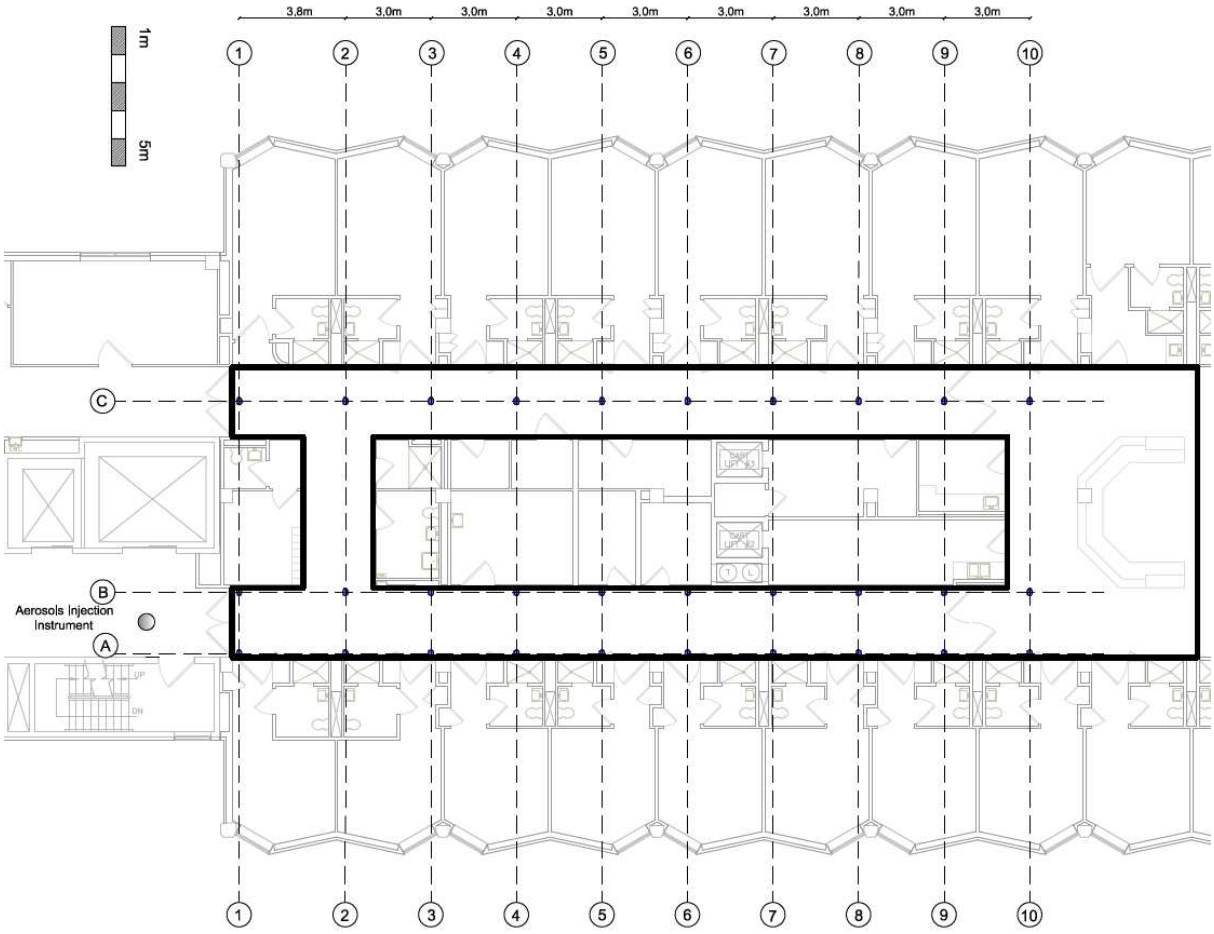

Figure 3-6 Particle Sampling Locations in General Patient Ward Corridors

Particle size distribution measurements (particles/L) ranging from 0.5-3.0µm were collected using a NUCON F-1000-DD forward light scattering photometric aerosol

detector at 30 sampling locations (Figure 3-6). The aerosol detector was a six channel instrument with ±1% reading accuracy and 0.0001 µg/L threshold sensitivity. Concentrations of aerosol were observed along the patient-room side of the main corridor (‘A’ series) and along the side of the corridor opposite the patient rooms (‘B’ series) at sampling heights of 0.6m, 1.2m and 1.8m above the floor (Figure 3-7). Concentrations of aerosol were also observed in the center of an adjacent corridor (‘C’ series) at a sampling height of 1.2m. For each spatial sample series, concentrations of aerosol were first observed at a distance of 3.3m from the aerosol release point, and then, at intervals ~3.0m over a total distance of 31.5m from the aerosol release point. Samples from each sampling point were drawn at 30 second intervals for a total of ~30 minutes each. Ambient concentrations of airborne particles were sampled for 30 minutes prior to aerosol injection (

Table 3-1).

Time (Neutral)	Time (Negative)	Instruments	Test Locations	Description
0:00-0:05	0:00-0:30	F-1000-DD/HH-3016-IAQ	A1, B1, C1	Background (3.3m)
0:05-0:30	0:30-1:00	“	A1, B1, C1	Injection started (3.3m)
0:30-1:00	1:00-1:30	F-1000-DD/HH-3016-IAQ	A2, B2, C2	Position movement (7.1m)
0:05-0:30	0:30-1:00	“	A1, B1, C1	Injection started (3.3m)
1:00-1:20	1:30-1:50	“	A3, B3, C3	Position movement (10.1m)
0:30-1:00	1:00-1:30	“	A2, B2, C2	Position movement (7.1m)
1:20-1:40	1:50-2:10	“	A4, B4, C4	Position movement (13.2m)
1:00-1:20	1:30-1:50	“	A3, B3, C3	Position movement (10.1m)
1:40-2:00	2:10-2:30	“	A5, B5, C5	Position movement (16.2m)
1:30-1:40	1:50-2:10	“	A4, B4, C4	Position movement (13.2m)
2:00-2:30	2:30-2:50	“	A6, B6, C6	Position movement (19.3m)
1:40-2:00	2:10-2:30	“	A5, B5, C5	Position movement (16.2m)
2:30-2:50	2:50-3:30	“	A7, B7, C7	Position movement (22.3m)
2:00-2:30	2:30-2:50	“	A6, B6, C6	Position movement (19.3m)
2:50-3:10	3:30-3:50	“	A8, B8, C8	Position movement (25.4m)
2:30-2:50	2:50-3:30	“	A7, B7, C7	Position movement (22.3m)
-	3:50-4:10	“	A9, B9, C9	Position movement (28.4m)
2:50-3:10	3:30-3:50	“	A8, B8, C8	Position movement (25.4m)
-	4:10-4:30	“	A10, B10, C10	Position movement (31.5m)
3:10-3:20	4:30-5:00	“	A10, B10, C10	Injection stopped (31.5m)
0:00-3:20	0:00-5:00	HH-3016-IAQ	Static	Nurses station (35.0m)

Table 3-1 Summary of Test Procedure in Corridors

Figure 3-7 Particle Sampling Equipment in General Patient Ward Corridors. Sampling Locations A1 (left) and B1 (right) Shown at Entrance to Patient Area at 0.6m, 1.2m, and 1.8m Sampling Heights Respectively. Aerosol Generator Approximately 3.3m Behind Closed Doors

3.2.1 Neutral mode

For testing under the *neutral* airflow mode, attempts were made to balance ventilation air supplied to the patient ward by manipulating variable frequency drive (VFD) controls. At 60Hz (maximum capacity) the ward was supplied 220.8m^3/min of ventilation air as verified by duct traverse measurements. A total of 232.4m^3/min of exhaust air was removed from the ward by a constant volume system, producing a neutral to slightly

negative pressure relationship relative to adjacent spaces. Flow hood measurements in the general patient rooms indicated that ventilation and exhaust air were on average, balanced (~2.4m^3/min), producing a neutral air pressure relationship with respect to the corridor. Measurements in the isolation rooms indicated that exhaust air exceeded ventilation air by 2.3m^3/min, producing a negative air pressure relationship with respect to the corridor.

3.2.2 Negative Mode

For testing under the *negative* airflow mode, the VFD on the ventilation system was reduced from 60Hz to approximately 35Hz, reducing ventilation air from 220.8m^3/min to 136.7m^3/min as verified by duct traverse measurements. Exhaust air removed from the ward remained relatively constant (227.6 m^3/min), producing a strongly negative pressure relationship relative to adjacent spaces. Flow hood measurements in the general patient rooms indicated that exhaust air exceeded ventilation air by ~0.4m^3/min, producing a negative air pressure relationship with respect to the corridor. Measurements in the isolation rooms indicated that exhaust air exceeded ventilation air by 4.2m^3/min, producing a strongly negative air pressure relationship with respect to the corridor.

For both tests, entry doors separating the elevator lobby and patient area were closed. Sampling instrumentation was calibrated using 2.5mg of polyaliphaticolefin per cubic meter of air as part of a procedure developed with guidance from ANSI 510 and 511, ASME AG-1 and ASHRAE 52.2 [68,69]. Indoor temperature, relative humidity and air density were continuously recorded at a centrally located nursing station during the tests. Wind speed and direction, precipitation, temperature, relative humidity and barometric

pressure were recorded from three outdoor meteorological stations. The average indoor temperature was 21.7°C during testing. The average indoor relative humidity was high (>70%) as there was little effort to control latent loads during the time this area of the hospital was vacated (and thus available for non-human subject testing). Barometric pressure remained near constant at 1,012mb and the average indoor air density was 1.17kg/m^3. Outdoor temperatures were mild (18.9-27.8^{o}C) and winds were light (5-7km/hr) and variable.

3.3 Computational Modeling Method

ANSYS Fluent 15.0R was used to construct the computational models. The first series of CFD models were constructed to replicate experimental procedures. As experimental results suggested, particle concentrations vanished approximately 30m away from the aerosol generator. Therefore, sections of the corridors from the entrance door up to the nurse station area were modeled to reduce the computational intensity. Model geometries consist of the main and opposite hallways from the entrance door (at the elevator lobby) to the nursing station area (Figure 3-6). Supply diffusers and exhaust fans were placed according to the mechanical plan. Infiltration and exfiltration from the patient rooms and ancillary function spaces were neglected.

3.3.1 Discretization and Mesh

The entire domain was discretized using tetrahedral mesh. The maximum size of the general mesh was primarily set to 20cm. The mesh was refined from 20 to 15cm and again from 15cm to 10cm to assure ‘mesh-independency’ (Table 3-2). In practice, using finer meshing in high velocity gradient regions can improve the rate of convergence.

Thus, 1cm and 5cm grid sizes were used at diffusers and wall, respectively. As a result of the meshing scheme, a total of 2,935,528 nodes were generated with an element volume range from 1.13×10^{-8} m^3 to 1.25×10^{-3} m^3. The maximum aspect ratio and the minimum orthogonal quality were 2.3667 and 0.20264, respectively.

Table 3-2 Meshing Accuracy Relative to Mass Flow Rate Values at Boundaries

Mode	Boundary	Mesh Size (cm) vs. Mass Flow Rate (kg/s)				
		20	15	Change (20 to15)	10	Change (15 to 10)
Neutral	Exhaust Fans	0.0938	0.0973	3.73%	0.0979	0.62%
	Supply Diffusers	0.0576	0.0587	1.91%	0.0590	0.51%
	Pressure Inlet	0.0043	0.0026	-39.53%	0.0027	3.85%
	Overall Continuity	0.0174	0.0056	-67.82%	0.0053	-5.36%
Negative	Exhaust Fans	0.0925	0.0965	4.32%	0.0979	1.45%
	Supply Diffusers	0.0288	0.0292	1.39%	0.0297	1.71%
	Pressure Inlet	-0.0890	-0.2391	168.49%	-0.2503	4.68%
	Overall Continuity	-0.3562	-0.5259	47.67%	-0.5406	2.80%

Ansys Fluent recommends using 10^{-3} as the convergence criterion; however, 5×10^{-4} was used for this study to assure the convergence (Table 3-3). The residuals decayed to some small value ("round-off") and then stopped changing ("level out").

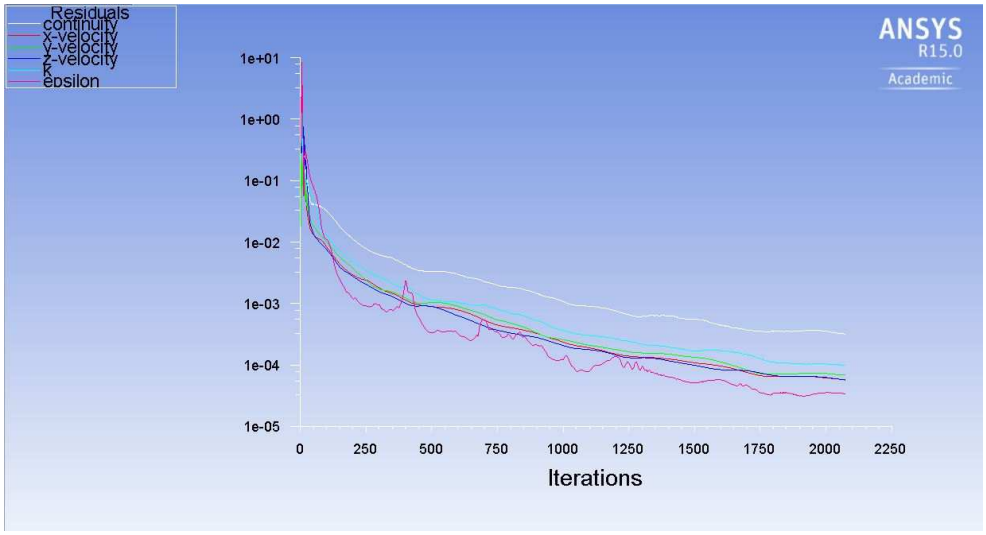

Figure 3-8 Scaled Residuals for Conserved Variables

Table 3-3 Scaled Residuals for Conserved Variables

Continuity	x-velocity	y-velocity	z-velocity	k	epsilon
3.1319e-4	5.7517e-5	6.8573e-5	5.6750e-5	1.0018e-4	3.4221e-5

Moreover, it is a good idea to judge convergence not only by examining residual levels, but also by monitoring relevant integrated quantities such as drag coefficient. Therefore, as per your request, convergence on average velocity field, pressure in Exhaust fan 3, and the drag coefficient on walls are also studied for convergence (Figure 3-9, Figure 3-10, Figure 3-11).

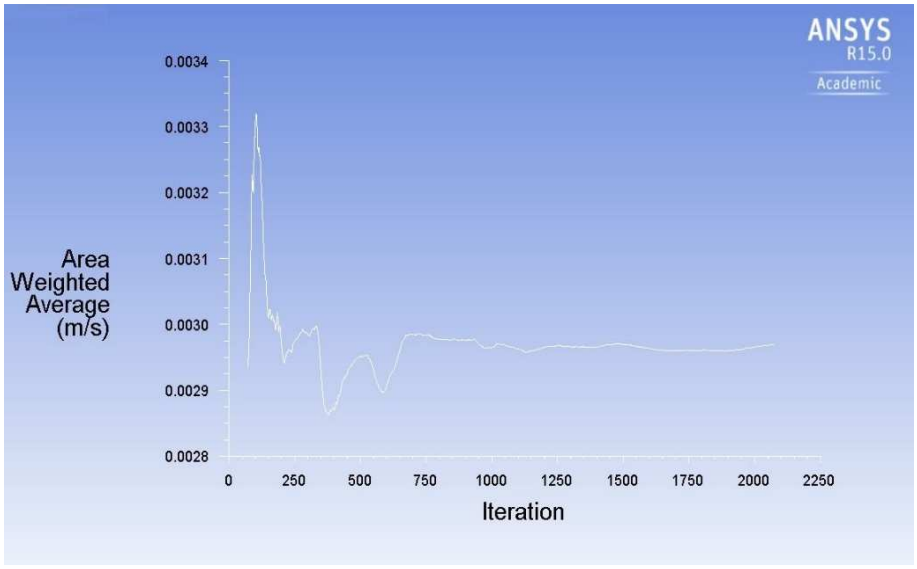

Figure 3-9 Weighted Average Velocity Field Convergence

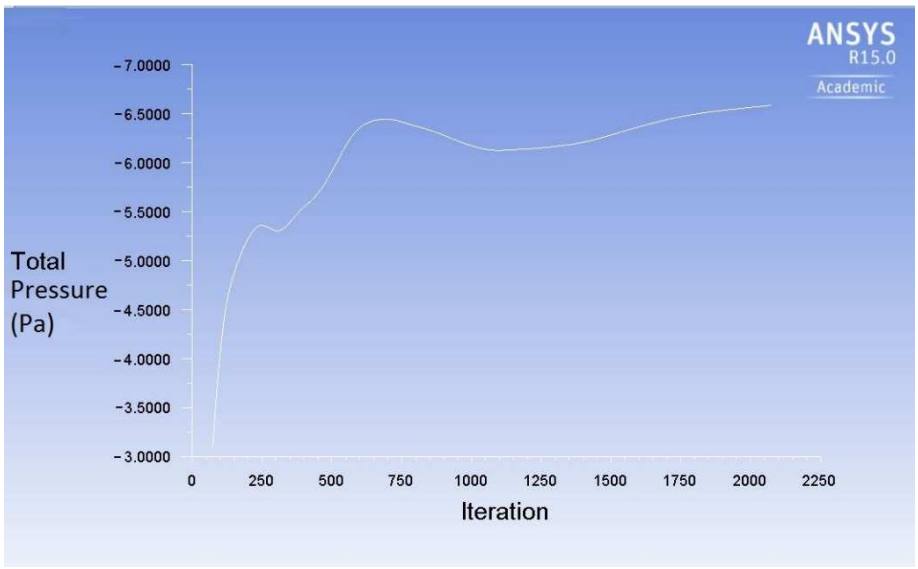

Figure 3-10 Total Static Pressure for Exhaust Fan 3

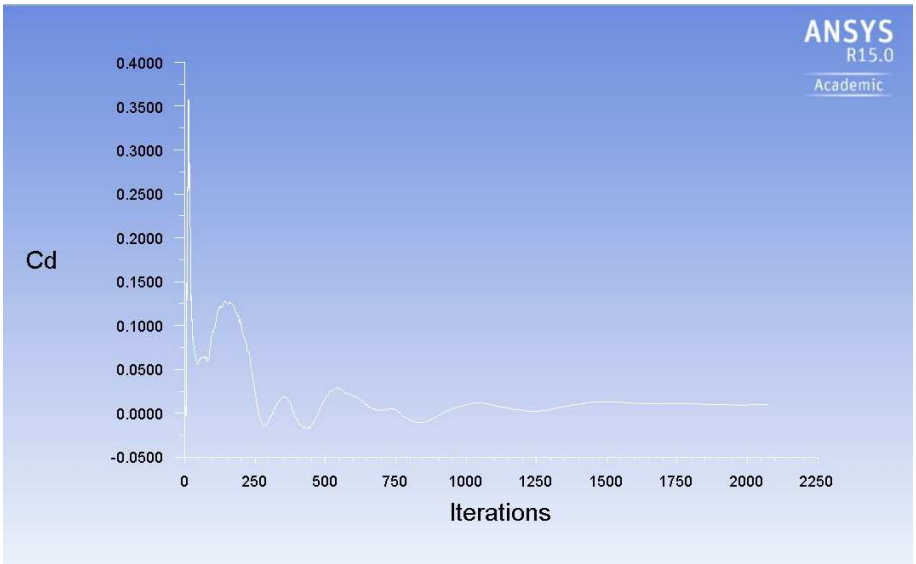

Figure 3-11 Drag Coefficient on Walls

Grid independency test was also conducted for the velocity field on a vertical plane in the middle of the hallway (y=1.25m), a horizontal plane at the release height (z=0.8m), and the boundaries for the neutral mode (Table 3-4).

Table 3-4 Meshing Accuracy Relative to Velocity Field

Mode	Boundary	Mesh Size (cm) vs. Velocity (m/s)				
		20	15	Change (20 to15)	10	Change (15 to 10)
Neutral	Exhaust Fans	1.2251	1.2709	3.73%	1.2787	0.62%
	Supply Diffusers	0.1306	0.1331	1.91%	0.1338	0.51%
	Pressure Inlet	0.0001	0.0001	-39.53%	0.0001	3.85%
	Mid Hallway Plane (y=1.25m)	0.0541	0.0496	-8.30%	0.0495	-0.22%
	Release Height Plane(z=0.8m)	0.0450	0.0396	-12.01%	0.0392	-1.05%

3.3.2 Material Properties

Air was deemed as a perfect gas where its density changes with local pressure and temperature values. The absolute viscosity of air was assumed constant ($\mu = 1.98\times10^{-5}$

Pa.s) in the ambient temperature [70]. Moreover, particle properties were similar to that of the surrogate particle in the tests (ρ=847 kg/m^3, C_p= 2217.5 J/kg.K).

3.3.3 Modeling and Solver

As alluded to earlier, turbulence is the intrinsic part of indoor air movement and it has to be modeled accordingly. Several previous works have suggested that the Realizable K-ε Reynolds-Averaged-Navier-Stokes method is appropriate for airflow modeling in enclosed spaces [71–73]. This model is of RANS type models which introduces two more partial differential equations for mathematical closure. Energy equation was also solved for the problem. Hence a total of 7 partial differential equations (conservation of mass, 1 equation; conservation of momentum, three equations; turbulence, two equations; and conservation of energy, one equation) were simultaneously solved to obtain the solutions. The SIMPLE algorithm [74] was utilized to iterate towards the solution. A second order upwind scheme was used to approximate the first and second derivatives of the unknowns (i.e. temperature, velocity, pressure, turbulent kinetic energy, and turbulent dissipation rate). Models were solved assuming the steady state condition since there was no time dependence in the variables.

3.3.4 Boundary Conditions

Aside from the governing equations, boundary conditions are required to attain the mathematical closure. In fact, boundary conditions are the inherent part of a physical problem that provides the unique, realistic solution. In this work four types of boundary conditions existed: walls, supply diffusers (velocity inlet), exhaust fans, and pressure outlets (Figure 3-12).

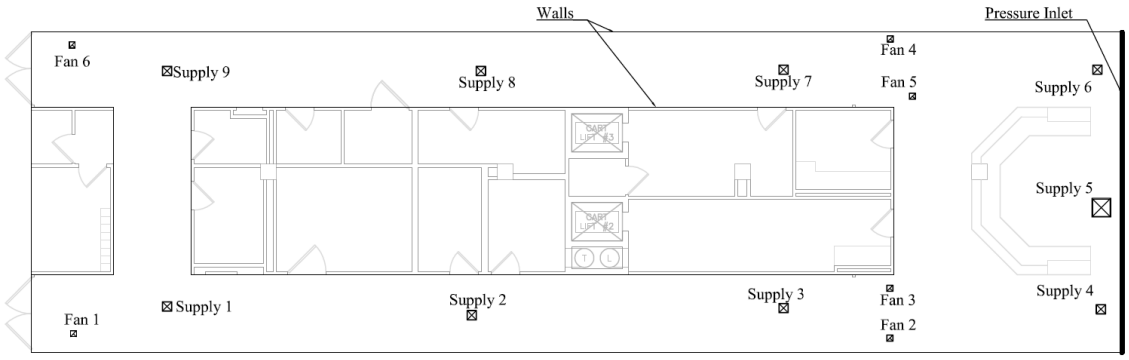

Figure 3-12 Boundary Conditions in General Patient Ward Corridors

3.3.4.1 Walls

Both the normal and tangential components of the velocity field were deemed to be zero at walls. In the technical sense, walls were non-porous with no-slip condition which makes the air stagnant in the wall vicinity. The log-law was implemented in the viscous sublayer as well as the buffer layer [70]. Also, walls were assumed to be stationary and adiabatic (i.e. no energy transfers through walls).

3.3.4.2 Supply Diffuser Modeling

Simulating supply diffusers is one of the most troublesome parts of creating CFD models. A typical diffuser is considerably smaller compared to the size of the room and has high flow velocities [73]. In addition, several types of diffusers (e.g. grille, square, displacement, vortex, etc.) exist in the market creating various flow conditions at the inlet. Thus, many researchers have defined modeling the inlet airflow a major limiting factor in using CFD techniques in indoor spaces [75–79]. It should be noted that the inflow through most of diffuser types is not completely identical to the classical fully developed free or attached

jet flow problems. Therefore, in its most general sense, the approaches to model diffusers are threefold:

1. Momentum modeling at the air supply devices [80]

   This method is called the momentum method and it decouples mass and momentum boundary conditions. The diffuser is represented in the CFD model with the same gross area, mass inflow, and momentum flux as the real diffuser. To apply the momentum method to a CFD model the following information is needed.

   - Airflow rate
   - Effective diffuser area
   - Supply air turbulence properties
   - Supply air temperature and contaminant level

2. Momentum modeling in front of the air supply devices [81]

   Several models have been suggested over a course of time using this approach including the box model [82,83], the prescribed velocity model [82], the diffuser specifications model [84] and the tiny box model [85]. The box model for instance, draws an imaginary box in front of the diffuser. The flow field inside the box is ignored, calculated of observed magnitudes of velocity is prescribed on the opposite side, and the surrounding faces are zero pressure inlet boundaries (Figure 3-13). Below are the required field information for the box method [85,86]:

   - The distribution of air velocities
   - The turbulence properties

- The distribution of temperature and contaminant concentrations

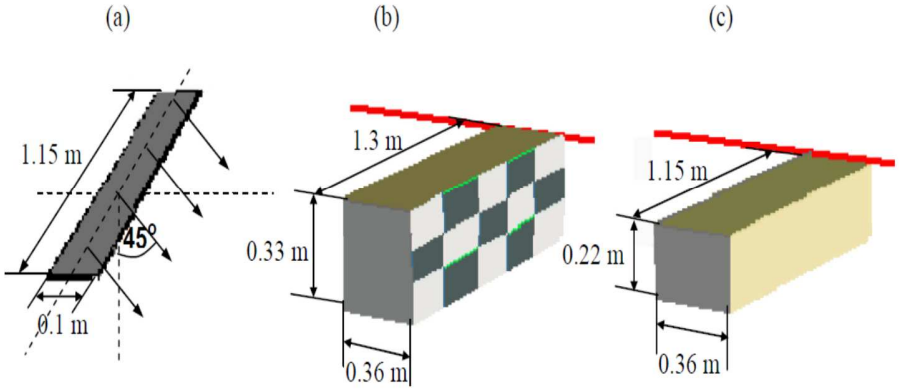

Figure 3-13.Simulation of the slot diffuser with (a) the momentum method (b) the box method, and (c) the tiny box method [85]

3. Modeling the airflow in the duct prior to the diffuser and retain all flow details at the diffuser.

   It should be noted that while the first two methods use simplifying assumptions to reduce the computations, this approach tends to keep the details. Hence, it is usually unaffordable for CFD modeling unless it is used to study the behavior of the diffuser.

For this study the momentum method was used since it was reported to work well for grille diffusers [85] .Air was modeled to entrain vertically. Airflow rates and the diffuser size were adopted from the experiments (Table 3-5). Supply air contaminant level was zero since it was 100% outdoor air and the temperature was set to 15.8 °C. Joubert et al. 1996 [87] found that turbulent intensity at the boundary does not influence the calculations. Lau et al. [88], on the other hand measured turbulence intensity for swirl supply diffusers. Azad et al. [89] reported 3% of turbulence intensity for conical grille diffusers which was

adopted for this study. Particles were reflected back into the space when reaching to the supply diffusers.

Figure 3-14 Supply Diffuser in Corridor-1

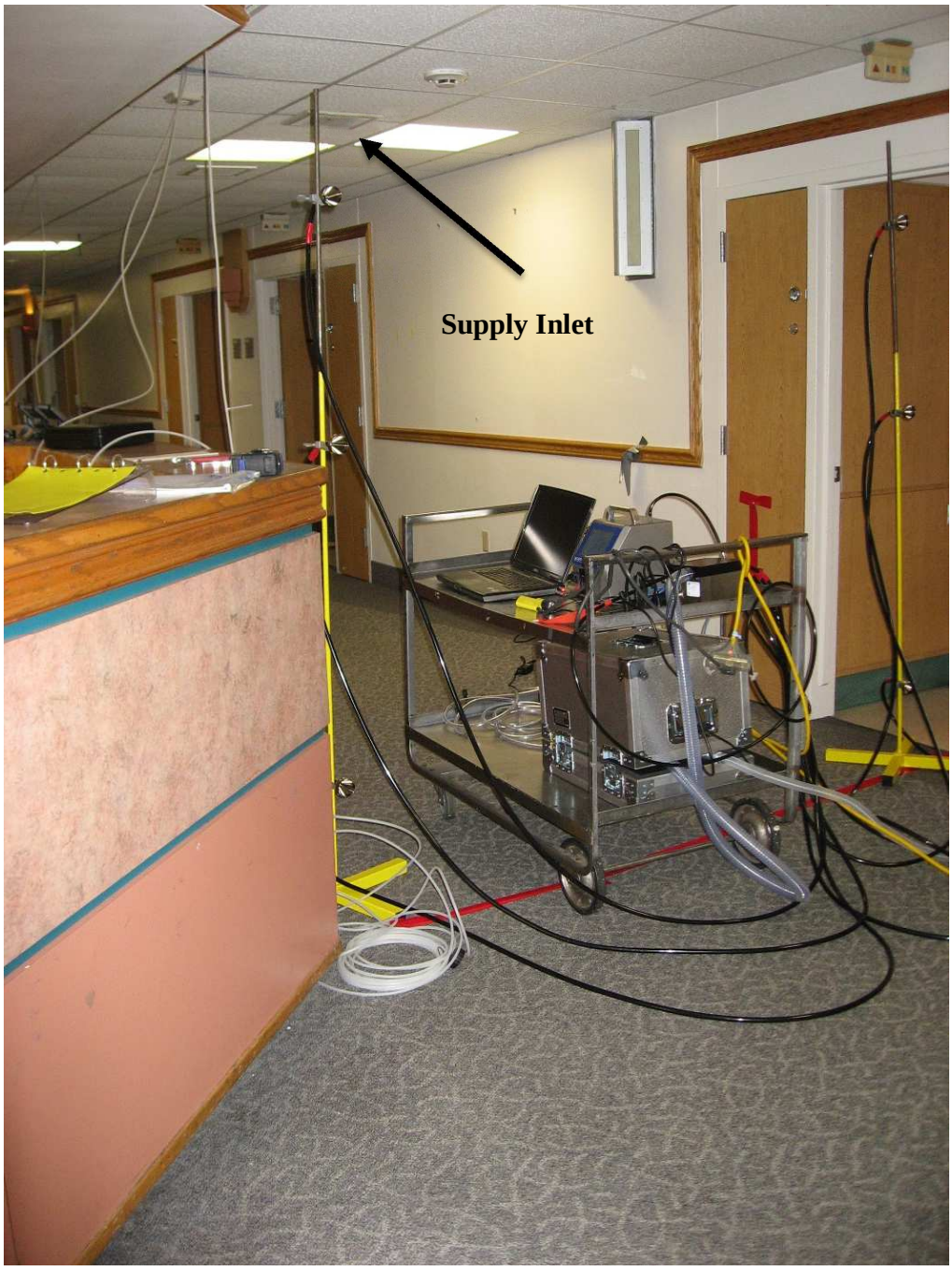

Figure 3-15 Supply Diffuser in Corridors-2

3.3.4.3 Exhaust Fans

Air was removed from the space and through the exhaust fan boundary condition by the same mass flow rate measured in the experiments (Table 3-5). The backflow temperature was set to the thermostat temperature (24°C) and particles were presumed to escape from the exhaust fans (removal).

3.3.4.4 Pressure Inlet

The 'make-up' air in the negative mode was designed to entrain from the section at the end of the hallway, behind the nursing station. Therefore, it was defined as a pressure inlet boundary condition whose flow information was calculated using the adjacent cells' information. The pressure was set to zero at this boundary to allow the free movement of air both inward and outward. Again, particles were presumed to escape from this boundary.

Table 3-5 Boundary Conditions of General Patient Ward Corridors, Neutral vs. Negative Modes

Boundary Name	Boundary Type	Size (m x m)	Flow rate (m^3/sec)	
			Negative	Neutral
Fan 1	Exhaust Fan	0.2 × 0.2	0.098	0.098
Fan 2	Exhaust Fan	0.2 × 0.2	0.098	0.098
Fan 3	Exhaust Fan	0.2 × 0.2	0.098	0.098
Fan 4	Exhaust Fan	0.2 × 0.2	0.098	0.098
Fan 5	Exhaust Fan	0.2 × 0.2	0.098	0.098
Fan 6	Exhaust Fan	0.2 × 0.2	0.098	0.098
Diffuser 1~4	Supply Diffuser	0.3 × 0.3	0.030	0.059
Diffuser 5	Supply Diffuser	0.6 × 0.6	0.060	0.119
Diffuser 6~9	Supply Diffuser	0.3 × 0.3	0.030	0.059
Pressure Inlet	Pressure Inlet	10.0 ×2.8	-0.291	0.007

3.3.5 Particle Tracking

Given the experimental outcomes, the maximum particle concentration was of the order of 10^4 per liter, while air contains approximately 10^{23} particles per liter. This suggested that the continuum condition was not met for the particle phase; it is rather a discrete phase. Thus, the Lagrangian-Eulerian method was selected to model the particle motion within the corridors (Eq.15). In addition to the drag force and gravity, the Brownian force, Saffman's lift force, virtual mass force, pressure gradient force were also considered. However, Zhao et al. [90] show that the last two forces' effect is proportional to the ratio of particle density to air density ($\approx 10^{-3}$). The Runge-Kutta method used to numerically solve Eq.15 with a maximum of 15,000 number of steps per iteration. Entrance doors were opaque, therefore particles were released linearly from the seams around the doors. The Cunningham slip correction factor was applied since the relative velocity may not be zero at the surface of small particles. The Discrete Random Walk (DRW) model with 500 number of tries was employed as the stochastic tracking scheme [65,91]. Hathway et al. [92] depict that using the DRW model will also improve the accuracy of deposition in the model. Particle generation rate was also adopted from the experiments (1.0g/min at 0.4L/s airflow rate). Particles were presumed to 'trap' when colliding with solid surfaces (deposition). This assumption was extensively used in the literature [52,55,65,67,92,93].

3.4 Model Validation

Computational results for the negative and neutral modes were validated using the experimental outcomes. To make a meaningful comparison, both data clusters were

casted into a dimensionless, unique form using the notion of probability of transport. The probability of transport was defined as the probability of a particle reaches a certain distance from the release point. It takes the following mathematical form:

$$P_T(x) = 1 - \frac{\int_0^x C_p d_x}{\int_0^\infty C_p d_x} \quad \textbf{21}$$

Where the probability of transport (P_T) is a function of distance from the release point (x) given the concentration distribution (C_p) throughout the domain. P_T was calculated for both the experimental and computational results under the negative and neutral modes for all particle sizes (Figure 3-16). To ensure that the stochastic motion of particles had no impact on the validity of the model, each model was run five times. Admittedly, computational results were slightly different each time.

Next, a proper statistical model was needed to evaluate the accuracy of CFD models. Two different approaches were used to address the similarity of the test and CFD results. The Pearson correlation coefficient (Figure 3-16) as well as the paired t-test (Table 3-6) was computed for all comparison cases. Although, the use of t-test entails normality of data, some suggest that violating this rule would not detrimentally affect the outcomes [94]. Since the data had to be tested point by point, the paired t-test was selected. Pearson correlation, on the other hand, tests if there is a statistically significant correlation between the data sets. For all the statistical analyses the confidence interval was 95% and the corresponding p-values were calculated. If the p-value was more than 5%, the null hypothesis was accepted and it was rejected otherwise.

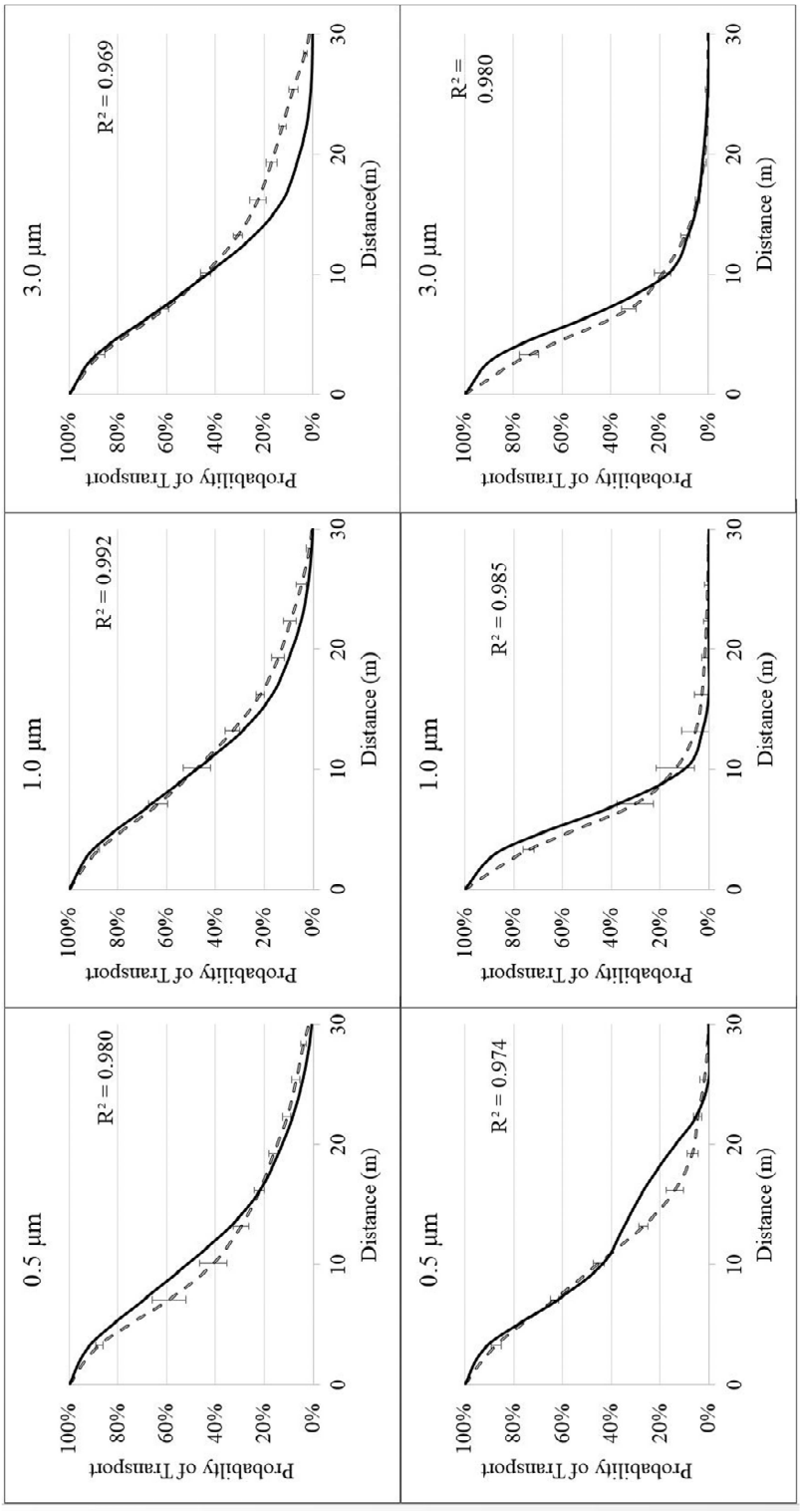

Figure 3-16 Computation validation with Experimental Results

Table 3-6 Statistical Analysis of Model Validation

Paired T-test			Data Linearization Results					
flow mode	particle size	p-value	exp. slope lower limit	model slope	exp. slope upper limit	exp. intercept lower limit	model intercept	exp. intercept upper limit
Negative	0.5µm	0.252	-8.069	-7.799	-5.37	1.49	2.038	6.923
	1.0µm	0.103	-6.686	-6.19	-4.378	1.642	3.931	7.21
	3.0µm	0.02	-5.021	-8.425	-2.864	1.928	2.741	8.785
Neutral	0.5µm	0.127	-10.06	-6.503	-5.177	-0.148	2.938	6.711
	1.0µm	0.781	-5.018	-4.697	-1.519	-1.4	1.29	5.549
	3.0µm	0.203	-1.107	-0.518	-0.023	4.813	11.155	17.656

To assure that non-normality of the data would not change the analysis outcomes and to prevent the β-type error (i.e. rejecting the null hypothesis while it is true), another statistical method was also adopted. In this case, the experimental data was linearized by taking the natural logarithm of the dependent variable and a linear function was fitted to it. The slope and intercept of the line was calculated with 95% confidence level. Similar process was undertaken to the CFD results. Similarity of the data clusters was accepted if the CFD linear fit fell into the range of experimental results.

A similarity analysis was rendered for three particle sizes (0.5µm, 1.0µm, and 3.0µm) and two flow modes (negative and neutral) and the results suggested that the CFD models were able to satisfactorily anticipate the experiments. Although, for the negative mode and 3.0µm particle size, slope of the line did not fall into the experimental range suggesting that the model failed to simulate the actual test. Otherwise, the results were

satisfactory and the model was deemed to be valid and can be used for modeling other plausible scenarios.

3.5 Computational Scenarios

The primary aim of this study was to observe the effect of flow direction and ventilation rates on particle transmission within the general patient ward corridors. Thus, a series of new CFD models were developed to specifically address the research question for 1.0µm particle size. The notion of directional flow was first raised and studied both experimentally and computationally. Next, the model was reconstructed by rearranging the outlet placements to determine if it mitigated particle transmission within the space. Finally, various ventilation rates were introduced to study particle transmission relative to ventilation rate.

3.5.1 Ventilation Arrangement (Existing versus Modified Configurations)

The existing ventilation arrangement in the general patient ward (Figure 3-4) had one exhaust fan close to the entrance door (Fan 1) and two exhaust fans in the vicinity of the nursing station (Fans 2 and 3). This arrangement seemed to have two major flaws. First, placing an exhaust fan near the entrance door could *potentially* create unfavorable pressure difference with the elevator lobby. Second, the other two exhaust fans down the hallway are fairly close to each other, where depending on the particle source, it could cause lower removal efficiency. For those reasons, a modified arrangement (Figure 3-17) was proposed to improve the ventilation performance. The new arrangement was perceived to create a pathway between inlets and outlets with minimum perturbation.

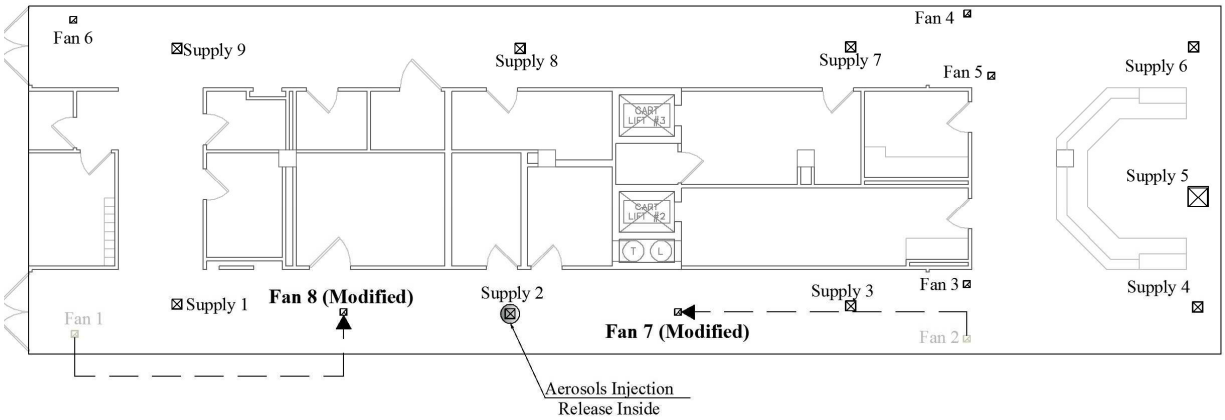

Figure 3-17 Modified Ventilation Arrangement in General Patient Ward Corridors

3.5.2 Directional versus Non-Directional Flow

In general, flow direction can be determined by two parameters: pressure relationship to adjacent spaces, and arrangement of inlets/outlets. Thus, the neutral mode, embodying the non-directional case, was contrasted to the negative (i.e. directional) mode. Both experimental and computational data were available to compare directional versus non-directional flows for the existing ventilation arrangement. For the modified ventilation arrangement and in the absence of experimental results, CFD models were designed to compare the negative versus the neutral mode. Ventilation rates and boundary conditions remained the same as before (Table 3-5) while the ventilation arrangement was amended.

3.5.3 Ventilation Rates

CFD models were constructed for four different ventilation rates (Table 3-7). The rationale for choosing these ventilation rates was to investigate the current (2 ACH) and former (4 ACH) ASHRAE Standard 170 recommendations. One value between the two recommended rates and one value beyond them was also selected. Moreover, to assure

the rigor of the methodology, particles were released inside and outside the corridor space. The outside release took place in accordance with the experimental setting. Whereas, the inside release was located at 14m away from the entrance door, underneath the supply diffuser (Supply 2). This point was selected since it was least affected by the new placement of exhaust fans. In fact, Supply 2 is remains intact when changes are in place from the existing to modified arrangements. The release point was in the middle of the hallways and 0.8m above the floor (Figure 3-17). Figure 3-18 shows overall flow of the methodology as well as the interchange and interconnection between the experimental and computational methods.

Table 3-7 Boundary Conditions for New CFD Models for Various Ventilation Rates

Boundary Name	Size (m x m)	Flow rates (m^3/s) at boundaries			
		2.0 ACH	3.0 ACH	4.0 ACH	5.0 ACH
Fan 1 (Fan 8)	0.2 × 0.2	0.051	0.098	0.145	0.126
Fan 2 (Fan 7)	0.2 × 0.2	0.051	0.098	0.145	0.126
Fan 3	0.2 × 0.2	0.051	0.098	0.145	0.126
Fan 4	0.2 × 0.2	0.051	0.098	0.145	0.126
Fan 5	0.2 × 0.2	0.051	0.098	0.145	0.126
Fan 6	0.2 × 0.2	0.051	0.098	0.145	0.126
Supply 1~4	0.3 × 0.3	0.038	0.059	0.094	0.083
Supply 5	0.6 × 0.6	0.076	0.119	0.189	0.165
Supply 6&9	0.3 × 0.3	0.038	0.059	0.094	0.083

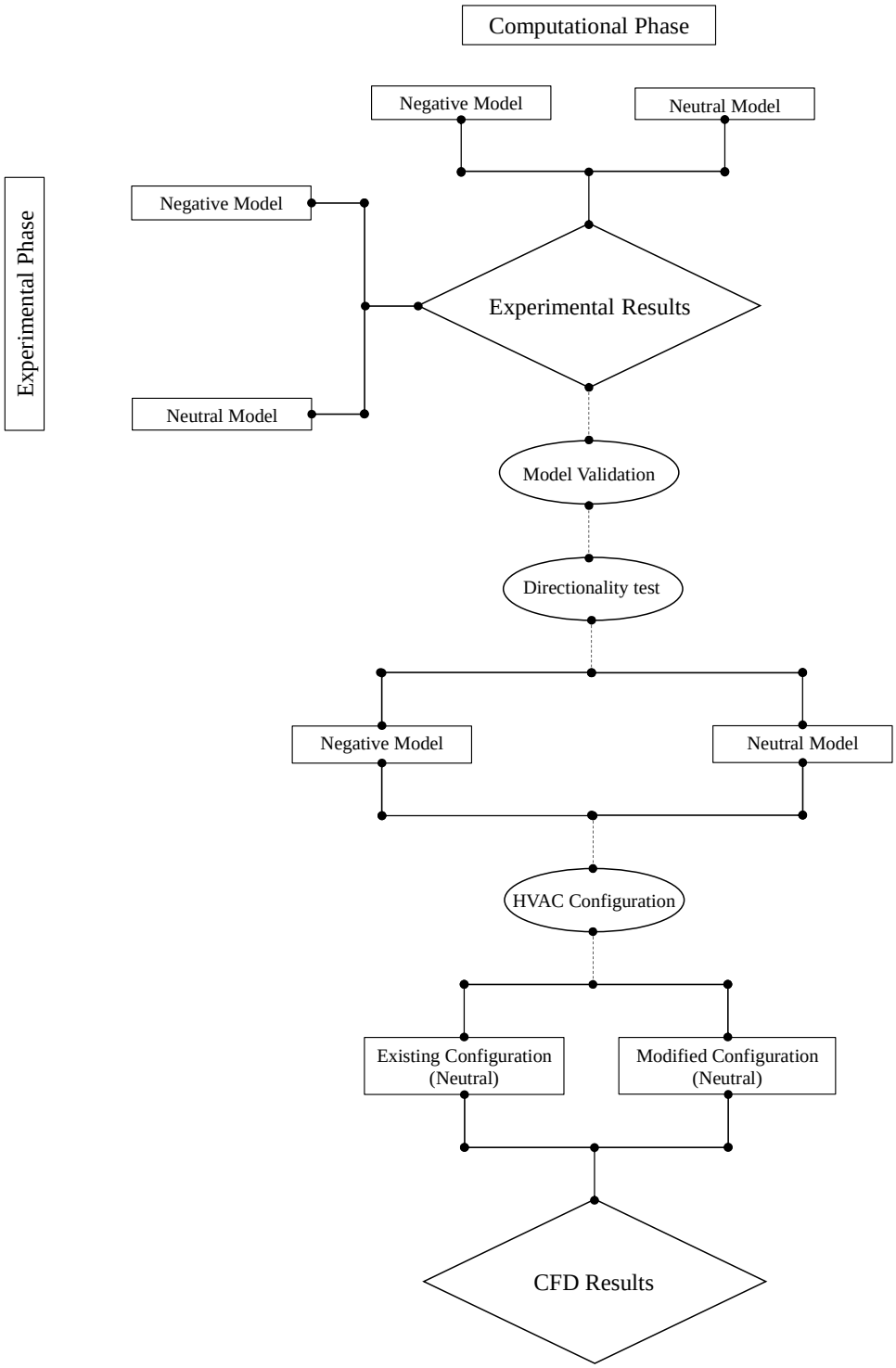

Figure 3-18 Research Methodology; Interchange and Interconnection between Experimental and Computational Method

CHAPTER 4: QUASI-EXPERIMENTAL RESULTS

4.1 Flow Direction

Particle concentrations for all size groups increased significantly when the aerosol injection was started (Figure 4-2). Particle concentrations then began to decrease with respect to time and distance from the aerosol release point. Differences, however, were observed with respect to particle size and airflow alignment (Table 4-1 and Figure 4-3).

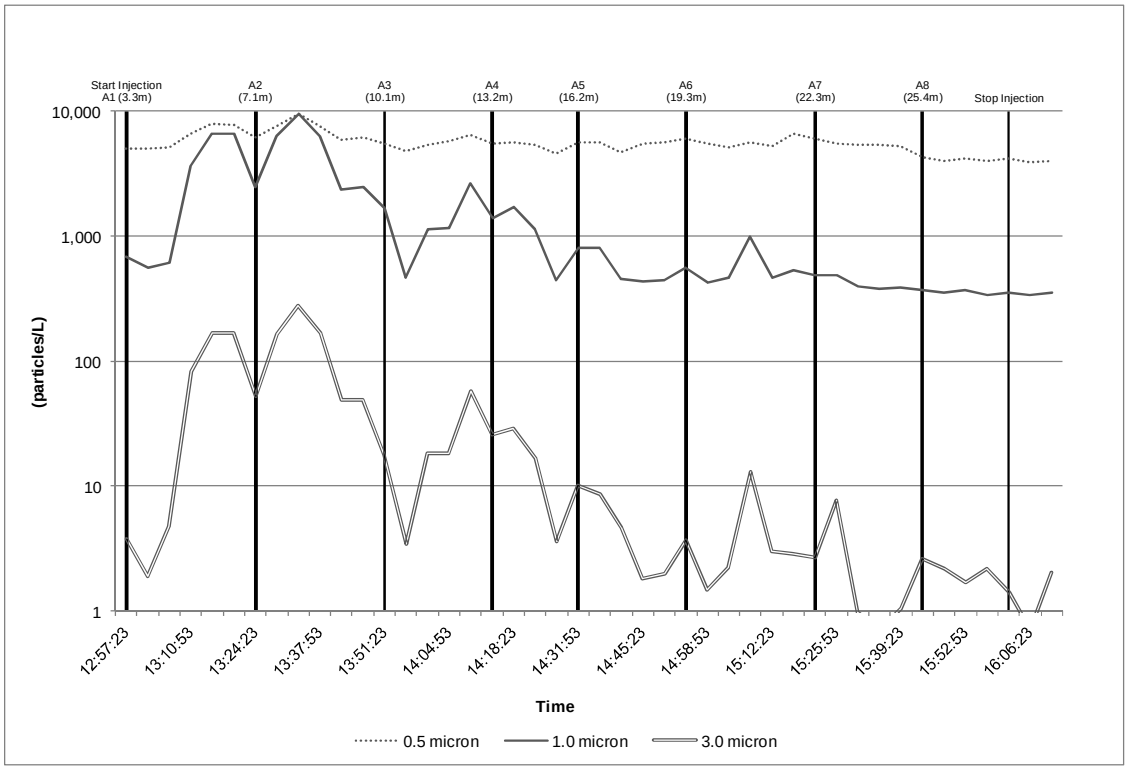

Figure 4-1 Aerosol Concentrations Relative to Particle Size (0.5µm-3.0µm), Time and Distance Under *Neutral* Ventilation Model for 'A' Series Sampling Locations (1.2m)

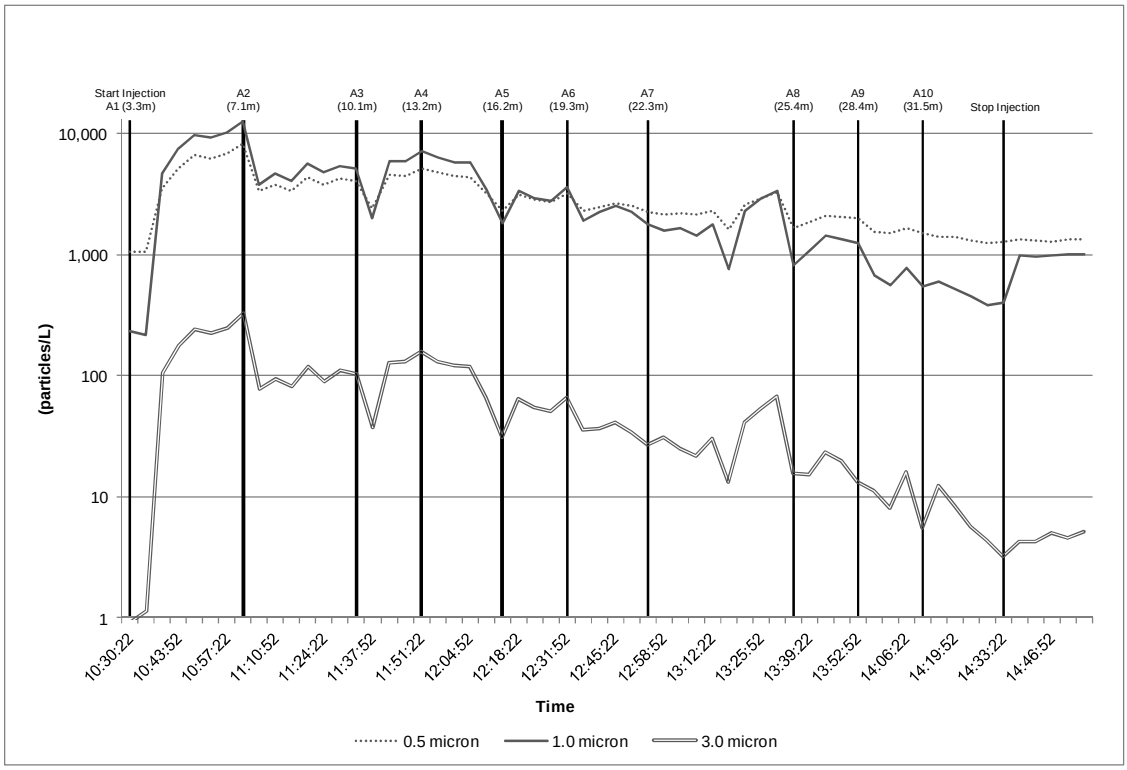

Figure 4-2 Aerosol Concentrations Relative to Particle Size (0.5µm-3.0µm), Time and Distance Under *Negative* Ventilation Mode for 'A' Series Sampling Locations (1.2m).

Table 4-1 Average Change in Particle Concentration Relative to Distance from Release

		Neutral Mode			Negative Mode		
Particle Size	Sample Height	Sample Series A	Sample Series B	Sample Series C	Sample Series A	Sample Series B	Sample Series C
0.5µm	0.6m	-6.9%	-4.3%	-	-8.2%	-7.6%	-
	1.2m	-6.1%	-4.9%	2.4%	-7.7%	-7.8%	-6.8%
	1.8m	-5.8%	-3.0%	-	-7.7%	-7.8%	-
1.0µm	0.6m	-15.6%	-14.1	-	-10.4%	-10.1%	-
	1.2m	-22.0%	-25.5	-25.6	-9.2%	-10.2%	-9.7%
	1.8m	-22.3%	-25.5	-	-9.1%	-10.1%	-
3.0µm	0.6m	-24.5%	-23.3	-	-11.9%	-11.6%	-
	1.2m	-19.3%	-24.2	-38.1%	-9.5%	-10.4%	-9.7%
	1.8m	-24.4%	-24.0	-	-9.4%	-10.3%	-

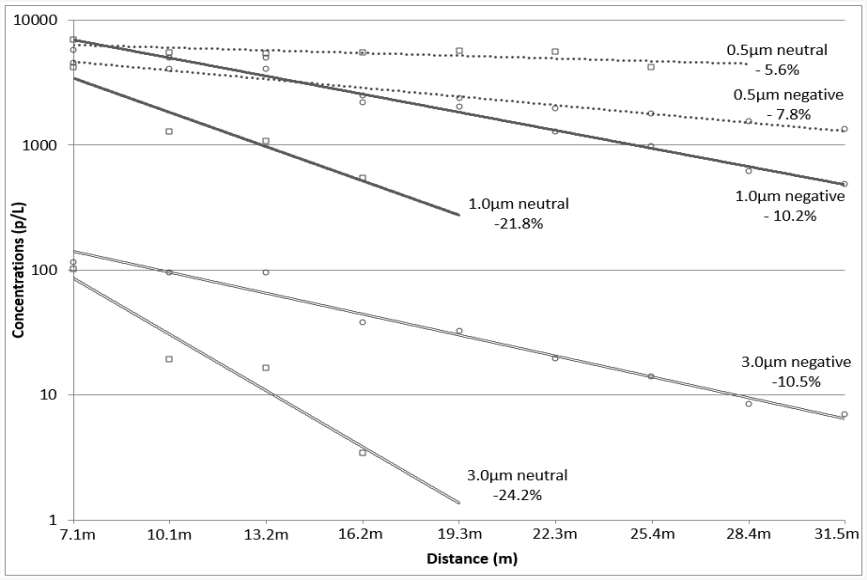

Figure 4-3 Aerosol Concentration Relative to Particle Size, Distance and Ventilation Mode

After peaking, concentrations of 0.5µm particles declined, on average, 5.6% every 3.0m ($R^2 = 0.57$) under the neutral airflow mode yet remained above background levels to distances of 22.3-25.4m. Under the negative airflow mode, concentrations of 0.5µm particles declined, on average, 7.8% every 3.0m ($R^2 = 0.96$) yet remained above background levels to distances exceeding 31.5m. No significant differences were observed with respect to sampling series or height for 0.5µm particles. Concentrations of 0.5µm particles under the neutral airflow mode, however, were approximately twice the concentration of 0.5µm particles observed under the negative airflow mode for each sampling series and height. In contrast, concentrations of 1.0µm and 3.0µm particles declined, on average, 21.8% and 24.2% every 3.0m ($R^2 = 0.91$ and 0.92, respectively) under the neutral airflow mode, and remained above background levels to distances of only 10.1-13.2m. Under the negative airflow mode, concentrations of 1.0µm and 3.0µm particles declined, on average, 10.2% and 10.5% every 3.0m ($R^2 = 0.98$ and 0.97,

respectively) and remained above background levels to distances of 28.4-31.5m. Concentrations of 1.0µm and 3.0µm particles were greater for 'A' series sampling locations when compared to 'B' series sampling locations for all sampling heights and airflow alignments, suggesting the possible influence of patient room ventilation, particularly in the negative mode. No significant differences were observed with respect to height for 1.0µm and 3.0µm particles. Concentrations of 1.0µm and 3.0µm particles under the neutral airflow mode, however, were on average, 50% less than concentrations of 1.0µm and 3.0µm particles observed under the negative airflow mode for each sampling series and height.

4.2 Particle Size

Data suggest that aerosols in the particle size range of 0.5µm exhibit somewhat different aerodynamic behaviors when compared to 1.0µm and 3.0µm particles subject to the same environmental conditions. Specifically, changes in aerosol concentrations among 0.5µm particles appeared significantly less influenced by airflow alignment. By comparison, changes in concentrations among 1.0µm and 3.0µm particles were three-to-four times higher in the neutral airflow mode when compared to changes among 0.5µm particles, indicating a greater potential for deposition (or removal). Under the negative airflow alignment, however, decay rates among 1.0µm and 3.0µm particles were reduced by half, indicating a greater potential for suspension and transport. In fact, under the negative airflow mode, concentrations of 1.0µm and 3.0µm particles remained above background levels roughly twice the distance, on average, than particles under the neutral airflow mode.

4.3 Probability of Transport

The probability of contamination, or, the chance that a particle could travel from the aerosol release point to a given distance in the main corridor, was calculated (Eq. 21) for each particle size and ventilation mode (Table 4-2).

Table 4-2 Probability of Contamination.

	Neutral Mode			Negative Mode		
Distance	0.5µm	1.0µm	3.0µm	0.5µm	1.0µm	3.0µm
3.3m	74.9%	56.1%	47.8%	76.7%	73.0%	65.1%
7.1m	50.9%	25.2%	18.4%	55.0%	49.1%	38.7%
10.1m	35.4%	11.1%	7.5%	41.3%	34.8%	25.0%
13.2m	22.5%	3.2%	2.1%	29.7%	23.4%	15.3%
16.2m	12.9%	-	-	20.8%	15.1%	9.1%
19.3m	5.8%	-	-	13.6%	8.8%	4.8%
22.3m	1.7%	-	-	8.3%	4.5%	2.3%
25.4m	-	-	-	4.4%	1.8%	0.8%
28.4m	-	-	-	1.9%	0.4%	-
31.5m	-	-	-	0.4%	-	-

For example, the average concentration of 1.0µm particles in the main corridor at a distance of 7.1m from the aerosol release point was 4,189 p/L under the neutral ventilation mode as determined by averaging 30 minutes of sample data from six sample points (sample locations A2 and B2 at 0.6m, 1.2m and 1.8m sample heights each). Similarly, the average concentration of 1.0µm particles was calculated over a total distance of 31.5m at ~3.0m intervals from the aerosol release point. An exponential function ($f(x) = \alpha e^{-\beta x}$) was then derived to estimate the average concentration of 1.0µm particles at any distance between the aerosol release point '0' and sample location '10' (31.5m). The area below the distribution function ($\int_0^{10} \alpha e^{-\beta x} dx$) and above the

background concentration was then calculated to represent the total concentration of synthetic (e.g. artificially generated) 1.0µm aerosol present in the main corridor. The ratio of the area under the distribution function at 7.1m ($\int_0^2 \alpha e^{-\beta x} dx$), for example, was determined to be approximately 74.8% of the total area under the distribution function curve, meaning that 25.2% of 1.0µm particles remain to pass through sample location AB2. As a result, the probability of contamination, or, the chance that a 1.0µm particle could travel from the aerosol release point to a distance of 7.1m (23.3ft) in the main corridor was calculated to be 25.2% under the neutral ventilation mode.

As shown (Table 4-2), the probability of contamination for all size groups decreases with respect to distance from the aerosol release point. The rate of decline, however, increases with respect to particle size and ventilation mode as larger particles under neutral (non-directional) airflow were observed to have higher rates of deposition when compared to smaller particles under negative (directional) airflow (Table 4-1). The greatest probability of contamination exists among 0.5µm particles in both neutral and negative ventilation modes. The ventilation mode, however, appears to have significantly less influence on the movement of 0.5µm particles when compared 1.0µm and 3.0µm particles. Specifically, the probability of contamination by 0.5µm particles at a distance of 13.2m from the aerosol release point increases only 30% from neutral to negative ventilation mode. By comparison, the probability of contamination by 1.0µm and 3.0µm particles increases more than seven-times in the negative ventilation mode. As a result, the probability of contamination among 1.0µm and 3.0µm particles becomes comparable to that of 0.5µm particles in the negative ventilation mode.

CHAPTER 5: COMPUTATIONAL MODELING RESULTS

In this section first a brief discussion will be presented as to the flaws of the existing ventilation arrangement and how the modified arrangement can improve the design. Next, the results on directional flow will be presented in conjunction with ASHRAE Standard 170 recommendations. Finally, particle transport phenomena relative to ventilation rate will be studied. It should be noted that computational results were generated only for **1.0μm** particle size, since a transition takes place in particle behavior at about this size [95]. In addition, even though each particle's trajectory is time-dependent, the overall particle concentrations can be safely assumed to be steady-state since the main carrier field (air) is in steady-state condition.

5.1 Preliminary Findings

By solely looking at the mechanical drawings one may suspect that the arrangement of diffusers/fans is not tactfully designed. In fact, placing an exhaust fan close to the entrance door could *potentially* provide a conducive environment for pathogens generated outside the corridor. Especially knowing that the elevator lobby area is a populated place with various types of occupants, one could become more concerned about impeding particles from migrating into the ward corridors and ultimately patient rooms. Moreover, the existing design could significantly reduce the dilution/ removal efficacy of the ventilation system. These issues must be taken into account before particle motion

analysis and modeling within the corridors is commenced. Therefore, supply air streamlines were drawn for the existing ventilation arrangement (Figure 5-1).

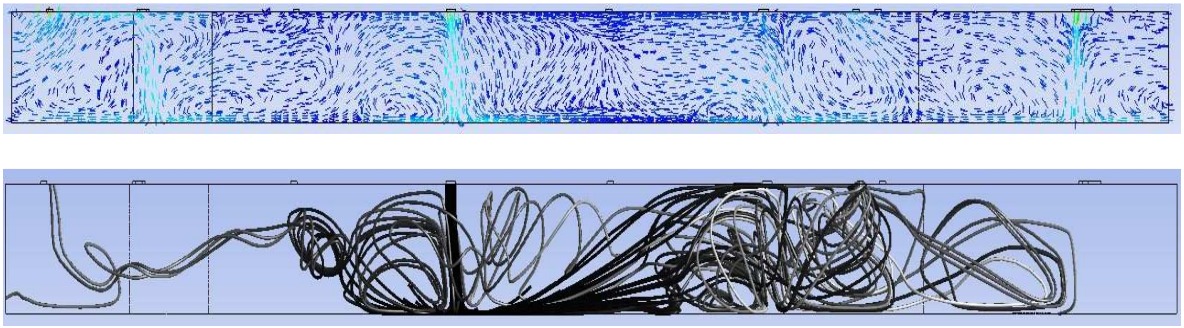

Figure 5-1 Velocity Vectors and Streamlines of the Air Entrained by Supply 2, Existing Arrangement. Nursing Station is on the Right Side

By definition, streamlines are a family of curves that are instantaneously tangent to the velocity vector and show the direction of the flow [70]. Streamlines of air entrained by Supply 2 are really cluttered in the existing arrangement. Once air is entrained, there is no conspicuous pathway it can follow. The modified arrangement could potentially rationalize the air motion (Figure 5-2). The arrangement could create air curtains that contain the entrained air within a certain range before being discharged.

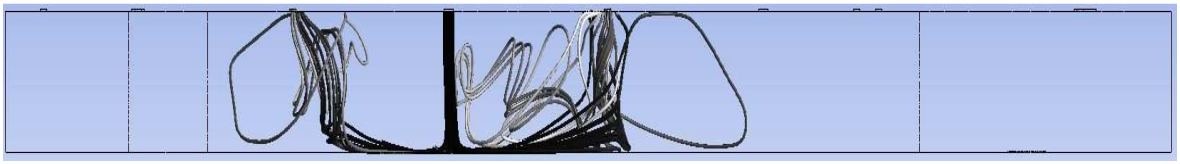

Figure 5-2 Streamlines of the Air Entrained by Supply 2, Modified Arrangement. Nursing Station is on the Right Side

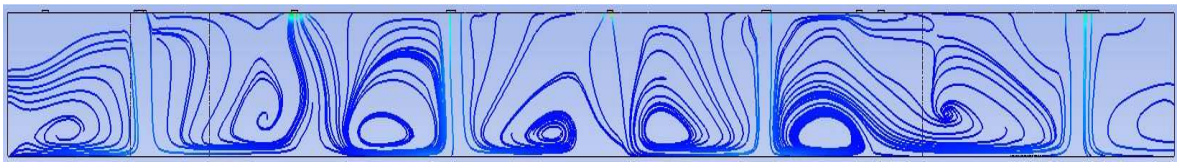

Figure 5-3 Vortices Created by Introducing New Exhaust Fans. Nursing Station is on the Right Side

Mass is not transferred between streamlines. Thus, Figure 5-3 clearly illustrates that the total length of the hallway could be compartmentalized into three blocks where each block starts with a supply diffuser. The idea of placing one exhaust fan between two supply diffusers then is substantiated by knowing that a particle released within one block can hardly migrate to another before being removed.

5.2 Flow Direction

5.2.1 Concentrations

Similar to the experimental results, particle concentrations decreased with distance under both ventilation alignments (Figure 5-4 Figure 5-5). CFD models however, provided the capability of performing a micro analysis of particle behavior. For the existing arrangement, the average particle concentrations was 0.034gr/m^3 and 0.009gr/m^3 under the negative and neutral modes respectively (Table 5-1) suggesting that the directional flow (i.e. negative mode) enhanced particle suspension in the domain. Also, particles were able to travel further under the negative mode (31.5m) compared to the neutral mode (19.3m). These findings were consistent with the experimental observations.

Similar trends were observed when the ventilation arrangement was modified (Table 5-1, Figure 5-5). In fact, despite a better performance by proposing the modified arrangement, particle concentrations were considerably higher under the negative mode (0.034gr/m^3) compared to the neutral mode (0.009gr/m^3). The new arrangement did not seem to effectively reduce the distance traveled by particles under the negative mode (31.5m). to flow direction created by negative pressurization and misplaced exhaust fans.

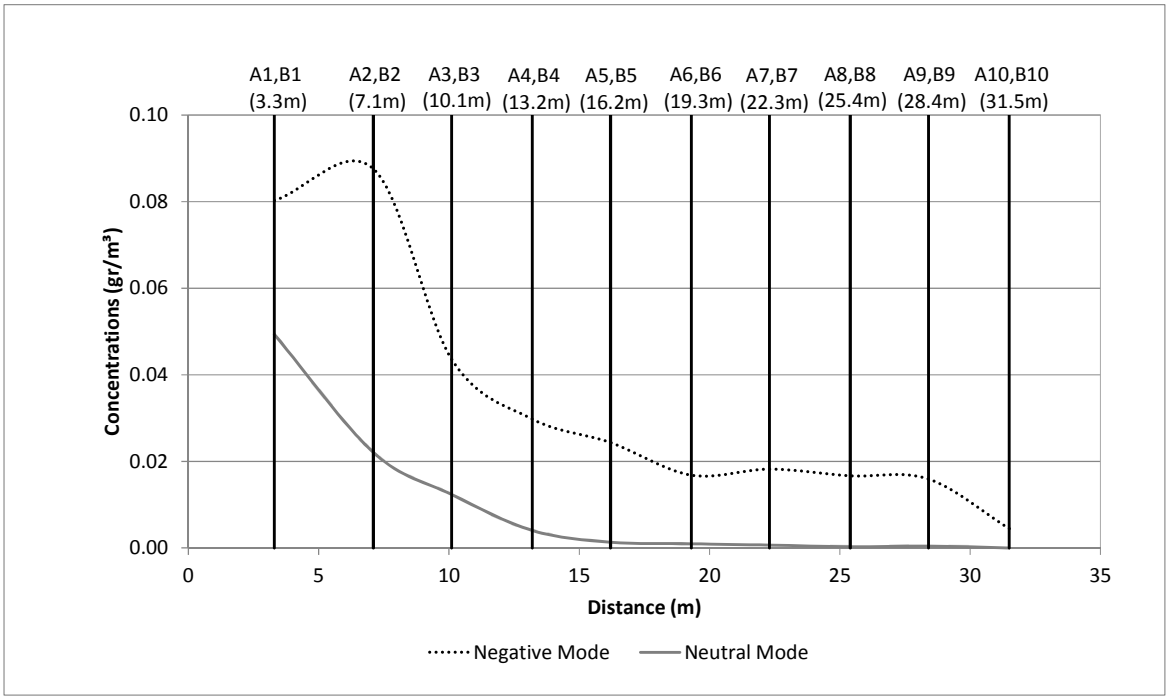

Figure 5-4 Average Particle Concentrations Relative to Distance, *Existing* Ventilation Arrangement Release *Outside (x=0m)*

Table 5-1 Particle Concentrations Relative to Distance; Negative vs. Neutral Modes, Existing vs. Modified Arrangements, Release *Outside (x=0m)*

Sampling Location	Distance (m)	Existing Arrangement		Modified Arrangement	
		Negative Mode	Neutral Mode	Negative Mode	Neutral Mode
Sample Location 1	3.3	0.080	0.049	0.075	0.056
Sample Location 2	7.1	0.088	0.022	0.070	0.007
Sample Location 3	10.1	0.044	0.012	0.036	0.013
Sample Location 4	13.2	0.030	0.004	0.031	0.001
Sample Location 5	16.2	0.024	0.001	0.011	0.000
Sample Location 6	19.3	0.017	0.001	0.057	0.000
Sample Location 7	22.3	0.018	0.001	0.011	0.000
Sample Location 8	25.4	0.017	0.000	0.007	0.000
Sample Location 9	28.4	0.016	0.000	0.006	0.000
Sample Location 10	31.5	0.004	0.000	0.002	0.000
Average Concentrations		0.034	0.009	0.031	0.008

However, no particles were observed past 13.2m from the release point under the neutral mode when the new arrangement was applied. It should also be noted that particle concentrations exhibited a local peak around the new exhaust fan locations. The fan around which concentrations peaked and amplitude of the peak changed relative to ventilation alignment. Under the neutral mode, particles accumulated near the closer fan (~10.0m) where the peak concentration was 1.85 times larger than the previous sample point. Under the negative mode, particles were prone to migrate farther to the vicinity of Fan 8 (~19.5m). The peak concentration was more than tripled compared to the previous sampling point. The results revealed a propensity for particles to move further and with higher concentrations under the negative mode. As alluded to in the experimental results, this behavior can be ascribed

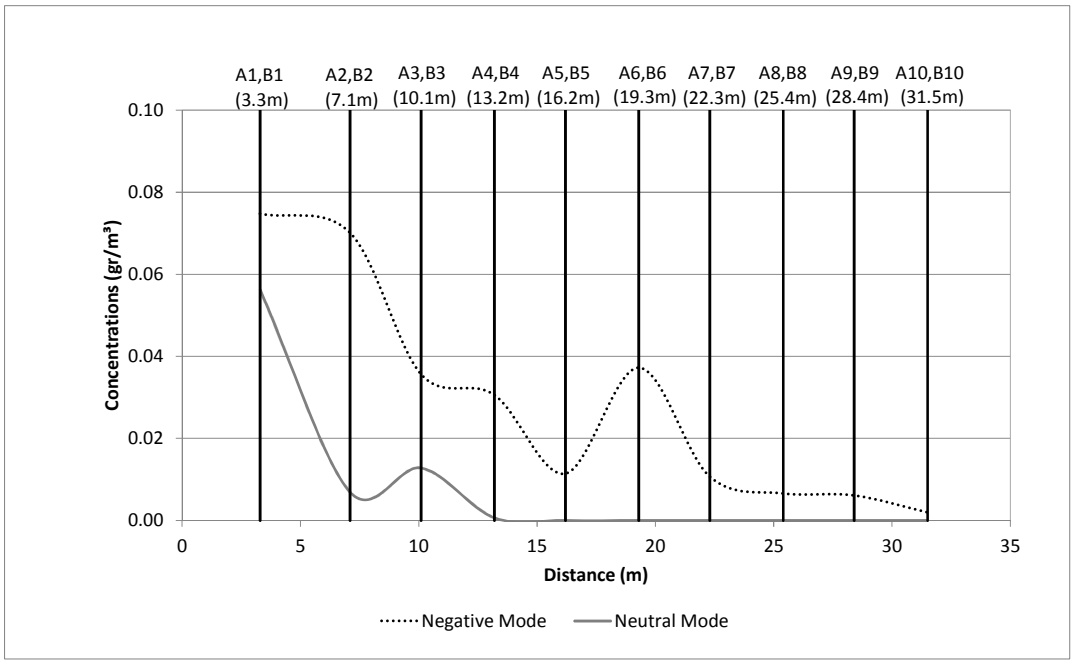

Figure 5-5 Average Particle Concentrations Relative to Distance, *Modified* Ventilation Arrangement Release *Outside (x=0m)*

Moreover, particles were released inside the corridor to examine if a change in the release point could lead to different results. Therefore, particles were released under the supply diffuser (supply 2) and 14m away from the entrance door. As the entry airstream pushed particles to the sides, a local minimum was observed in the vicinity of supply 2. This trend was observed for all ventilation arrangements and alignments. The local maximum however, was dependent on the placement of the exhaust fans. For the existing condition, concentrations peaked near the exhaust fans (3m and 25m) under the negative mode, suggesting a strong directional flow towards the outlets. Concentrations were much lower and peaked closer to the release point (14m) under the neutral mode (Figure 5-6).

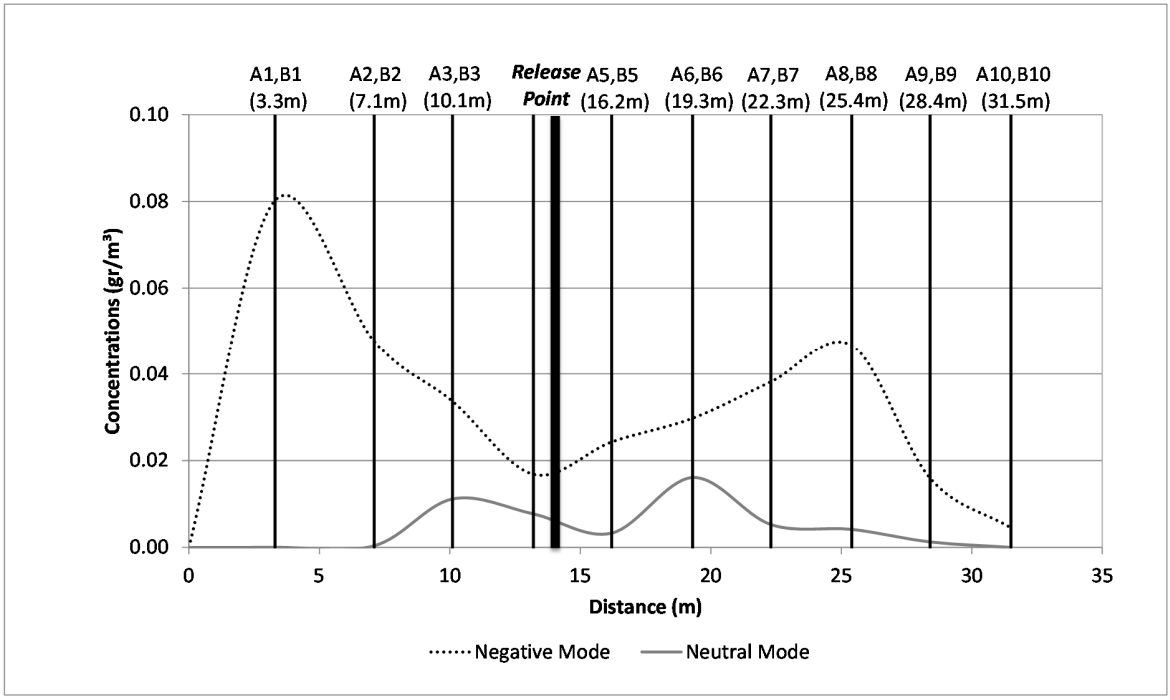

Figure 5-6 Average Particle Concentrations Relative to Distance, Existing Ventilation Arrangement and Release Inside (x=14m)

The average particle concentrations declined nearly one order of magnitude relative to ventilation alignment for both arrangements (Table 5-2). For the existing (modified) arrangement, the average concentration was 0.031gr/m^3 (0.023gr/m3) and 0.004gr/m^3 (0.001gr/m3) under the negative and neutral modes, respectively. In Summary, a similar trend was observed for all cases with different breadth and intensity.

The local maximum concentrations shifted towards the new location of exhaust fans (Fan 7 and 8) by modifying the arrangement (Figure 5-7). Under the negative mode, the maximum concentrations (0.075gr/m^3) were approximately twenty times larger than that of the neutral mode (0.004gr/m^3).

Table 5-2 Particle Concentrations Relative to Distance; Negative vs. Neutral Modes, Existing vs. Modified Arrangements, Release *Inside (x=0m)*

Sampling Location	Distance (m)	Existing Arrangement		Modified Arrangement	
		Negative Mode	Neutral Mode	Negative Mode	Neutral Mode
Sample Location 1	3.3	0.080	0.000	0.031	0.000
Sample Location 2	7.1	0.048	0.000	0.036	0.001
Sample Location 3	10.1	0.034	0.011	0.075	0.004
Sample Location 4	13.2	0.017	0.008	0.020	0.002
Sample Location 5	16.2	0.024	0.003	0.011	0.004
Sample Location 6	19.3	0.030	0.016	0.057	0.004
Sample Location 7	22.3	0.038	0.005	0.011	0.001
Sample Location 8	25.4	0.047	0.004	0.007	0.000
Sample Location 9	28.4	0.016	0.001	0.006	0.000
Sample Location 10	31.5	0.004	0.000	0.002	0.000
Average Concentrations		0.031	0.004	0.023	0.001

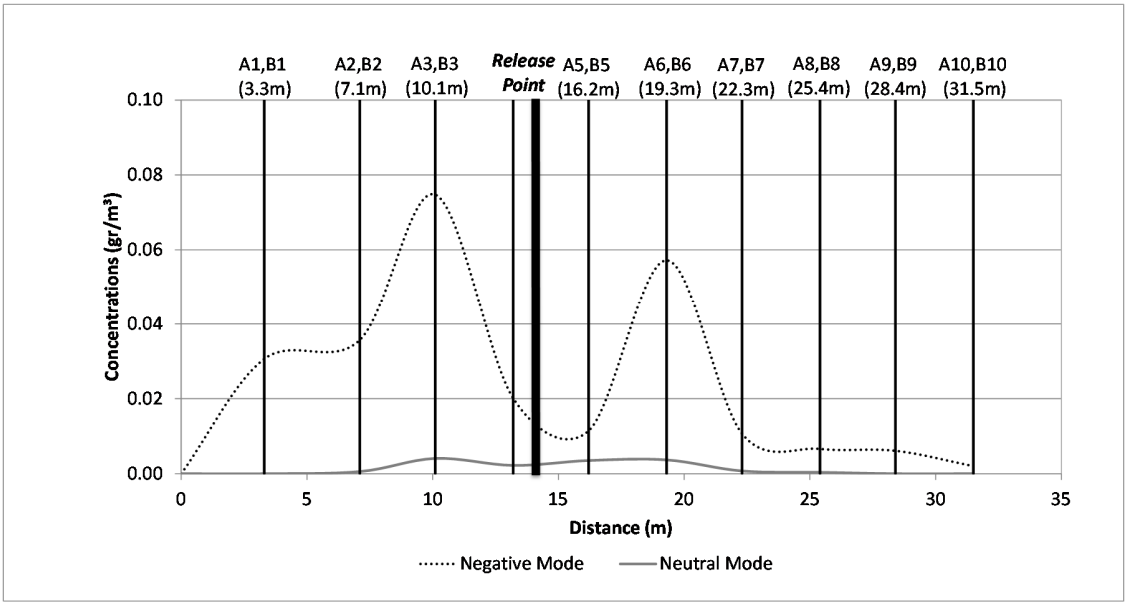

Figure 5-7 Average Aerosol Concentrations Relative to Distance, Modified Ventilation Arrangement and Release Inside (x=14m)

The Results suggested that the best design strategy is the neutral mode with modified ventilation arrangement. Again, modifications brought about a series of vortices from each supply diffuser to the closest exhaust fans. This way, particles are nearly contained within a block consisting of a supply fan and its surrounding exhaust fans. When particles were released inside, modifications in the ventilation arrangement caused a 24% and 69% decline in particle concentrations under the negative and neutral modes respectively. Modifications also seemed effective when particles were released outside. Particle concentrations were reduced by 16.3% and 15.5% under the negative and neutral modes respectively. The improvements were less significant when particles were released outside mainly because the idea of compartmentalization of the corridor was designed to contain particles generated by an internal source. Thus, an outside source is less affected by the change scenario in the ventilation arrangement. Particles were able to move farther

away from the release point with higher concentrations under the negative mode when released inside. In conclusion, regardless of the release point, particle concentrations were highest under the negative mode and for the existing ventilation arrangement (Table 5-3). Reducing particle concentrations is necessary for a decent design but not sufficient. Thus, particle distributions were also studied for all cases.

Table 5-3 Average Particle Concentrations Relative to Ventilation Alignment; Negative versus Neutral

Ventilation Arrangement	Release Point	Negative (gr/m^3)	Neutral (gr/m^3)	Change (%)
Existing Arrangement	Outside	0.034	0.009	-73.5%
	Inside	0.031	0.004	-87.1%
Modified Arrangement	Outside	0.031	0.008	-74.2%
	Inside	0.023	0.001	-95.7%

5.2.2 Distributions

For each case, the statistical distribution of particles is of interest. In fact, apart from the average particle concentrations, how particles are distributed is also important. Thus, statistical analyses on the vertical and lateral (along the hallway) particle distributions, maximum residence time, and total distance traveled by particles were performed for all cases. The maximum residence time is the duration each particle is suspended within the space before its final fate. Moreover, the distance particles can travel during suspension (between zero and maximum residence time) is referred to as the distance traveled by particles.

5.2.2.1 Case 1: Existing Arrangement, Release Outside *(x=0m)*

Under the negative mode, particles migrated to the nursing station (32m) through the main and opposite hallways when released outside (Figure 5-8). A histogram was used to depict the vertical distribution of particles in 0.2m increments (Figure 5-9). The upward directional flow caused by ceiling exhaust fans culminated in higher particle heights. More than one-third of all particles were observed within the breathing zone (0.8m to 1.8m) and the average particle height was 1.65m which is the mode height of a women in the United States [96]. The results were consistent with the experimental findings.

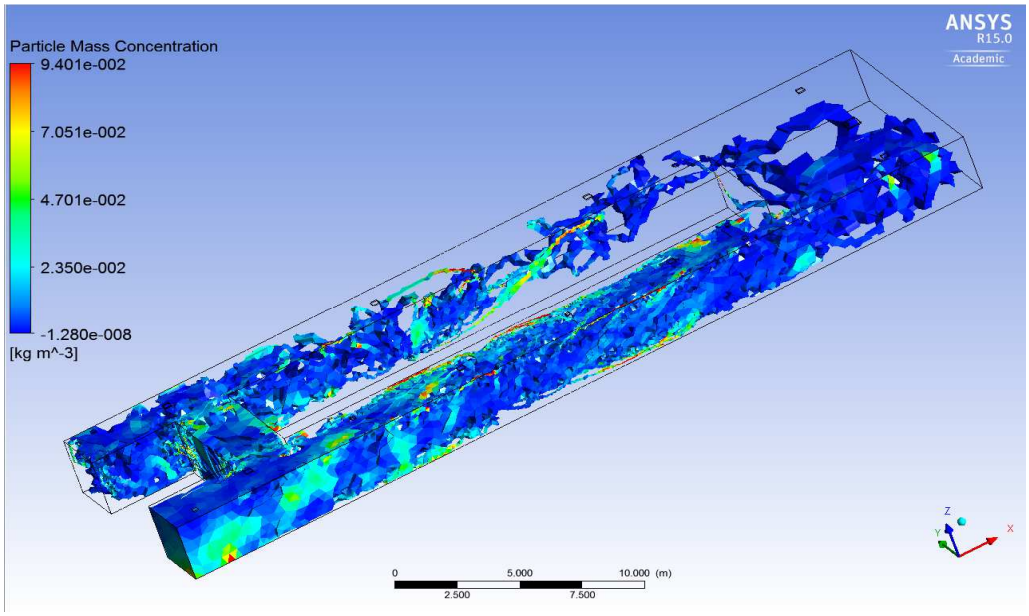

Figure 5-8 Particle Distribution, Negative Mode, Case 1

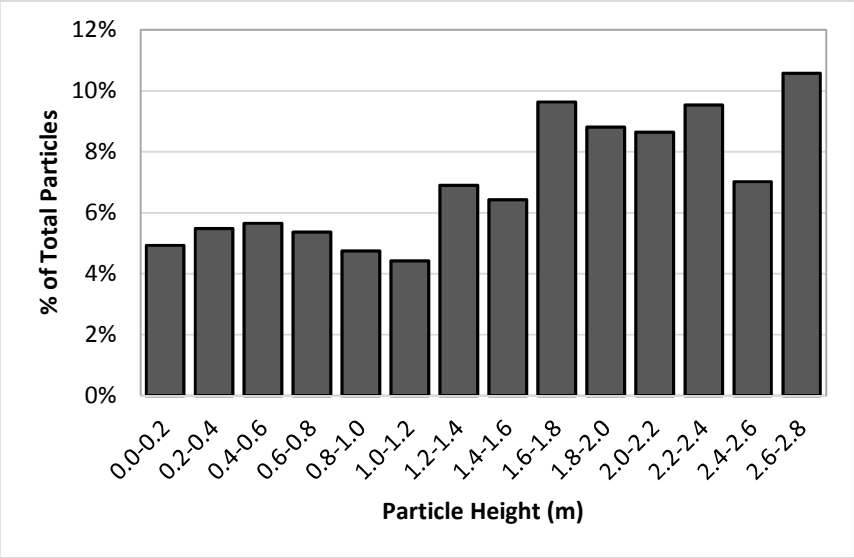

Figure 5-9 Vertical Distribution of Particles under *Negative* Mode, *Case 1*

Particles were dispersed within the corridors almost ubiquitously under the negative mode. Particle average distance from the source was 5.55m (σ=7.41). The standard deviation is higher for flawed distributions since it represents a higher probability of particles to travel farther from the source. Higher mean values also exhibit how much particles are prone to distance away from the source. Dispersion ratio or the range in which 90% of particles existed divided by the length of the hallway (37.0m) was also calculated. The dispersion ratio is a number between zero and unity where a smaller ratio shows better containment. This ratio was 0.54 under the negative mode, for existing condition when particles were released outside (Figure 5-10).

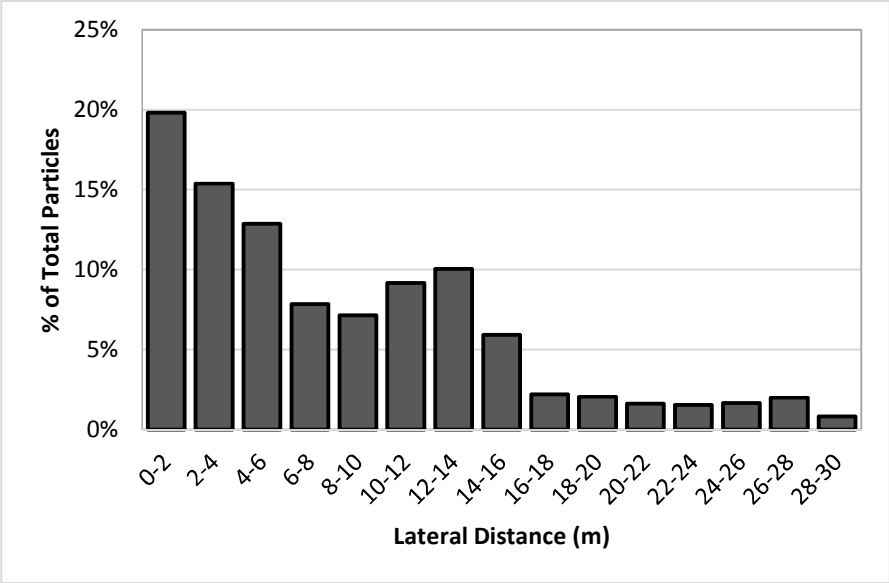

Figure 5-10 Lateral Distribution of Particles under Negative Mode, Case 1

More than one-third (34%) of particles were removed from the space by the ventilation system. Half of the particles were removed by Fan1 whereas Fans 2 and 3 were responsible for 35% of the removal (Table 5-4).

Table 5-4 Removal By Ventilation System Relative to Exhaust Fan Placement; *Negative* Mode, *Case 1*

Exhaust Fan	Fan1	Fan2	Fan3	Fan4	Fan5	Fan6
Rate of Removal	50%	15%	20%	1%	1%	14%

Particles were suspended within the space for 7.0 minutes on average (σ=12.9) before they were eliminated from the domain (Figure 5-11). Also, the average distance traveled by a particle was 22.0m (σ=23.6) (Figure 5-12).

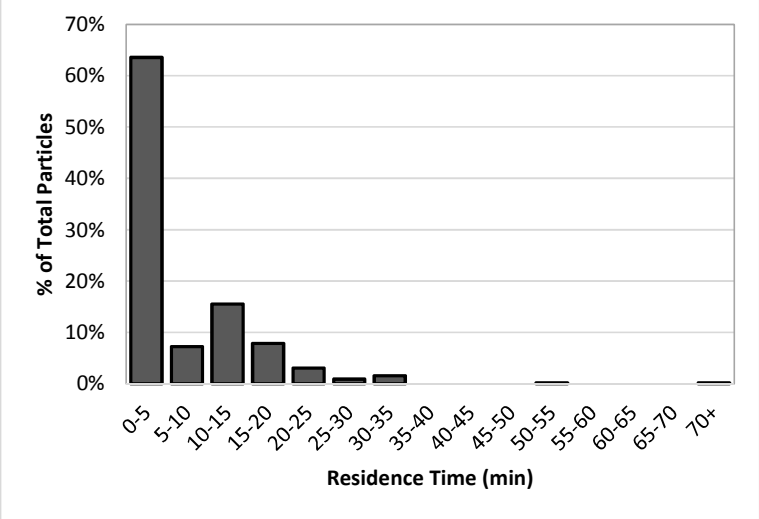

Figure 5-11 Particle Maximum Residence Distribution; Negative Mode, Case 1

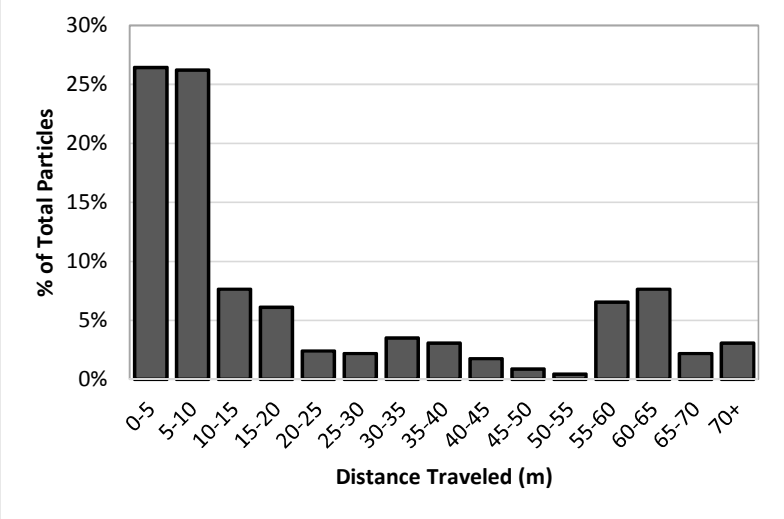

Figure 5-12 Particle Distance Traveled Distribution; Negative Model, Case 1

Under the neutral mode however, both particle concentrations and distribution were mitigated (Figure 5-13). Particles were able to migrate to the opposite hallway, but the migration was limited to the vicinity of the exhaust fan.

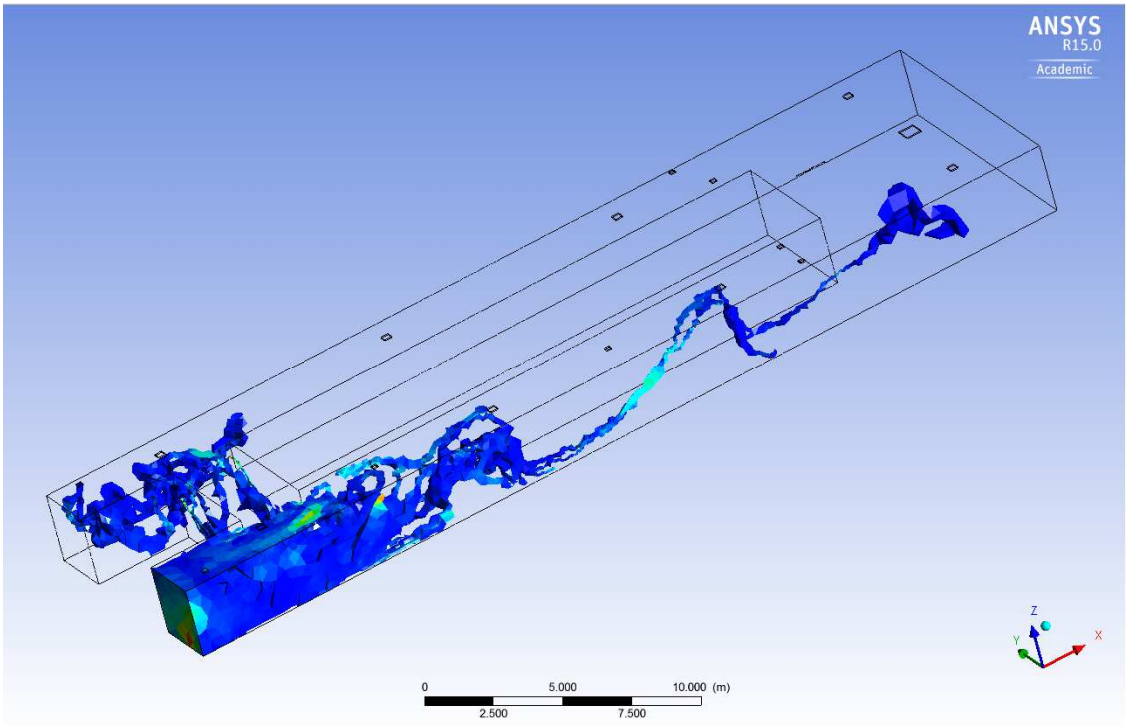

Figure 5-13 Particle Distribution, Neutral Mode, Case 1

Discharging air the ceiling level inevitably caused a tendency for particles to rise. This trend was observed for all cases under both ventilation alignments. Under the neutral mode however, the particle average height (1.43m) was lower compared to the negative mode. The vertical distribution's standard deviation (σ=0.92) was also lower than the negative mode (Figure 5-14).

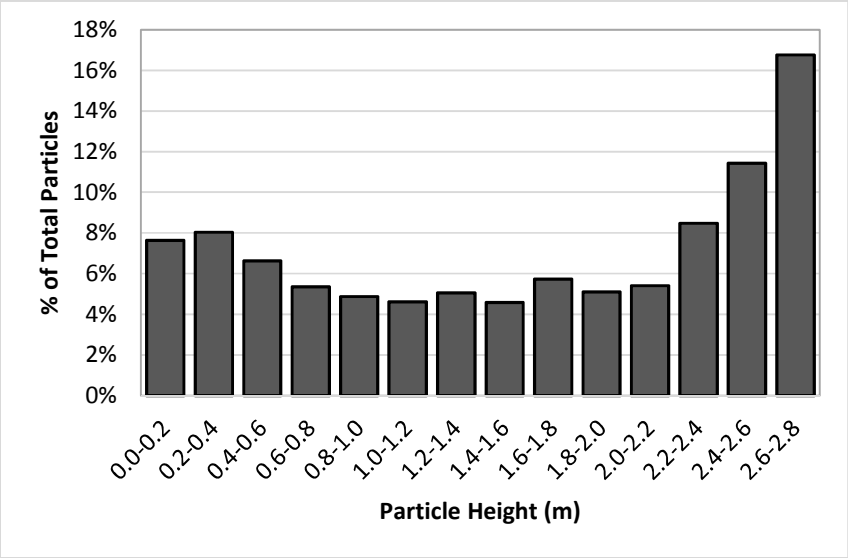

Figure 5-14 Vertical Distribution of Particles under Neutral Mode, Case 1

Moreover, only slightly more than a quarter of particles (27%) existed within the breathing zone range. The convex appearance of the distribution suggested that particles are more likely to either gravitationally settle or be removed by the exhaust fans. Also, particles average distance from the source (x=0m) was 4.65m (σ=5.63) under the neutral mode. Compared to the negative mode, this number reduced by 16% meaning that particles were prone to more displacement under the negative mode. The dispersion ratio was 0.35 under the neutral mode which reflects a 35% improvement (Figure 5-15). As depicted in Figure 5-15, particles were mostly observed in the range of zero to 8m from the source. However, a full containment was not attained in this case suggesting that a small fraction of particles could migrate even to the nursing station area (Figure 5-13).

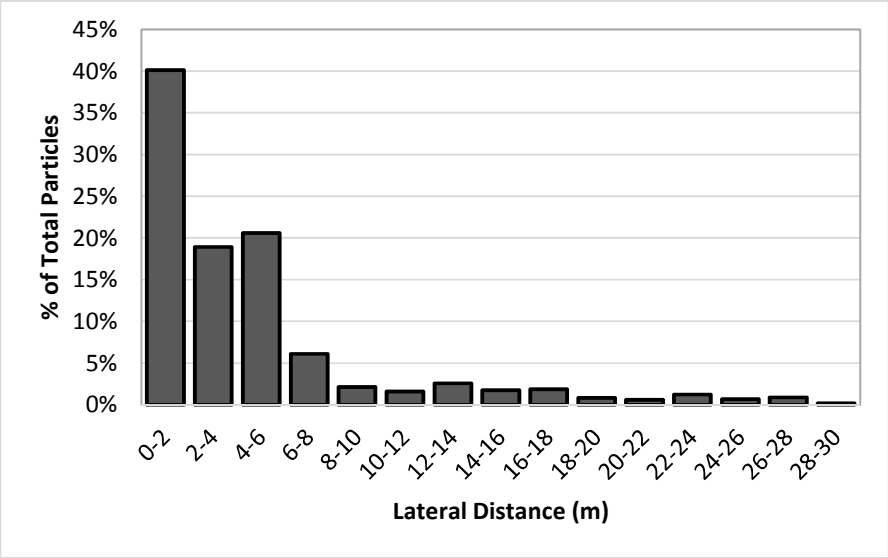

Figure 5-15 Lateral Distribution of Particles under Neutral Mode, Case 1

Particles, on average, remained within the system for 3.0 minutes (σ=4.90) which is half the corresponding time under the negative mode (Figure 5-16).

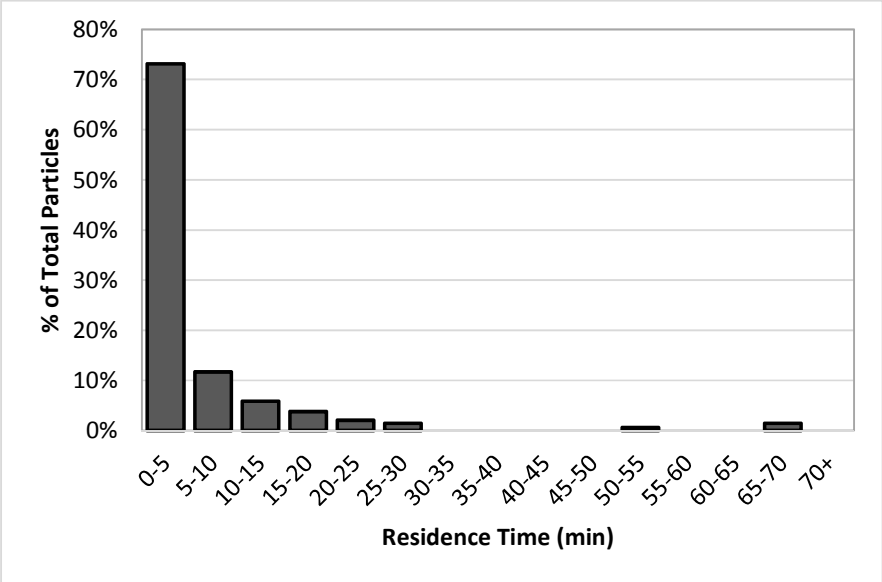

Figure 5-16 Particle Maximum Residence Distribution; Neutral Mode, Case 1

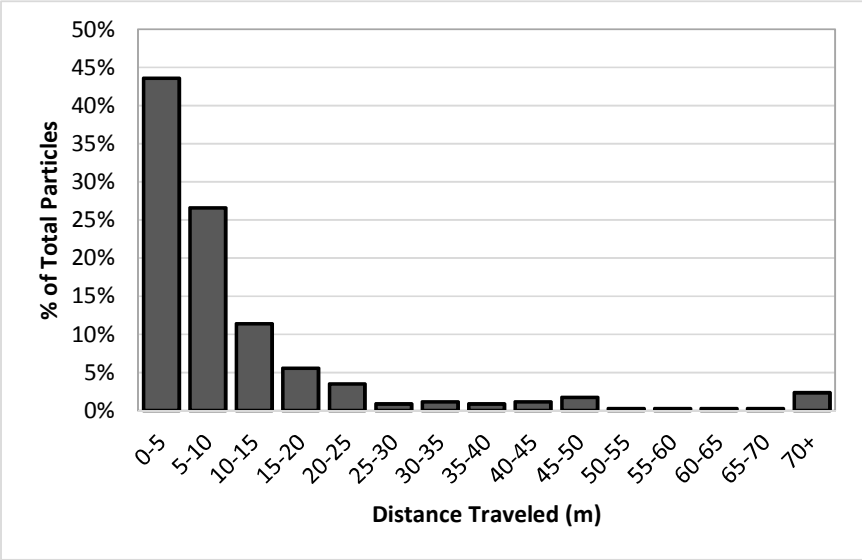

Figure 5-17 Particle Distance Traveled Distribution; Neutral Model, Case 1

The average distance traveled by particles was 11.33m (σ=16.5) under the neutral mode. The distance traveled halved compared to the negative mode. Although, 2% of particles could travel more than 70m which was twice the distance between the entrance door and the nursing station area. Again, this was a sign of incomplete containment.

Approximately 30% of particles were removed by the ventilation system from which 90% were removed by Fan 1 suggesting a more reliable containment under the neutral mode (Table 5-5). The removal from the opposite hallway was one-third of the negative ventilation alignment.

Table 5-5 Removal By Ventilation System Relative to Exhaust Fan Placement; *Neutral* Mode, *Case 1*

Exhaust Fan	Fan1	Fan2	Fan3	Fan4	Fan5	Fan6
Rate of Removal	90%	5%	0%	0%	0%	5%

As a results, analyses on case 1 revealed that the neutral mode performed better in terms of particle distributions within the corridors (Table 5-6).

Table 5-6 Distribution Parameters Relative to Ventilation Alignment, *Case 1*

Ventilation Alignment	Average Height	Breathing Zone Concentration	Distance form Source	Dispersion Ratio	Max. Time	Distance Traveled
Units	[m]	[%]	[m]	[-]	[min]	[m]
Negative	1.65	34.7	5.55	0.54	7.0	22.0
Neutral	1.43	27.47	4.65	0.35	3.0	11.35
Change	-13%	-21%	-16%	-35%	-57%	-48%

5.2.2.2 Case 2: Modified Arrangement, Release Outside *(x=0m)*

In the previous subsection, distribution parameters were appraised relative to ventilation alignment. Similar analyses for the modified arrangement were needed to assure that the results were independent of ventilation arrangement. Thus, for Case 2, particles were released at the entrance door while Fan 1 and Fan 2 were displaced as described in the computational method section (Figure 3-17).

Under the negative mode and similar to observations for the existing condition, particles existed all along the main hallway. In the opposite hallway however, particles mostly congregated around Fan 6 (Figure 5-18).

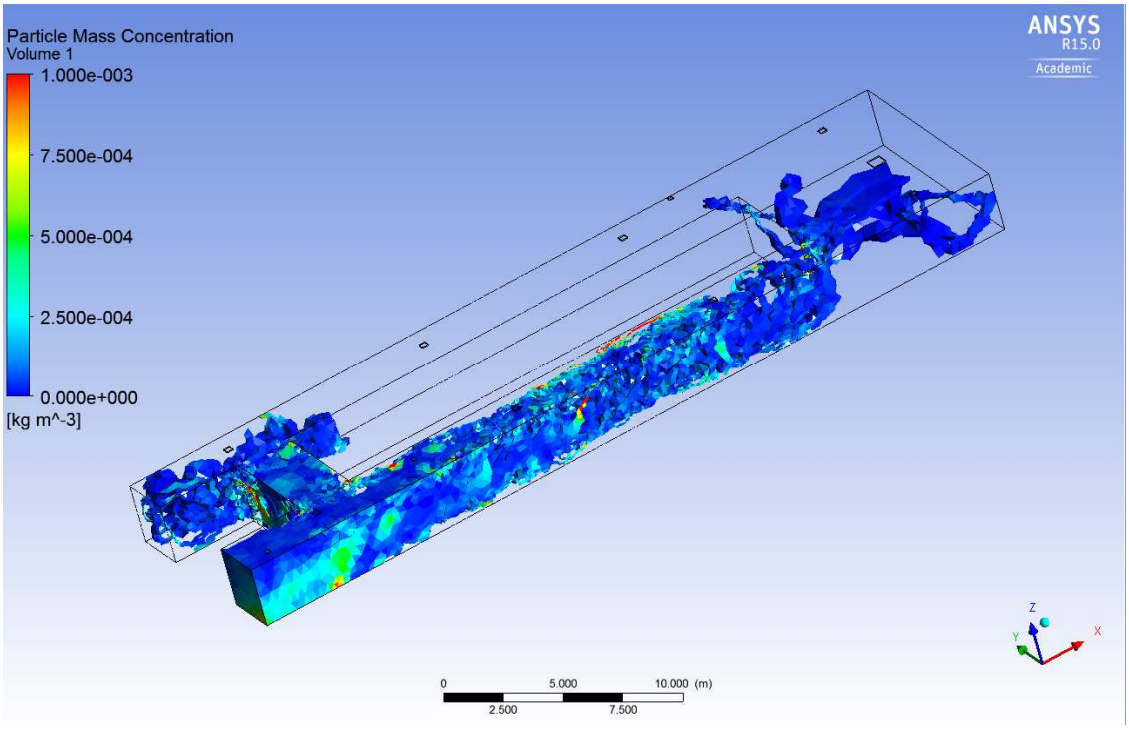

Figure 5-18 Particle Distribution, Negative Mode, Case 2

Particle height was nearly uniformly distributed from zero to 2.2m and profoundly increased thereafter (Figure 5-19).

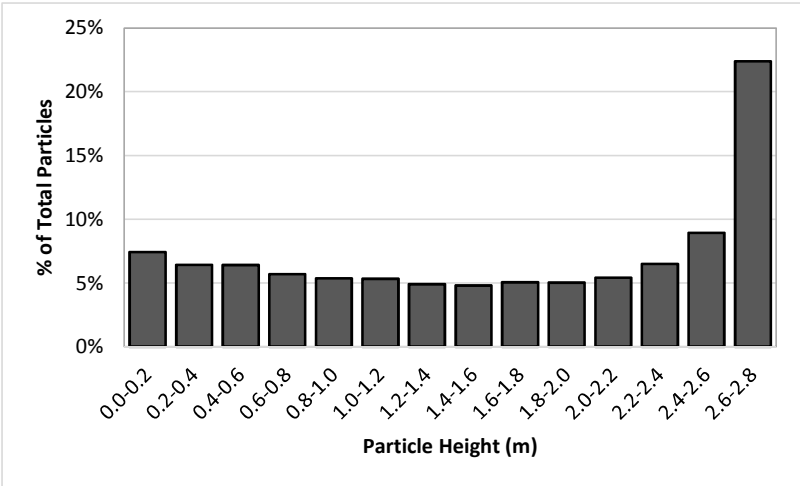

Figure 5-19 Vertical Distribution of Particles under Negative Mode, Case 2

Particle average height was slightly under 2m (1.97m, σ=0.75) which again conceded the fact that the general vertical direction of particle movement was upward. This motion contradicted with the gravitational settling of particles, and hence, placed 28% of particles in the breathing zone.

Average lateral distance from the source was 6.7m (σ=6.95) under the negative mode (Figure 5-20). Concentrations decreased relative to distance from the source and more than 90% of particles were within 18m from the source. Given a relatively large dispersion ratio (0.48), containment was not fully achieved under the negative mode (Figure 5-18) suggesting that particles were dragged towards the end of the hallway by means of the exhaust fans. Although the exhaust fans were uniformly placed in the modified arrangement, the effect of flow direction remained prominent due to negative pressurization.

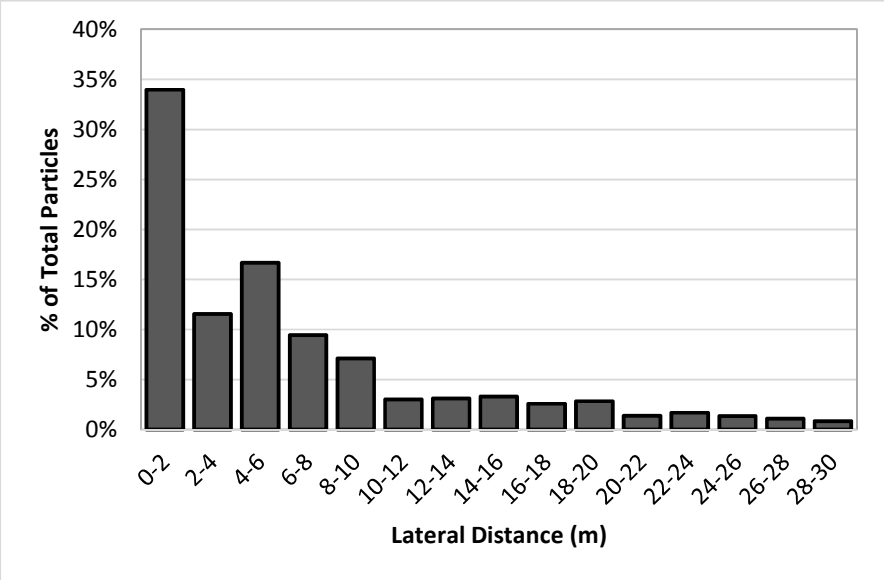

Figure 5-20 Lateral Distribution of Particles under Negative Mode, Case 2

On average, particles were suspended for 5.3 minutes (σ=7.1) within the corridors where nearly two-third of them were decayed within the first five minutes (Figure 5-21).

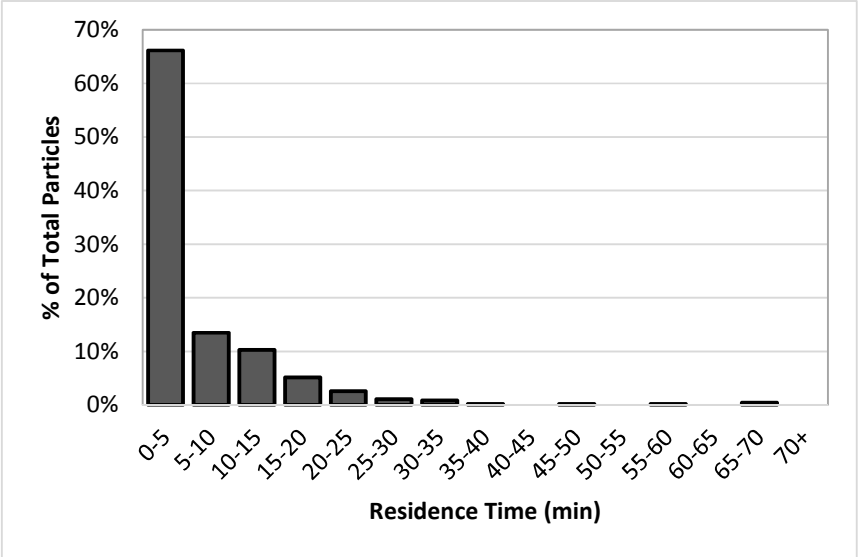

Figure 5-21 Particle Maximum Residence Distribution; Negative Mode, Case 2

The average distance traveled by particles was 19.3m (σ=19.1) under the negative mode, showing that particles tended to remain suspended due to a balance between upward flow and gravity (Figure 5-22). In fact, few particles traveled more than 100m which is equivalent to three time the length of each hallway. Particles primarily followed the vortices created by the modified arrangement. Thus, the modified arrangement oriented the motion of air entrained through a supply diffuser towards an exhaust fan which was replaced to its proximity.

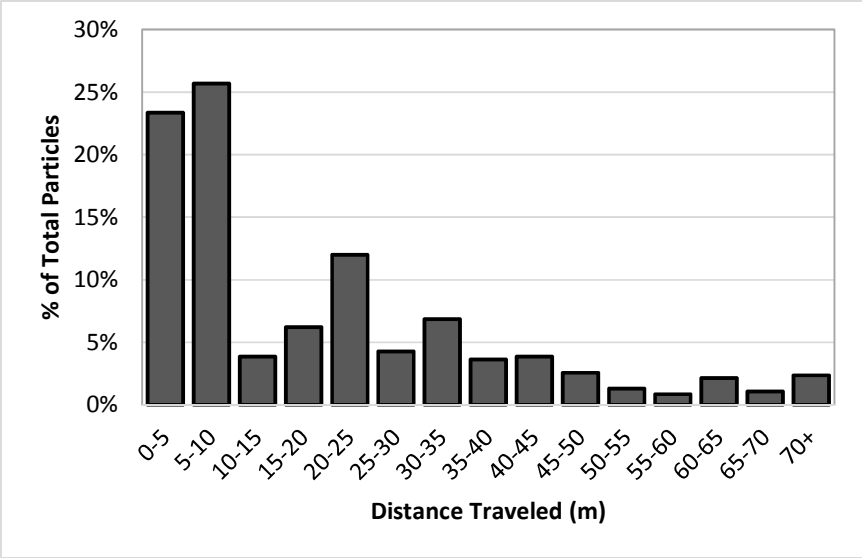

Figure 5-22 Particle Distance Traveled Distribution; Negative Model, Case 2

Similar to the existing arrangement, nearly one-third of particles were removed by the ventilation system. The removal rate was incrementally declined as fans distanced from the source (Table 5-7). Although the overall removal rate of the main hallway exhaust fans (Fans 7, 8, and 3 in the modified arrangement) was similar to that of the existing arrangement, particles were removed closer to the source, and consequently, faster. This observation described the difference between the existing and modified modes in terms of the average residence time and distance traveled. Moreover, it reinforced the improvements due to modifications in the outlet arrangement.

Table 5-7 Removal By Ventilation System Relative to Exhaust Fan Placement; *Negative* Mode, *Case 2*

Exhaust Fan	Fan7	Fan8	Fan3	Fan4	Fan5	Fan6
Rate of Removal	37%	27%	21%	2%	0%	13%

For case 2 and under the neutral mode, a clear-cut containment was observed. Particles solely existed within 14m from the entrance and the opposite hallway was clear (Figure 5-23).

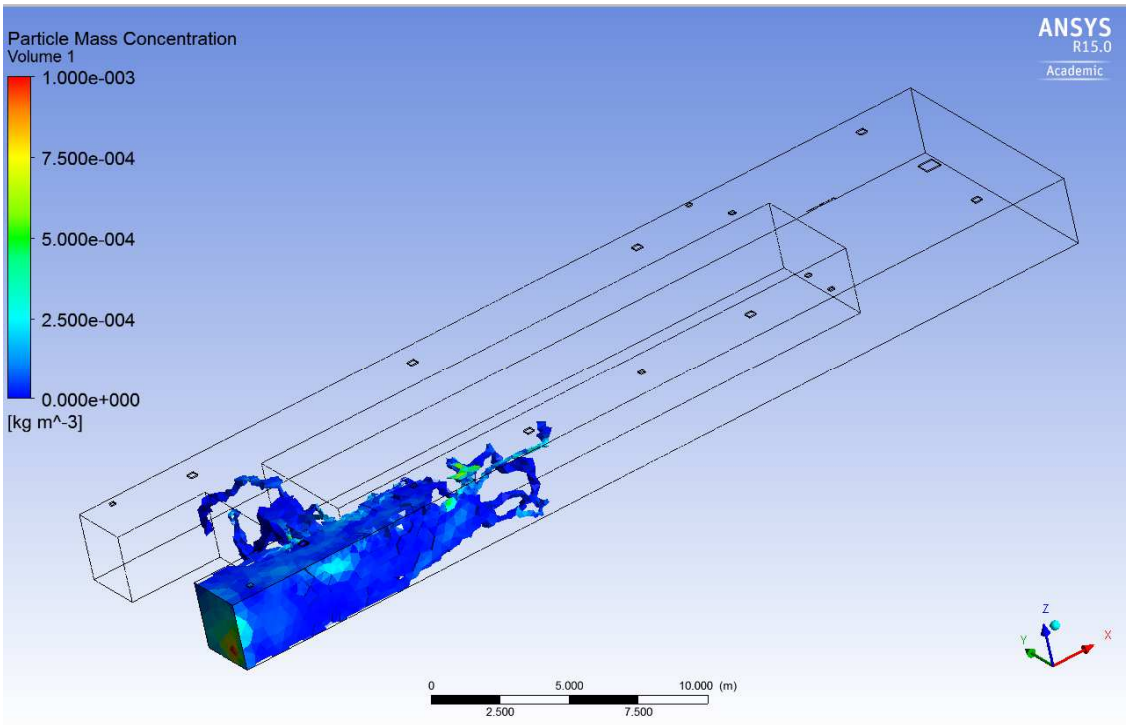

Figure 5-23 Particle Distribution, Neutral Mode, Case 2

Average height of particles were 1.58m (σ=0.83) where 25.6% of particles were within the breathing zone range (Figure 5-24) under the neutral mode. Vertical distribution seemed to remain intact when the ventilation arrangement was modified. Intuitively, a change in the location of exhaust fans should not alter the vertical distribution of particles since it is delineated by the resultant of forces acting on particles. These forces are regardless of the placement of a fan, yet depending on its flowrate.

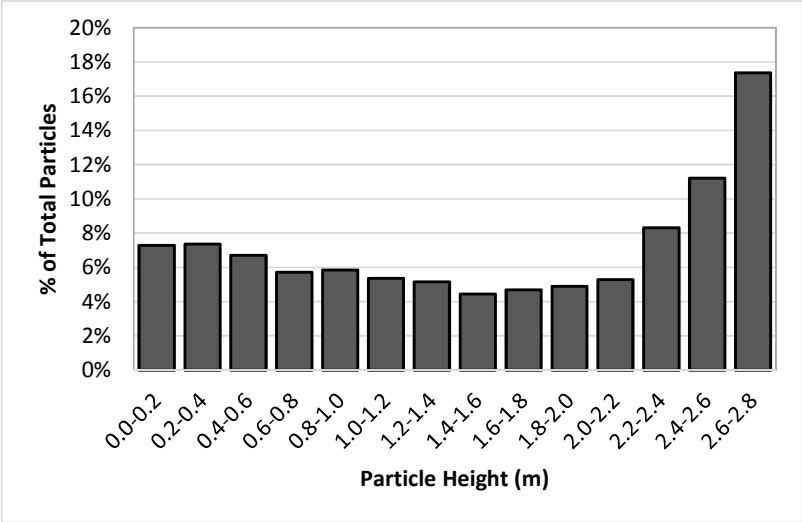

Figure 5-24 Vertical Distribution of Particles under Neutral Mode, Case 2

The lateral distribution was seemingly desirable under the neutral mode. The mean lateral distance from the source was reduced to 2.6m (σ=2.3) suggesting that the modified arrangement allied to the neutral alignment could generate relatively favorable conditions (Figure 5-25).

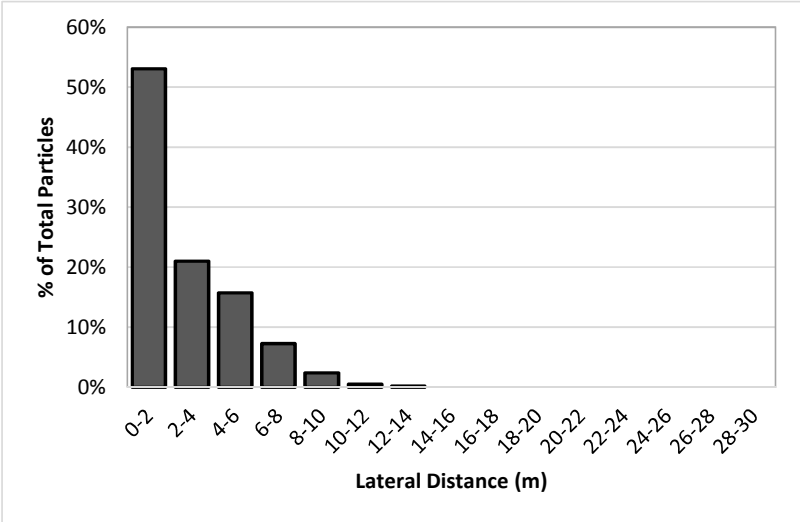

Figure 5-25 Lateral Distribution of Particles under Neutral Mode, Case 2

Under the neutral mode, the dispersion ratio was 0.16 where a full containment was achieved mainly because air motion form Supply 2 and Fan7 created a negative velocity field in the x-direction in that region (9m-14m). Moreover, the average residence time of particles was 2 minutes (σ=3.4) indicating that particles were decayed faster when compared to the neutral mode under the existing arrangement (Figure 5-26).

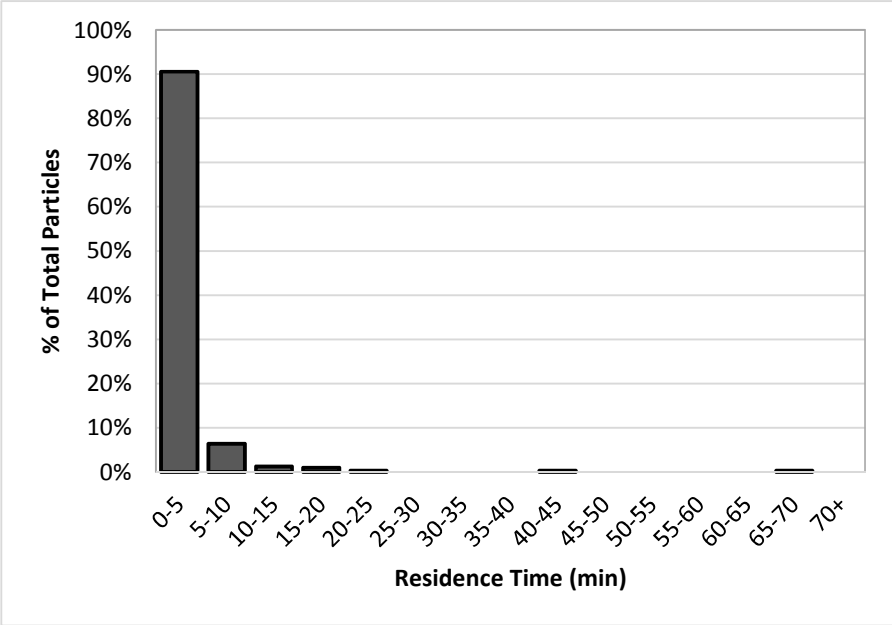

Figure 5-26 Particle Maximum Residence Distribution; Neutral Mode, Case 2

As stated earlier, modifications enhanced the removal mechanism of particles by placing exhaust fans uniformly throughout the corridor. The average distance traveled by particles was 9.1m (σ=9.3) under the neutral mode (Figure 5-27). Compared to the negative mode, particles tended to move around shorter. Also, compared to the neutral mode in case one, the average distance traveled by particles reduced by 20% upon implementing the modifications.

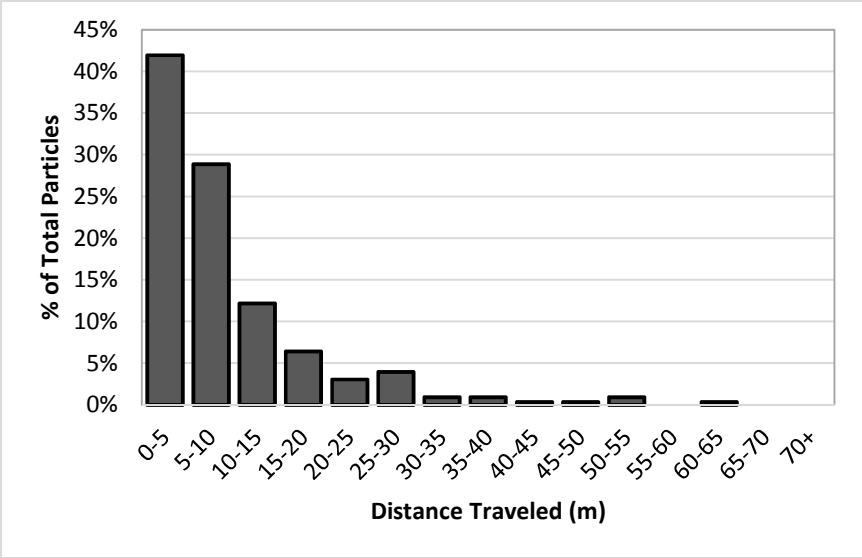

Figure 5-27 Particle Distance Traveled Distribution; *Neutral* Model, *Case 2*

The removal rate was 28% under the neutral mode which was slightly lower than that under the negative mode. The reason lied in the roots of higher tendency for upward motion under the negative mode. As expected though, particles were entirely removed by Fan7 or deposited onto surfaces as another plausible destiny.

Table 5-8 Removal By Ventilation System Relative to Exhaust Fan Placement; *Neutral* Mode, *Case 2*

Exhaust Fan	Fan7	Fan8	Fan3	Fan4	Fan5	Fan6
Rate of Removal	100%	0%	0%	0%	0%	0%

A conclusion to analyses on Case 2 is presented in Table 5-9. Similar to Case 1, all of the distribution parameters improved under the neutral mode suggesting that the neutral mode was the more rational design strategy regardless of the placement of domain boundaries.

Table 5-9 Distribution Parameters Relative to Ventilation Alignment, *Case 2*

Ventilation Alignment	Average Height	Breathing Zone Concentration	Distance form Source	Dispersion Ratio	Max. Time	Distance Traveled
Units	[m]	[%]	[m]	[-]	[min]	[m]
Negative	1.97	28.2	6.7	0.48	5.3	19.3
Neutral	1.58	25.6	2.6	0.16	2.0	9.10
Change	-20%	-9%	-61%	-67%	-62%	-53%

To refrain any bias in data analysis, distributions were tested against the release point. Thus far, Cases 1 and 2 investigated particles average and distributions when released outside the hallway. In order to find the prominent design strategy, cases where release took place inside was also studied. The release point was 14m away from the entrance. The results were analyzed using similar procedure for Cases 1 and 2, however, nuances in terms of release point were accounted. For instance, for a release inside case, particles normally distribute both ways (i.e. toward the entrance and nursing station). Therefore, unlike releasing outside, the distribution evolves around the point of release. As a result, other parameters such as skewness and kurtosis became of interest. Generally, a symmetric distribution has skewness close to zero and is more desirable. Moreover, higher kurtosis implies that particles are congregated near the source (Figure 5-28).

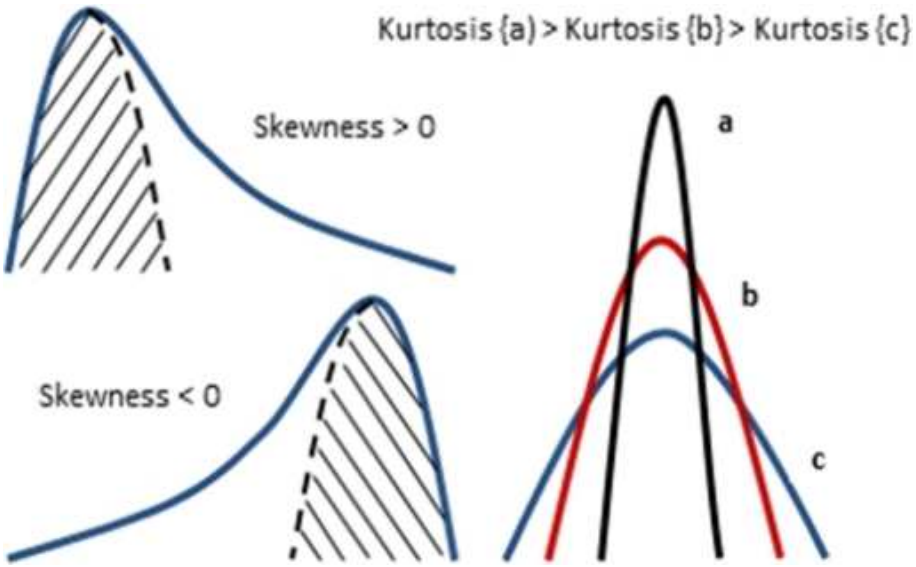

Figure 5-28 Skewness and Kurtosis in Distributions [97]

With that in mind, two new cases with an internal source of particles were defined and analyzed.

5.2.2.3 Case 3: Existing Arrangement, Release Inside *(x=14m)*

For Case 3 and under the negative mode, particle concentrations were considerably high in both the main and opposite hallways (Figure 5-29). However, placing the exhaust fans near each other impeded particle migration to the nursing area.

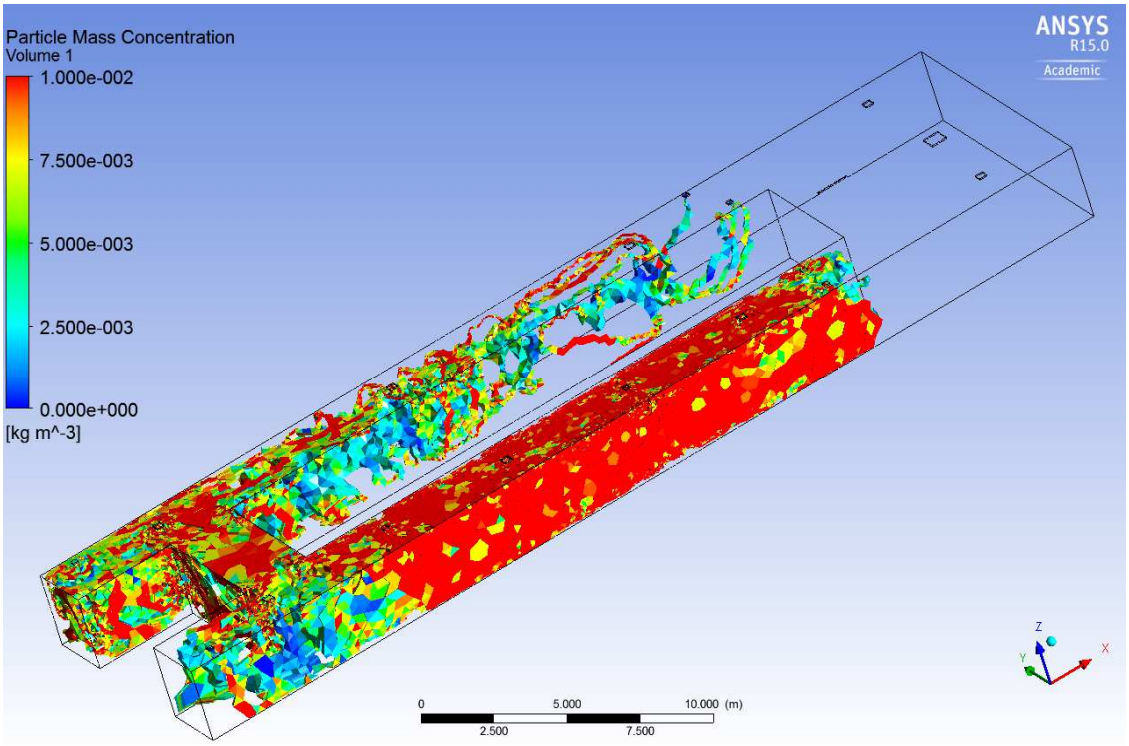

Figure 5-29 Particle Distribution, Negative Mode, Case 3

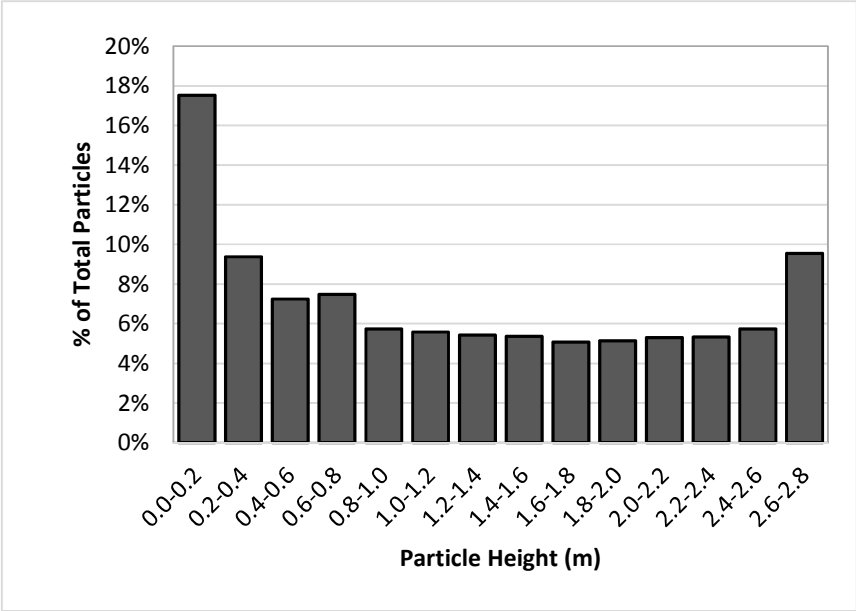

Figure 5-30 Particle Distribution, Negative Mode, Case 3

Particles tend to settle down more easily when released inside (Figure 5-30). The average height of particles were 1.35m (σ=0.89) depicting the equilibrium between gravity and the drag force. Also, 31.5% of particles existed within the breathing zone range. The lateral dispersion, on the other hand, was positively skewed (g=2.48) because of the non-uniform placement of exhaust fans under the existing arrangement (Figure 5-31).

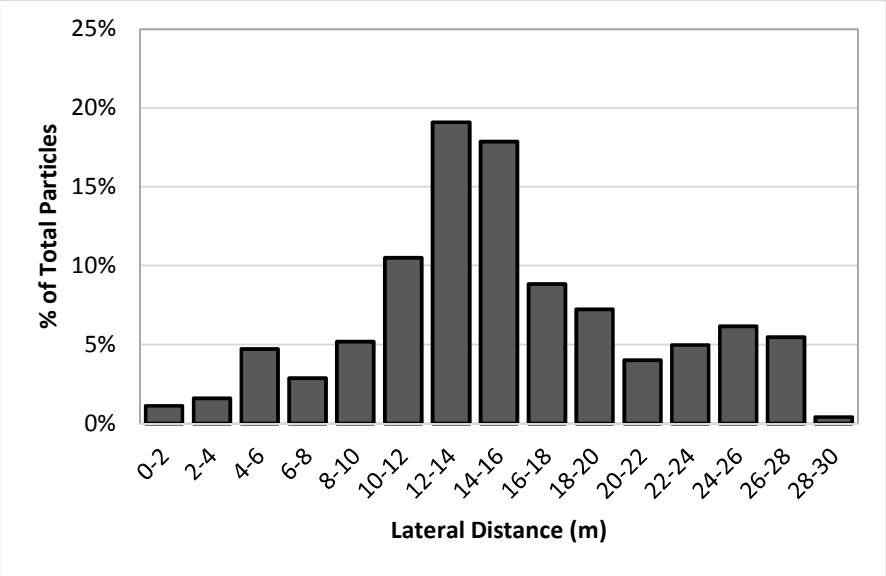

Figure 5-31 Lateral Distribution of Particles under Negative Mode, Case 2

Under the negative mode, the average distance from the source (x=14m) was +1.76m with 9.33 standard deviation. Dispersion ratio was 0.62 given the fact that 90% of particles were sought on both sides of the release point. For example in this case, 90% particles existed in a range starting from 3m to 25m with a center at x=14m. Kurtosis was 1.81 under the negative mode. It should be noted that kurtosis is three (β=3) for a normal distribution (mesokurtic), thus when β=1.81, the distribution was considered 'flat' and is called platykurtic.

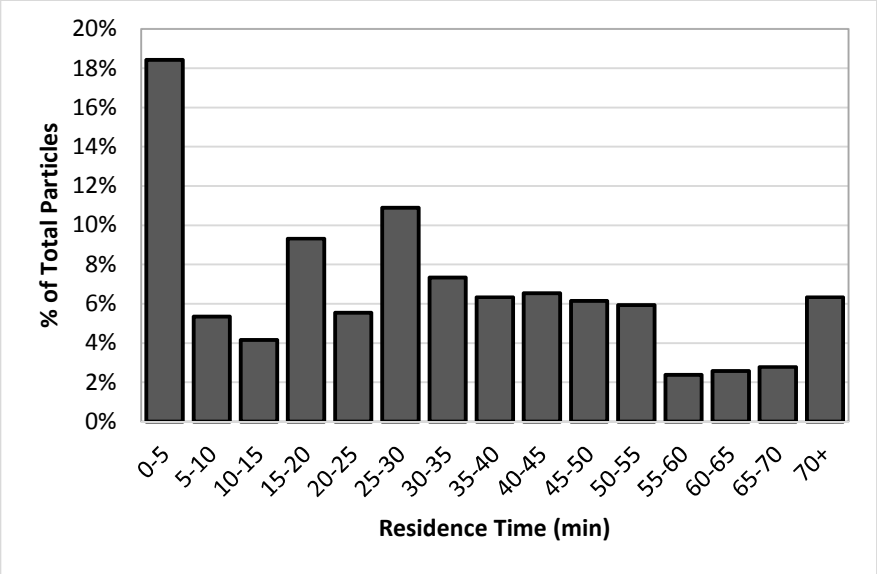

Figure 5-32 Particle Maximum Residence Distribution; Negative Mode, Case 3

Particle residence time was, on average, 31.5 minutes (σ=29.4) where only 18% of particles were decayed within the first five minutes.

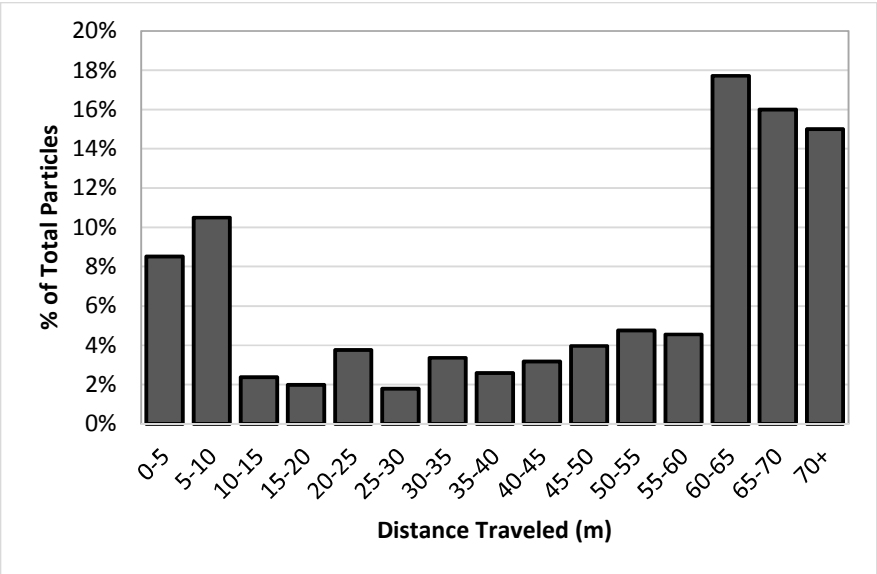

Figure 5-33 Particle Distance Traveled Distribution; *Negative* Model, *Case 3*

The mean distance traveled by particles was 67m (σ=39.4) under the negative mode (Figure 5-33). As can be seen, particles either traveled no more than 10.0m or stayed suspended and traveled more than 60m within the space.

Approximately 40% of particles were removed through the ventilation system compared to other mechanisms under the negative mode. From the removed particles slightly less than 90% were removed by Fan1 and Fan2 (Table 5-10).

Table 5-10 Removal By Ventilation System Relative to Exhaust Fan Placement;

Negative* Mode, *Case 3

Exhaust Fan	Fan1	Fan2	Fan3	Fan4	Fan5	Fan6
Rate of Removal	0%	43%	43%	1%	1%	13%

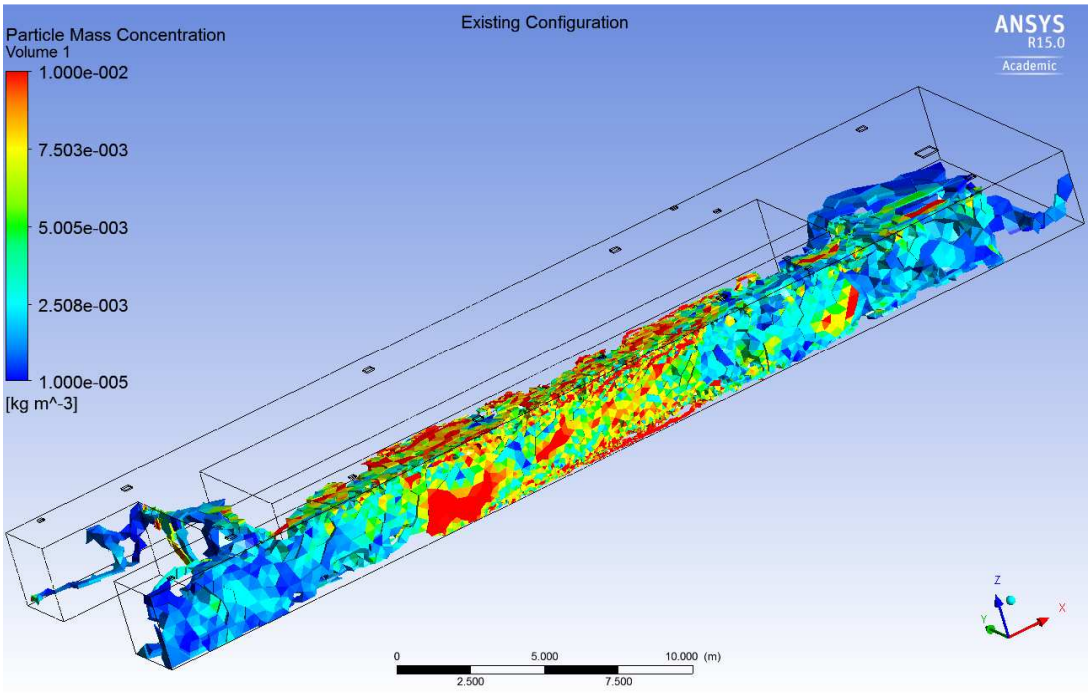

Figure 5-34 Particle Distribution, Neutral Mode, Case 3

Under the neutral mode, the opposite hallway was clear and particles were distributed within the main hallway with appreciably lower concentrations (Figure 5-34). Particles tended to remain closer to the floor level where the average height was 1.25m (σ=0.85) and 29.8% of all particles were within the breathing zone (Figure 5-35).

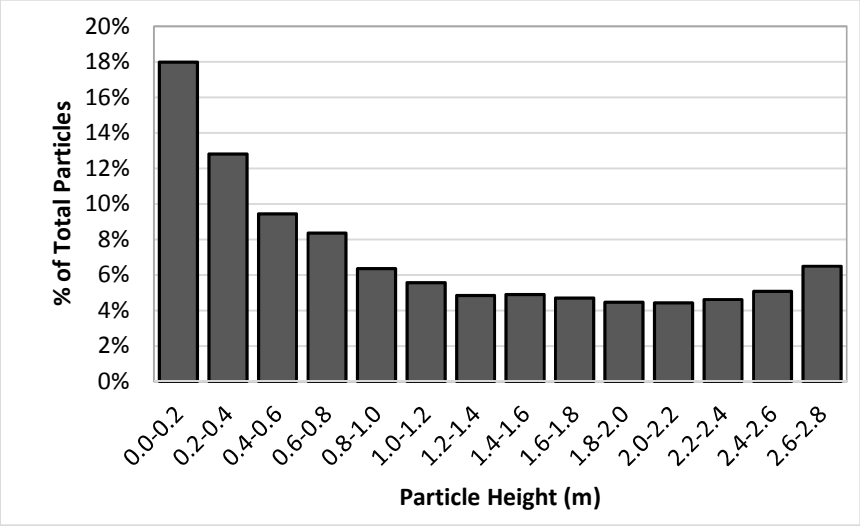

Figure 5-35 Vertical Distribution of Particles under Neutral Mode, Case 3

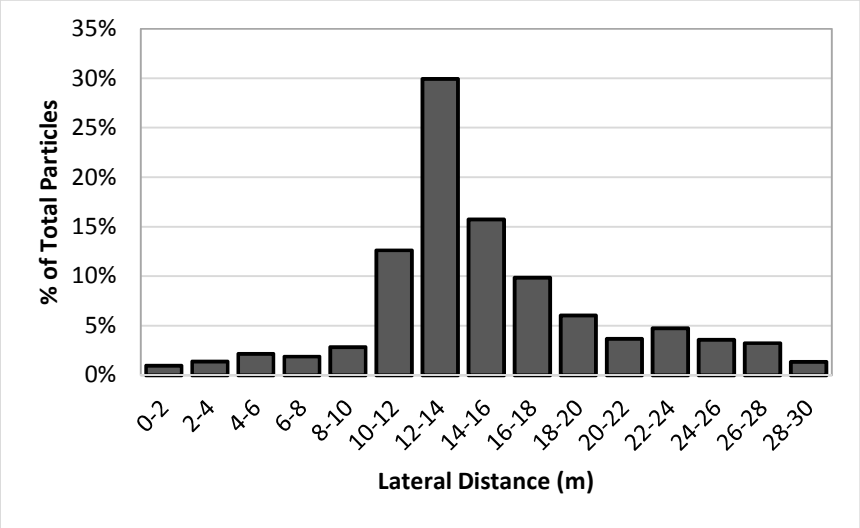

Figure 5-36 Lateral Distribution of Particles under Neutral Mode, Case 3

The weighted average lateral distribution of particles were 15.2m (σ=5.52) which drifted away 1.2m from the source (x=14.0m) (Figure 5-36). The lateral distribution was slightly skewed to the left (g=0.6) and kurtosis was 2.97 under the neutral mode. The dispersion ratio under the neutral mode was 0.56 which was 12.5% lower than the corresponding value under the negative mode.

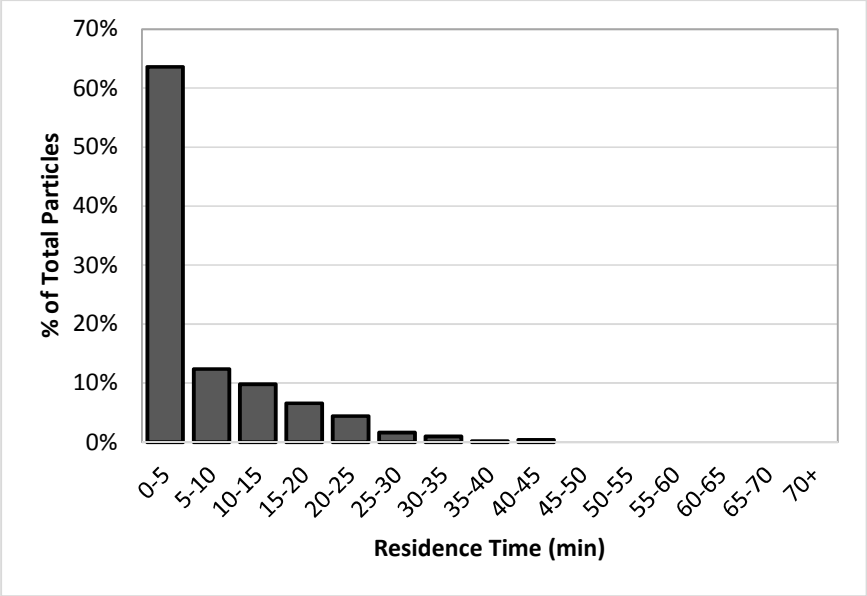

Figure 5-37 Particle Maximum Residence Distribution; Neutral Mode, Case 3

The average time particles remained within the space was 6 minutes (σ=8.1) under the neutral mode which was nearly one-fifth of the corresponding time under the negative mode (Figure 5-37). Particles traveled, on average, 31.3m (σ=24.1) before they either settled or egress through the ventilation system (Figure 5-38).

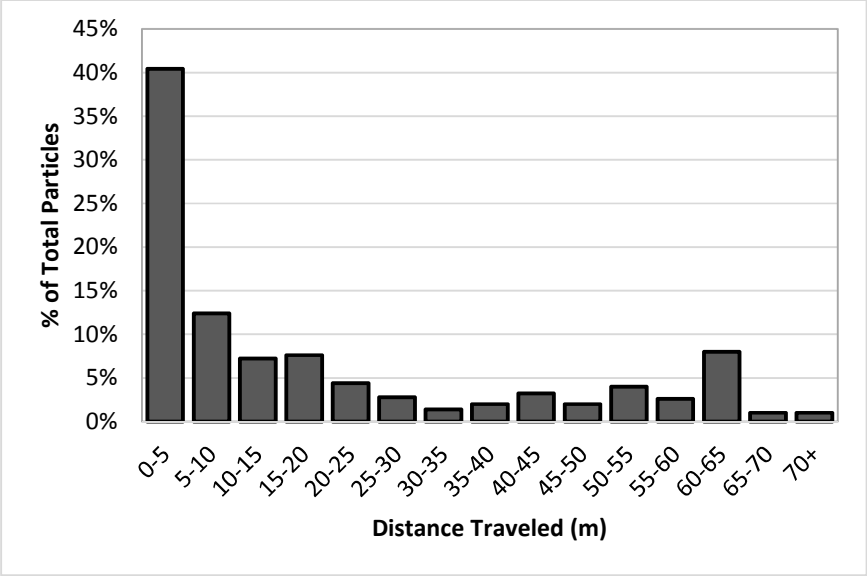

Figure 5-38 Particle Distance Traveled Distribution; Neutral Model, Case 3

19% of the total removed particles escaped from Fan1 while the rest escaped from Fans 2 and 3 under the neutral mode. Unlike the negative mode, exhaust fans in the opposite hallway did not contribute to the removal process (Table 5-11).

Table 5-11 Removal By Ventilation System Relative to Exhaust Fan Placement;

Neutral* Mode, *Case 3

Exhaust Fan	Fan1	Fan2	Fan3	Fan4	Fan5	Fan6
Rate of Removal	19%	56%	25%	0%	0%	0%

Comparison between ventilation alignment and distribution parameters in Case 3 revealed that the neutral mode exhibited more reliable performance in terms of particle distribution (Table 5-12).

Table 5-12 Distribution Parameters Relative to Ventilation Alignment, *Case 3*

Ventilation Alignment	Average Height	Breathing Zone	Lateral Distribution Parameters					Max. Time	Distance Traveled
Units	[m]	[%]	DS1	σ	g	β	DR2	[min]	[m]
Negative	1.35	31.5%	1.76	9.33	2.48	1.81	0.62	31.5	67
Neutral	1.26	29.8%	1.27	5.52	0.61	2.97	0.57	5.6	31
Change	-7%	-6%	-28%	-41%	-75%	-64%	-8%	-82%	-54%

[1] DS = Distance from Source

[2] DR = Dispersion ratio

5.2.2.4 Case 4: Modified Arrangement, Release Inside *(x=14m)*

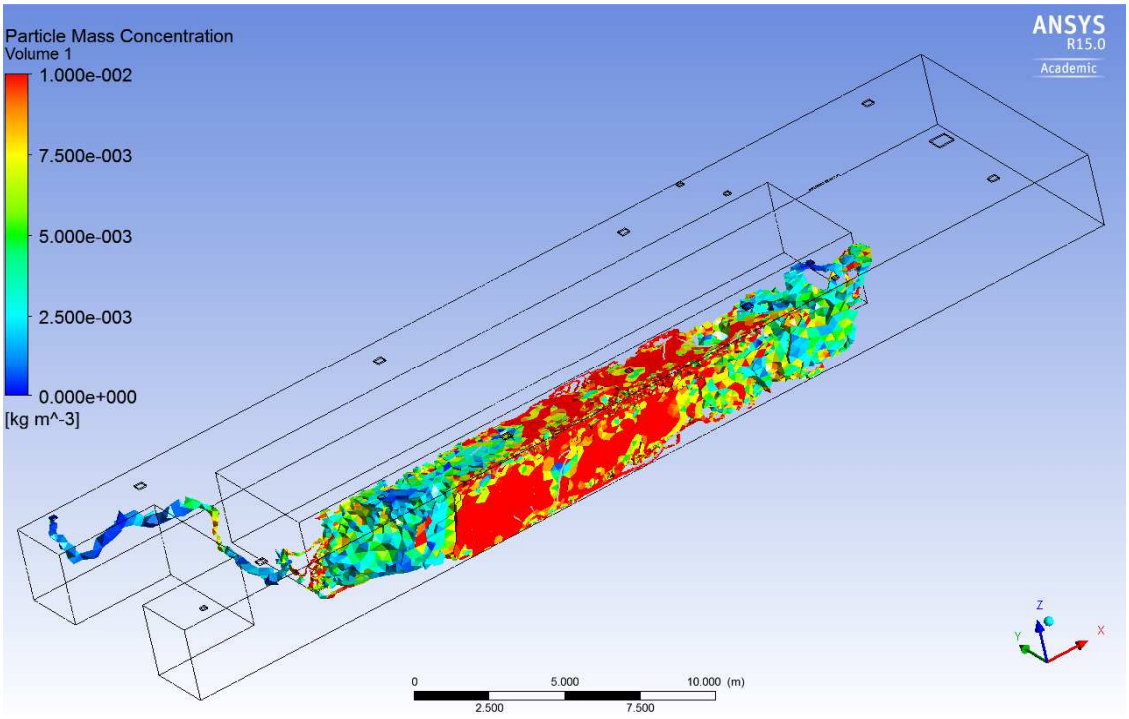

Figure 5-39 Particle Distribution, Negative Mode, Case 4

Final case, was defined as a case in which particles were released inside and the ventilation arrangement was amended. In Case 4 and under the negative mode, particle

concentrations were relatively high but contained within the range of the main hallway (Figure 5-39).

The average height of particles was 1.38m (σ=0.81) with a tendency towards settling. 30.5% of particles existed within the breathing zone and particles outside this range were likely to settle out. More than 40% of particles were below the breathing zone range (height ≤ 0.8m).

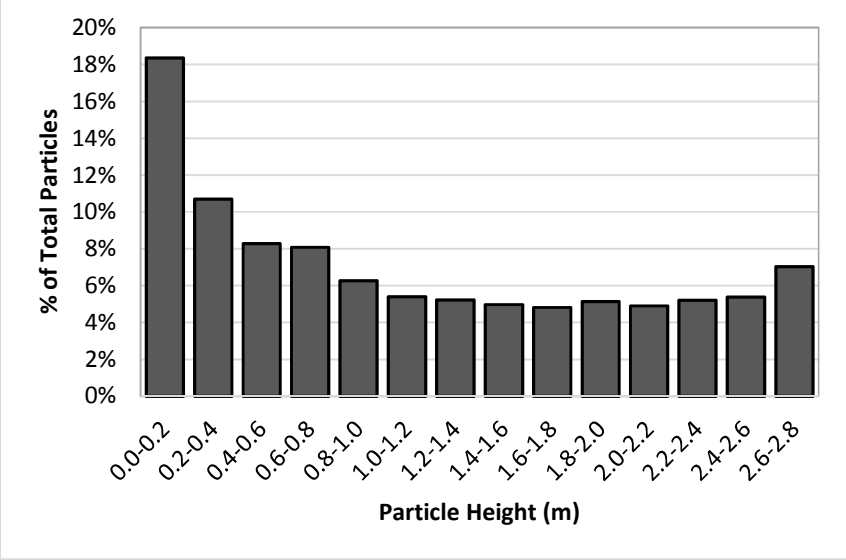

Figure 5-40 Vertical Distribution of Particles under Negative Mode, Case 4

Similar to Case 3, the lateral distribution was positively skewed (g=+0.76) however the skewness was considerably smaller than that of the existing arrangement (Figure 5-41).

Under the negative mode, the mean value of the lateral distribution was 15.80m creating 1.80m distance from the source (x=14.0m). Standard deviation was 2.96 which was more than one-third of the corresponding value under the existing arrangement. Kurtosis was 2.20 meaning that the distribution was platykurtic (β<3).

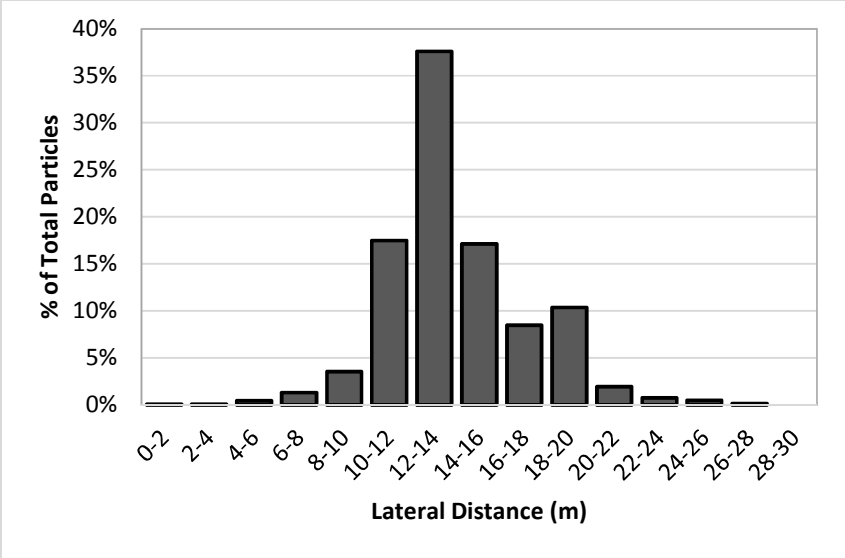

Figure 5-41 Lateral Distribution of Particles under Negative Mode, Case 4

The dispersion ratio was 0.32 under the negative mode which was nearly half of the dispersion ratio under the existing arrangement (Case 3). Moreover, modifications were proven to culminate in a design that was less prone to unfavorable particle dissemination. In fact, comparing Case 3 and Case 4 under the negative mode revealed that changing the ventilation arrangement could, to a good extent, affect particle distributions.

The average residence time of particles were 9.0 minutes (σ=9.8) where slightly less than half of the particles were either decayed or deposited in the first five minutes.

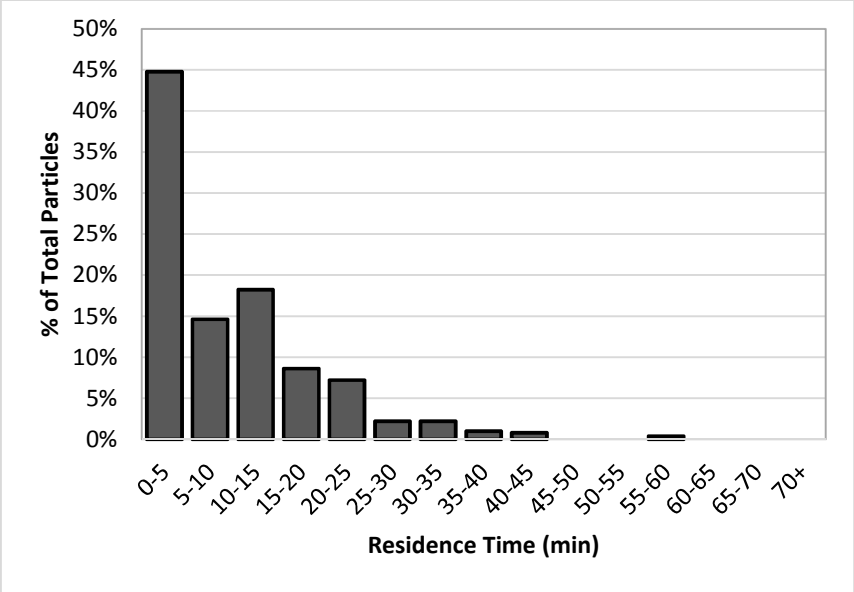

Figure 5-42 Particle Maximum Residence Distribution; Negative Mode, Case 4

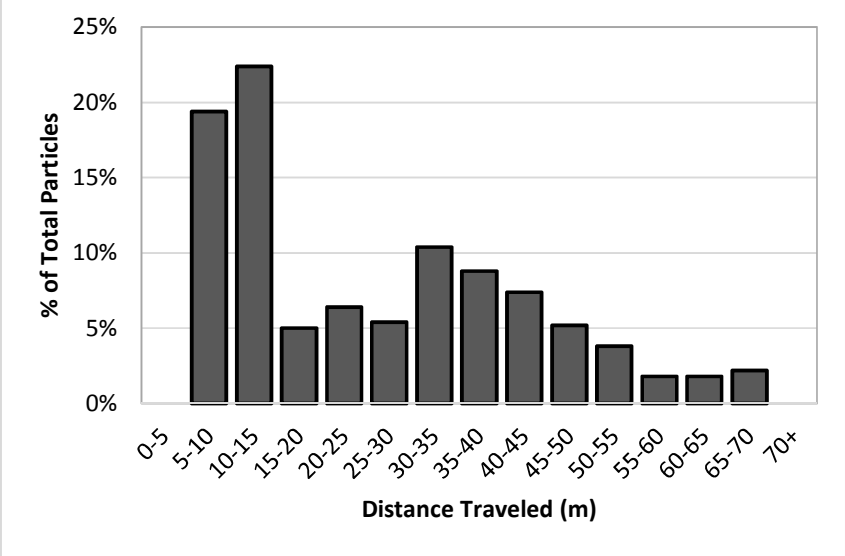

Figure 5-43 Particle Distance Traveled Distribution; Negative Model, Case 4

The average distance traveled by particles was 31.0m (σ=17.3), however, nearly 40% of particles did not travel more than 15m (Figure 5-43).

More than a quarter (27%) of particles were removed by the ventilation system of which 83% and 16% were removed by the displaced exhaust fans (Fans 7 and 8 respectively). Other exhaust fans did not really contribute to the removal process (Table 5-13).

Table 5-13 Removal By Ventilation System Relative to Exhaust Fan Placement;

Negative* Mode, *Case 4

Exhaust Fan	Fan7	Fan8	Fan3	Fan4	Fan5	Fan6
Rate of Removal	16%	83%	0%	0%	0%	1%

Under the neutral mode however, particle concentrations decreased, and similar to Case 2, an absolute containment was also achieved. An absolute containment is the situation in which 100% of particles existed in the limited part of the hallway.

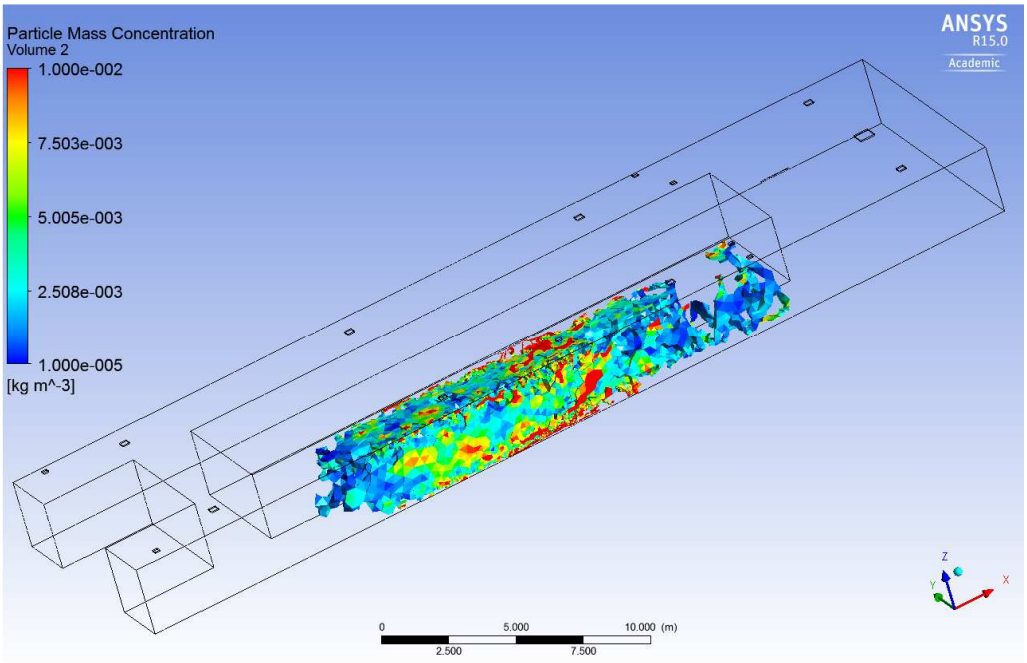

Figure 5-44 Particle Distribution, Neutral Mode, Case 4

The average height of particles was 1.19m (σ=0.85) under the neutral mode and 34% of particles were within the breathing zone (Figure 5-45).

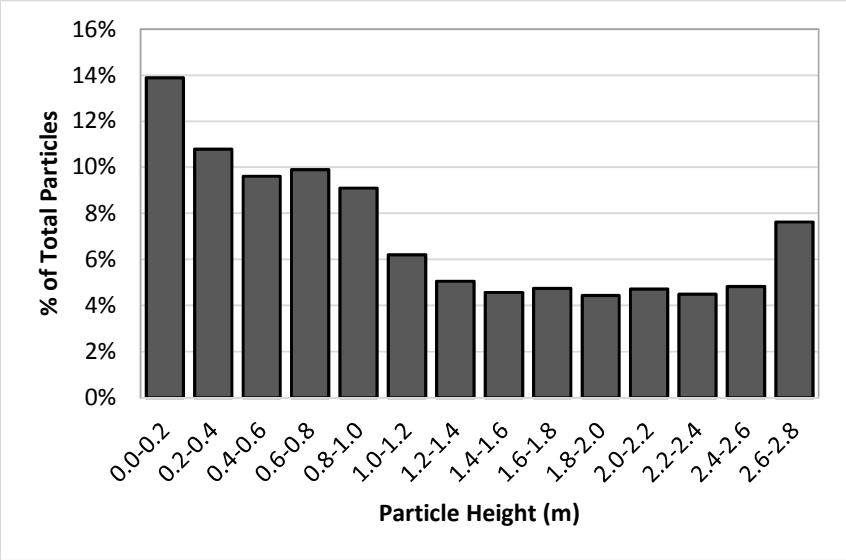

Figure 5-45 Vertical Distribution of Particles under *Neutral* Mode, *Case 4*

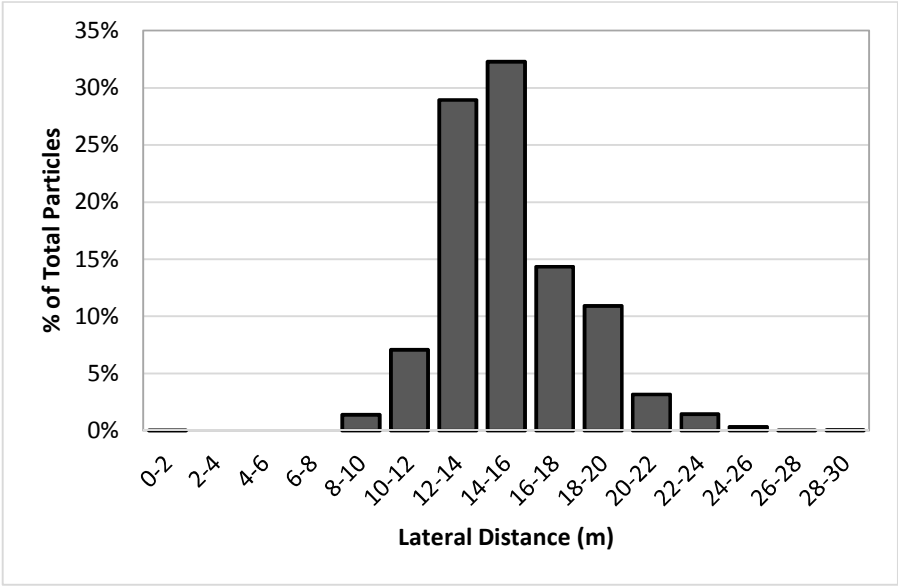

Figure 5-46 Lateral Distribution of Particles under *Neutral* Mode, *Case 4*

On average, particles were distributed away from the source only by 1.17m (Figure 5-46). The standard deviation of lateral distribution was 2.8 and it was positively skewed (g=1.1). Also, under the neutral mode, kurtosis was 3.2 which was the only case with a leptokurtic distribution. In fact, in this case and under the neutral mode, more than 60% of particles existed in a 4m range from the source. Therefore, the dispersion ratio was 0.29 which was the lowest value among all the release-inside cases.

More than 90% of particles remained within the domain for less than five minutes (Figure 5-47) and particles traveled 25.6m on average (σ=10.15) while nearly half of them transported for less than 10m before decay(Figure 5-48).

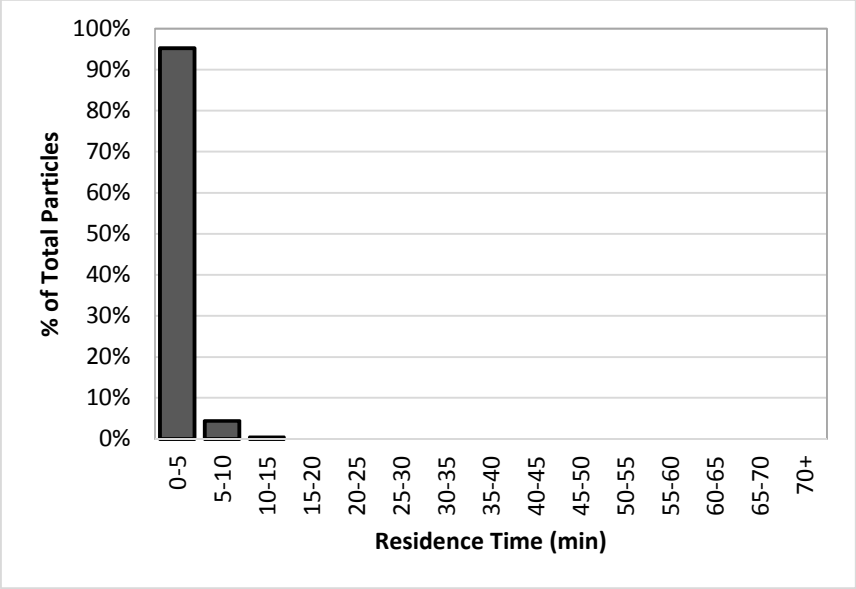

Figure 5-47 Particle Maximum Residence Distribution; *Neutral* Mode, *Case 4*

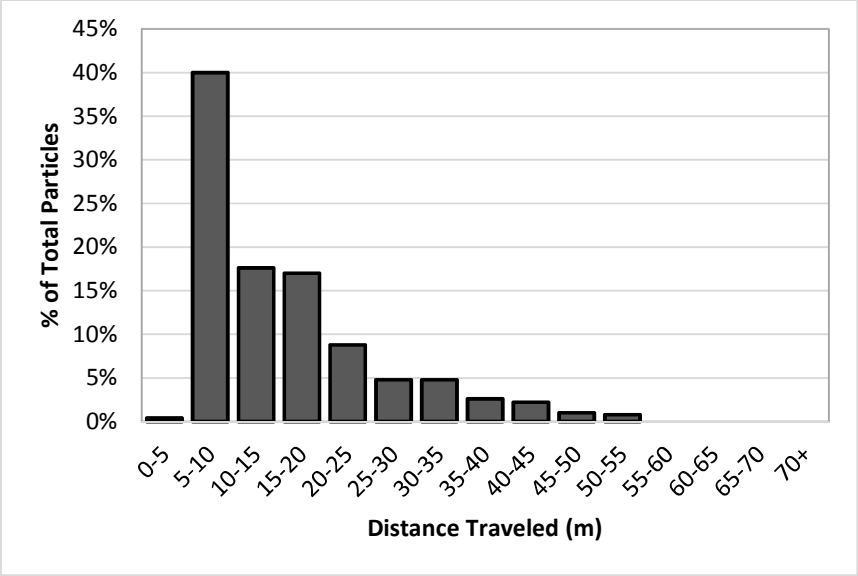

Figure 5-48 Particle Distance Traveled Distribution; *Neutral* Mode, *Case 4*

The removal rate was 28% under the neutral mode which was slightly higher than that of the negative mode. From this portion, 15% and 85% were removed by Fan7, and 8 respectively (Table 5-14).

Table 5-14 Removal By Ventilation System Relative to Exhaust Fan Placement; *Neutral* Mode, *Case 4*

Exhaust Fan	Fan7	Fan8	Fan3	Fan4	Fan5	Fan6
Rate of Removal	15%	85%	0%	0%	0%	0%

The results from the comparison between the negative and neutral modes were presented in Table 5-15. Skewness in addition to breathing zone concentration were the only parameters with a better performance in the negative mode compared to the neutral mode.

Table 5-15 Distribution Parameters Relative to Ventilation Alignment, *Case 4*

Ventilation Alignment	Average Height	Breathing Zone	Lateral Distribution Parameters					Max. Time	Distance Traveled
Units	[m]	[%]	DS1	σ	g	β	DR2	[min]	[m]
Negative	1.38	30.5%	1.80	2.96	0.76	2.2	0.32	9.0	31
Neutral	1.19	34.0%	1.17	2.79	1.10	3.2	0.29	2.0	25.6
Change	-15%	11%	-45%	-6%	45%	-45%	-9%	-78%	-19%

[1] DS = Distance from Source

[2] DR = Dispersion ratio

In summary, both particle concentrations and distributions dramatically improved under the neutral mode suggesting that any directional flow within corridors of a healthcare setting should be avoided. As alluded to in the introduction section, ASHRAE standard 170-2013 has no requirements in terms of pressure relationship with adjacent spaces. The results suggested that although no particular relationship with adjacent spaces is required, corridors must be balanced in terms of the amount of intake and exhaust air.

Furthermore, advertent modifications in the ventilation arrangement could greatly mitigate the issue of particle transmission in corridors. In other words, corridors should be designed to deliver a non-directional flow. This can be achieved by avoiding negative pressurization and designing a symmetric pattern for the ventilation arrangement. The latter could, to some extent, control the unfavorable outcomes of an unbalanced ventilation system.

5.3 Ventilation Rate

Results from the previous section suggested that a non-directional air distribution serves best in terms of particle removal and containment. Therefore, the **neutral mode** was studied under various ventilation rates. As stated in the method section (Table 3-7), four (4) ACH levels were selected to represent the previous and current ASHRAE requirements (4ACH and 2ACH respectively), in addition to one data point between and above these requirements. As per previous section discussion, CFD models were developed for two ventilation arrangements (existing vs modified) and two release points (inside vs. outside). Moreover, particle concentrations and distributions were analyzed separately to ensure rigorous and thorough outcomes.

5.3.1 Concentrations

Concentrations of particles declined with distance from the release point. This trend was observed for all ventilation rates and arrangements. Under the existing arrangement, concentration trends seemed independent of the ventilation rate (Figure 5-49). Relatively high concentrations were observed at the first 10m and then, on the average, concentrations decreased by 80%. For 2ACH however, particle concentrations were sustained up to the nursing station area. Changes in the ventilation rate brought about nearly 2.5% reduction in the average particle concentrations (Table 5-16). This was obviously not commensurate with the amount of air to be conditioned for ventilation rates. To demonstrate this issue, cost of ventilation in US dollars were calculated for each case. The annual cost for conditioning 1 cfm of air was $6 according to Memarzadeh [16].

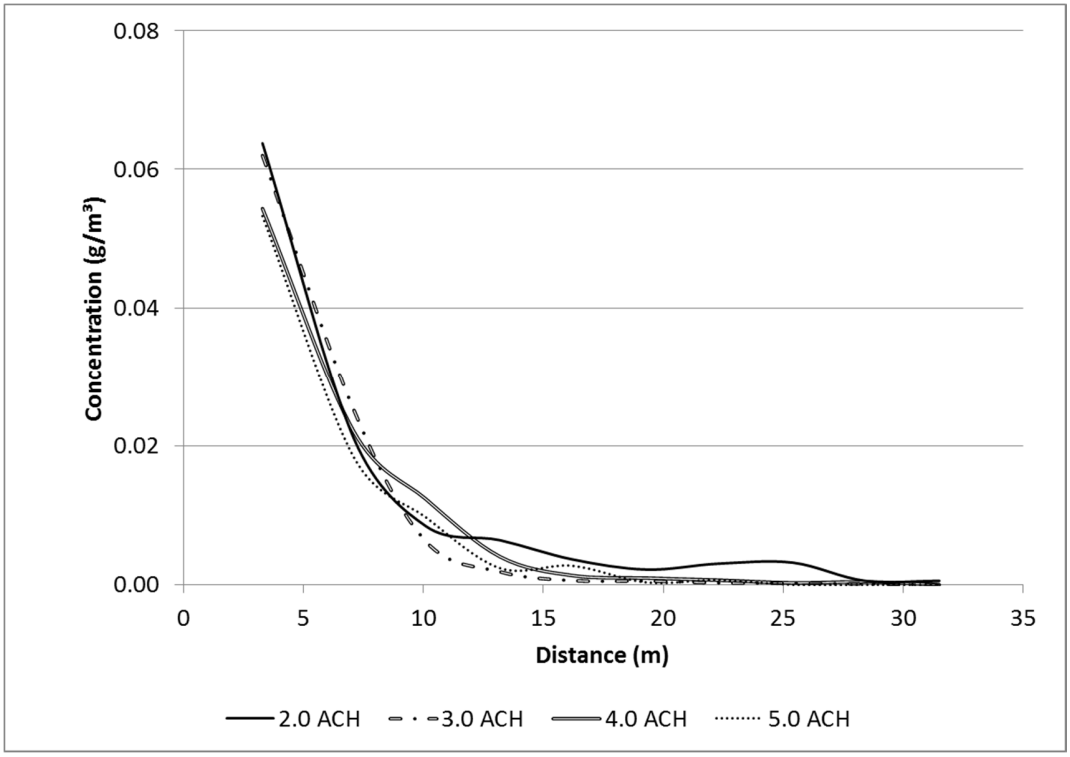

Figure 5-49 Particle Concentrations versus ACH, Existing Arrangement, Release Outside (x=0m)

Table 5-16 Particle Concentrations (gr/m^3) versus Ventilation Rate; *Existing* Arrangement, Release *Outside (x=0m)*

Sampling Location	Distance (m)	Ventilation Rates			
		2.0ACH	3.0ACH	4.0ACH	5.0ACH
Sample Location 1	3.3	0.0638	0.0620	0.0543	0.0533
Sample Location 2	7.1	0.0211	0.0252	0.0221	0.0184
Sample Location 3	10.1	0.0085	0.0063	0.0124	0.0097
Sample Location 4	13.2	0.0064	0.0019	0.0040	0.0024
Sample Location 5	16.2	0.0037	0.0006	0.0013	0.0027
Sample Location 6	19.3	0.0022	0.0006	0.0010	0.0003
Sample Location 7	22.3	0.0030	0.0003	0.0007	0.0007
Sample Location 8	25.4	0.0032	0.0002	0.0003	---
Sample Location 9	28.4	0.0006	0.0001	0.0004	---
Sample Location 10	31.5	0.0006	---	---	---
Average Concentrations		***0.0113***	***0.0097***	***0.0096***	***0.0087***

Considering the fact that introducing more energy will decrease concentrations, one can claim that the optimal case would take place when the product of the ventilation cost and average concentrations is minimum (Table 5-17).

Table 5-17 Ventilation Costs Relative to Average Concentrations; Existing Arrangement, Release *Outside (x=0m)*

Ventilation Rate (ACH)	2.0ACH	3.0ACH	4.0ACH	5.0ACH
Cost of Ventilation ($)	$719	$1,078	$1,438	$1,797
Average Concentrations (gr/m^3)	0.0113	0.0097	0.0096	0.0087
Cost × Concentration	*$8.12*	$10.48	$13.87	$15.74

As can be seen, when the release point was placed outside and for the existing arrangement, introducing more energy did not result in proportionally lower concentrations. Thus, the 2ACH case was the worthiest of all cases. A similar trend was observed for the modified arrangement. Particle concentrations decreased by distance from the source. The decline however, was more pronounced for the modified arrangement suggesting that interventions were successful in particle removal and containment (Figure 5-50). Furthermore, particles tended to accumulate around the new exhaust fan (Fan7) and thus created a local maximum around it. In fact, the increase in concentrations around the new fan was the main reason of effective containment. Near-the-source concentrations were more sensitive to ventilation rate. This can be attributed to eliminating the exhaust fan close to the entrance (Fan1) and thus higher flowrates did not cause an unfavorable suction at the door, which in turn, could elevate the near-the-source concentration by introducing more energy.

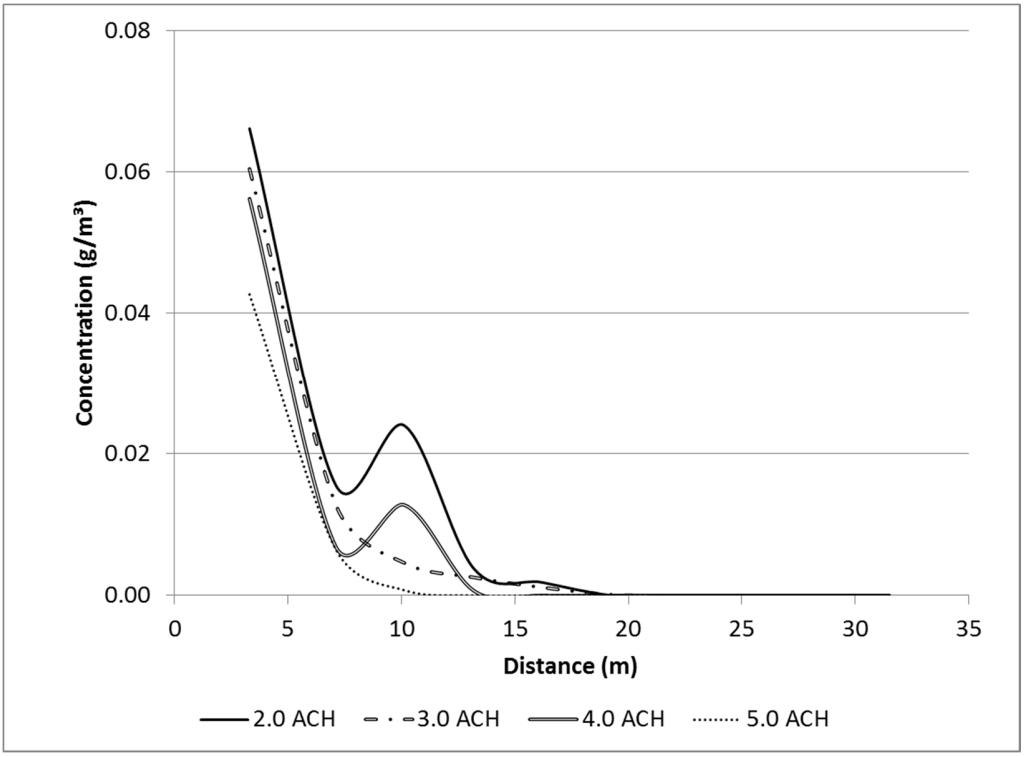

Figure 5-50 Particle Concentrations versus ACH, *Modified* Arrangement, Release *Outside (x=0m)*

Table 5-18 Particle Concentrations (gr/m^3) versus Ventilation Rate; *Modified* Arrangement, Release *Outside (x=0m)*

Sampling Location	Distance (m)	Ventilation Rates			
		2.0ACH	3.0ACH	4.0ACH	5.0ACH
Sample Location 1	3.3	0.0662	0.0604	0.0562	0.0427
Sample Location 2	7.1	0.0156	0.0128	0.0069	0.0065
Sample Location 3	10.1	0.0240	0.0046	0.0128	0.0008
Sample Location 4	13.2	0.0037	0.0025	0.0006	---
Sample Location 5	16.2	0.0018	0.0011	---	---
Sample Location 6	19.3	---	0.0001	---	---
Sample Location 7	22.3	---	---	---	---
Sample Location 8	25.4	---	---	---	---
Sample Location 9	28.4	---	---	---	---
Sample Location 10	31.5	---	---	---	---
Average Concentrations		***0.0111***	***0.0081***	***0.0076***	***0.0050***

Cost analysis showed that higher ventilation rates were not proportionally effective to remove particles from the space (Table 5-19)

Table 5-19 Ventilation Costs Relative to Average Concentrations; *Modified* Arrangement, Release *Outside (x=0m)*

Ventilation Rate (ACH)	2.0ACH	3.0ACH	4.0ACH	5.0ACH
Cost of Ventilation ($)	$719	$1,078	$1,438	$1,797
Average Concentrations (gr/m^3)	0.0111	0.0082	0.0077	0.0050
Cost × Concentration	*$8.01*	$8.81	$11.01	$8.98

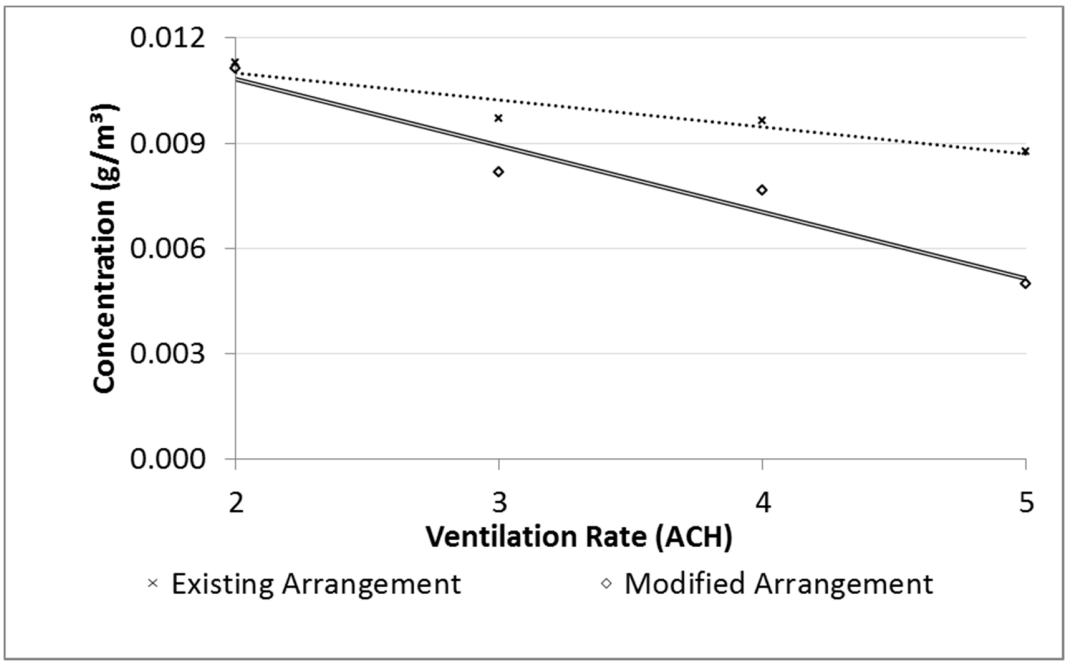

Figure 5-51 Particle Average Concentration Relative to ACH, *Released Outside (x=0m)*

As a general trend when the release point was outside, the average concentration disproportionately decreased by introducing more energy. This trend was almost linear

and more pronounced for the modified configuration meaning that the ventilation system was more efficient when the arrangement of grilles were adjusted (Figure 5-51).

Particle concentrations dramatically increased when the release point was placed inside. Since particles could move both directions when released inside, the distributions peaked near the release point and then concentrations decreased relative to distance (Figure 5-52).

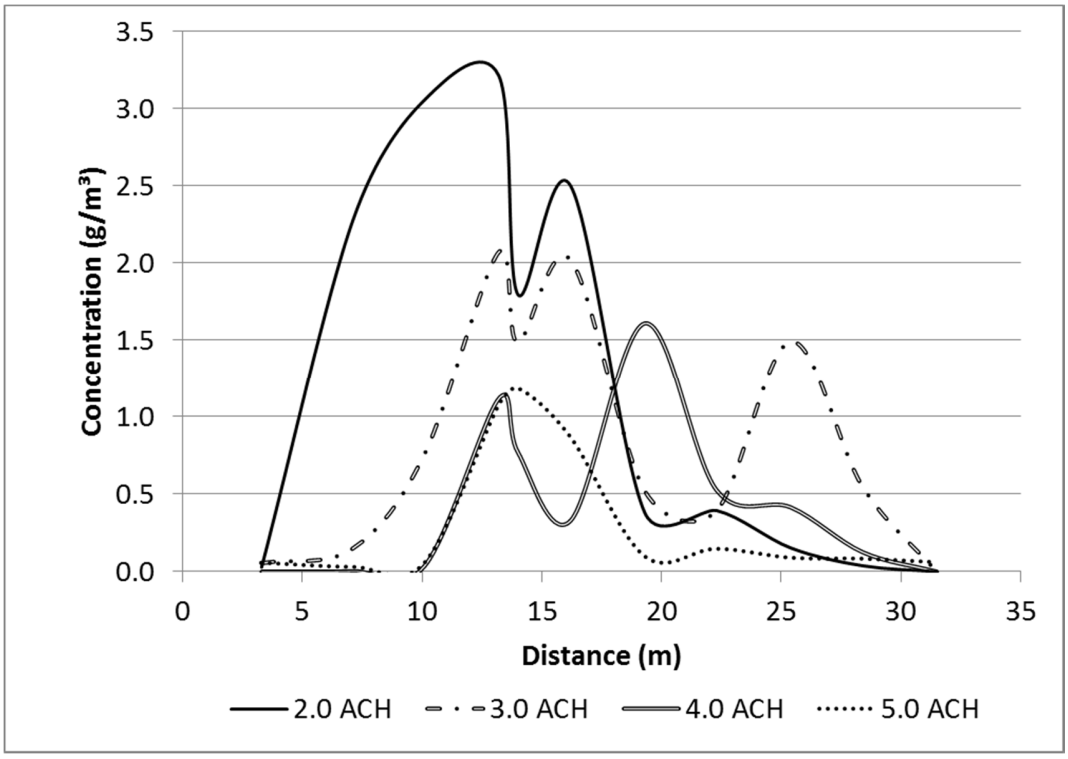

Figure 5-52 Particle Concentrations versus ACH, *Existing* Arrangement, Release *Inside (x=14m)*

As can be seen, 2ACH did not provide sufficient flow rate to drag the particles towards the nursing station area and the Brownian motion of particles was the dominant transport mechanism. On the other hand, there existed a second concentration peak by the location

of exhaust fans 2 and 3 (x≈25m) for higher ventilation rates (e.g. 3ACH and 4ACH). Since the release occurred right underneath the supply diffuser (Supply2), particles were forced to the sides swiftly and moved toward the nearest exhaust fans.

Table 5-20 Particle Concentrations (gr/m^3) versus Ventilation Rate; *Existing* Arrangement, Release *Inside (x=14m)*

Sampling Location	Distance (m)	Ventilation Rates			
		2.0ACH	3.0ACH	4.0ACH	5.0ACH
Sample Location 1	3.3	0.028	0.056	---	0.061
Sample Location 2	7.1	2.273	0.148	0.003	0.034
Sample Location 3	10.1	3.057	0.754	0.037	0.058
Sample Location 4	13.2	3.215	2.067	1.116	1.073
Release Point	14.0	1.797	1.485	0.770	1.184
Sample Location 5	16.2	2.502	2.021	0.329	0.871
Sample Location 6	19.3	0.380	0.523	1.610	0.102
Sample Location 7	22.3	0.394	0.392	0.525	0.151
Sample Location 8	25.4	0.153	1.490	0.415	0.092
Sample Location 9	28.4	0.038	0.549	0.126	0.087
Sample Location 10	31.5	---	---	---	0.633
Average Concentrations		***1.258***	***0.862***	***0.448***	***0.343***

Particle concentrations decreased when higher flowrates were introduced (Table 5-20). However, unlike the release outside cases, the trend was no longer linear and the average concentration changed exponentially relative to ventilation rate. This fact was also observed when calculating the cost-concentration correlation (Table 5-21). Cost of ventilation was commensurate with the decrease in concentration level.

Table 5-21 Ventilation Costs Relative to Average Concentrations; *Existing* Arrangement, Release *Inside (x=14m)*

Ventilation Rate (ACH)	2.0ACH	3.0ACH	4.0ACH	5.0ACH
Cost of Ventilation ($)	$719	$1,078	$1,438	$1,797
Average Concentrations (gr/m^3)	1.26	0.86	0.45	0.34
Cost × Concentration	$904	$930	$644	$617

Concentrations of particles declined considerably by rearranging the ventilation entries. It seemed that the modified arrangement could enhance the removal process when particles were released inside (Figure 5-53). This observation consolidated the influence of a proper ventilation arrangement for an internal contaminant source. Although in smaller amplitude, particle concentrations peaked at the whereabouts of new exhaust fans (x=11m and x=19m).

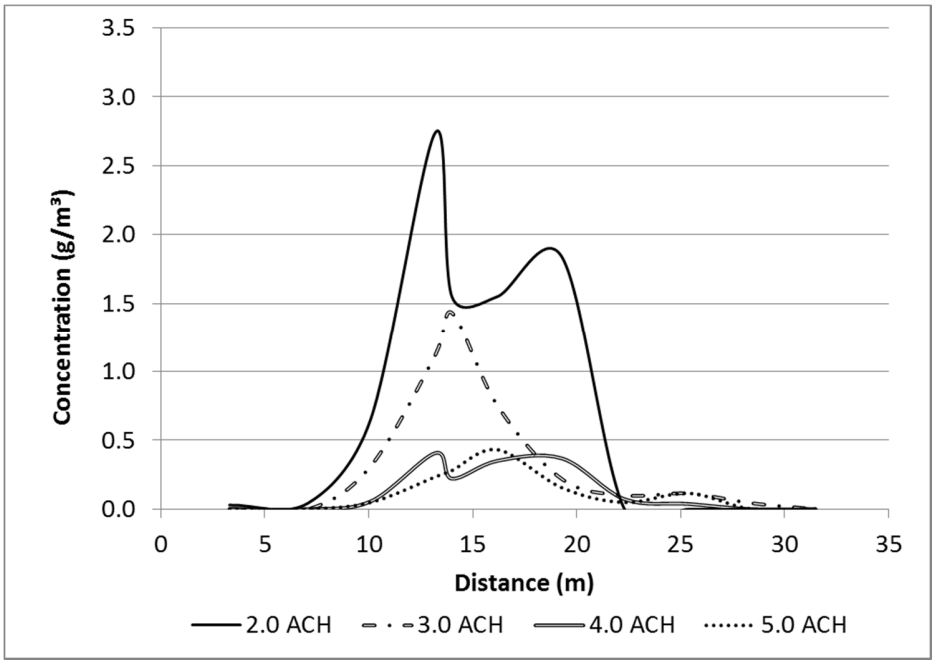

Figure 5-53 Particle Concentrations versus ACH, *Modified* Arrangement, Release *Inside (x=14m)*

Again, since lower ACH produced lower velocities, particles were less affected by the drag force caused due to difference in air-particle velocities. This in turn, resulted in a type of containment in which the concentration level was high. By introducing higher flowrates, particles were dispersed widely and had a better chance of reaching to the exhaust fans and eventually be removed from the domain (Table 5-22).

Table 5-22 Particle Concentrations (gr/m^3) versus Ventilation Rate; *Modified* Arrangement, Release *Inside (x=14m)*

Sampling Location	Distance (m)	Ventilation Rates			
		2.0ACH	3.0ACH	4.0ACH	5.0ACH
Sample Location 1	3.3	0.030	---	---	---
Sample Location 2	7.1	0.045	---	---	---
Sample Location 3	10.1	0.656	0.314	0.056	0.048
Sample Location 4	13.2	2.741	1.121	0.407	0.233
Release Point	14.0	1.550	1.431	0.221	0.279
Sample Location 5	16.2	1.552	0.749	0.351	0.429
Sample Location 6	19.3	1.836	0.217	0.368	0.153
Sample Location 7	22.3	---	0.100	0.072	0.047
Sample Location 8	25.4	---	0.113	0.037	0.114
Sample Location 9	28.4	---	0.043	---	---
Sample Location 10	31.5	---	---	---	---
Average Concentrations		***0.765***	***0.372***	***0.138***	***0.119***

Compared to the corresponding average concentrations for the existing arrangement, particle concentrations nearly halved. The reduction was more pronounced for higher ventilation rates (e.g. 65% reduction under 4ACH). However, the cost-concentration analysis revealed that adding more flowrate did not necessarily result in a proportional concentration decrease (Table 5-23). Therefore, concentration-wise, the modified arrangement and 4ACH were the optimum ventilation strategy for an internal source.

Table 5-23 Ventilation Costs Relative to Average Concentrations; *Modified* Arrangement, Release *Inside (x=14m)*

Ventilation Rate (ACH)	2.0ACH	3.0ACH	4.0ACH	5.0ACH
Cost of Ventilation ($)	$719	$1,078	$1,438	$1,797
Average Concentrations (gr/m^3)	0.76	0.37	0.14	0.12
Cost × Concentration	$550	$401	*$198*	$213

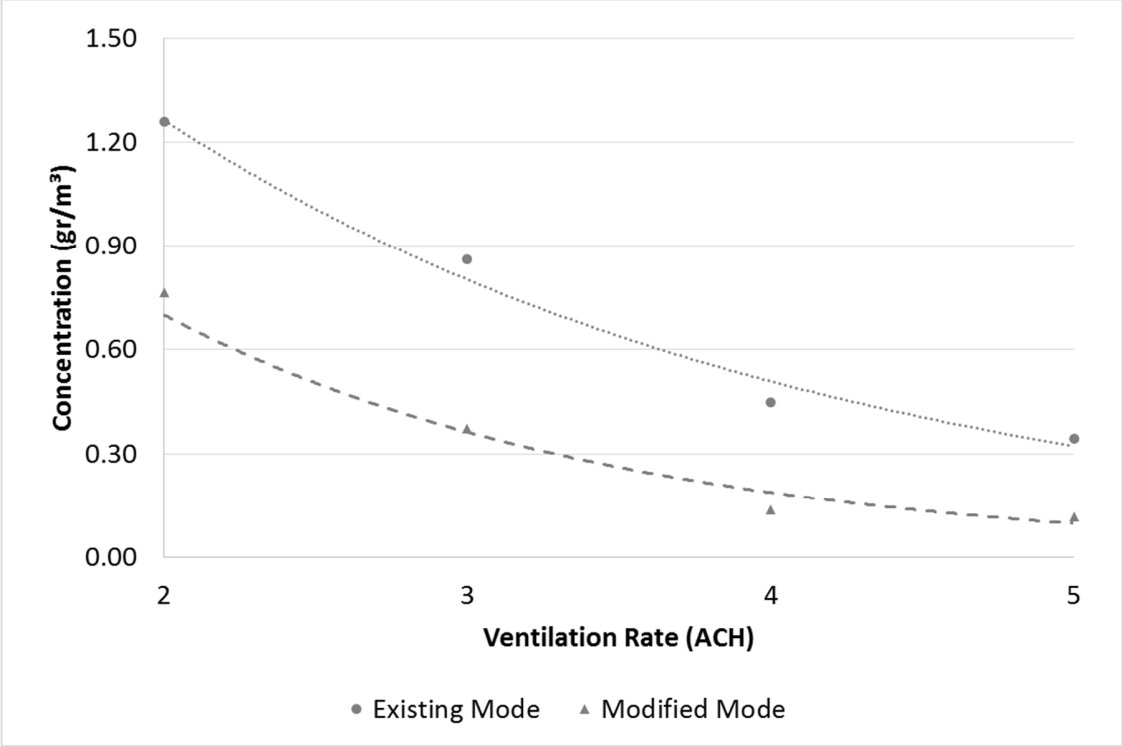

Figure 5-54 Particle Average Concentration Relative to ACH, *Released Inside (x=14m)*

Figure 5-54 demonstrates an exponential trend between the particle average concentration and ventilation rate. The trend is more pronounced for the modified arrangement meaning that an advertent modification in ventilation arrangement could potentially elevate the removal capacity of the ventilation system, holding the flow rate constant. Moreover, the exponential trends reached to a similar concentration magnitude when predicting the

0ACH (e.g. no ventilation). Essentially when the ventilation rate approaches zero, the placement of air entries and exists should not matter. Thus, particle average concentrations must be similar for both cases.

5.3.2 Distributions

In this section the distribution of particles will be scrutinized relative to ventilation rate. Results from the previous section revealed that releasing particles inside and underneath the supply diffuser (x=14m) may lead to a different *'cost-effective'* ventilation rate. Thus, a similar analyses are conducted to examine the effect of ventilation rate on particle distributions. For that purpose, four cases were defined based on the ventilation arrangement (existing vs. modified) and release point (outside vs. inside).

5.3.2.1 Case 1: Existing Arrangement, Release Outside *(x=0m)*

Particle distribution parameters were studied relative the ventilation rate. Particle average height increase for higher ventilation rates considering the upward movement of particle because of the ceiling level exhaust fans (Table 5-24).

Table 5-24 Distribution Parameters Relative to Ventilation Rates, *Case 1*

Ventilation Rate	Average Height	Breathing Zone Concentration	Distance form Source	Dispersion Ratio
Units	[m]	[%]	[m]	[-]
2ACH	1.08	18.5	5.50	0.39
3ACH	1.22	19.3	3.99	0.27
4ACH	1.43	27.5	4.65	0.35
5ACH	1.68	26.1	4.38	0.36

Admittedly, the average height was an indicative of concentration levels within the breathing zone. The average height of particles was determined by the balance between gravitational settling and the drag force. Since gravity was constant, higher ventilation rates caused a higher rate of presence within the breathing zone. Although by increasing the flowrates over a certain level (4ACH), the removal process became effective in such a way that the breathing zone concentration decreased. The distance from the source (x=0) represented how containment was achieved. Again, lower ventilation rates (e.g. 2ACH) could not effectively bring about the removal process and particles were transformed mostly due to diffusion. While, particles were oriented toward the exhaust fans at higher ventilation rates. Particularly for the existing arrangement, particles were more prone to migrate to the nursing station area (Figure 5-55). Similar trend was observed for the dispersion ratio parameter.

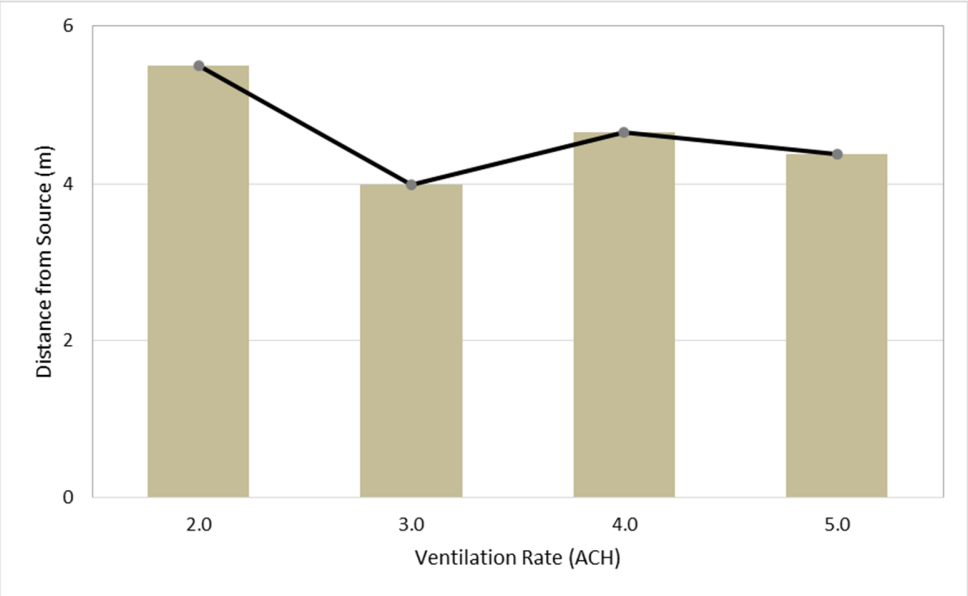

Figure 5-55 Distance from Source Relative to Ventilation Rate, *Case 1*

Potential improvements in this section come with the attributed cost of ventilation. Thus, all the distribution parameters were analyzed considering the extra cost of ventilation for higher rates. Breathing zone concentration, dispersion ratio, and the distance from the source divided by the length of the hallway used as the distribution parameters. The product of the ventilation cost and each distribution parameter were computed and added to find the overall cost (Table 5-25).

Table 5-25 Ventilation Costs Relative to Distribution Parameters, *Case 1*

Ventilation Rate	Ventilation Cost	Breathing Zone Concentration	Distance form Source	Dispersion Ratio	Total Cost
Units	[$]	[%]	[-]	[-]	[$]
2ACH	$719	0.185	0.14865	0.39	$520
3ACH	$1,078	0.193	0.10784	0.27	$616
4ACH	$1,438	0.275	0.12568	0.35	$1079
5ACH	$1,797	0.261	0.11838	0.36	$1328

Data suggested that the increase in flowrates did not end in a better distribution of particles. In fact, despite the use of more energy, particles were scattered within the hallway and remained suspended in a flow vortex even indefinitely. Thus, when particles were released outside and for the existing arrangement (Case 1), 3ACH exhibited the best performance while 2ACH is the worthies of all considering the extra cost of ventilation.

5.3.2.2 Case 2: Modified Arrangement, Release Outside *(x=0m)*

The particle average height were observed to have increased with ventilation rate. As alluded to earlier and in Case1, this can be ascribed to the ceiling height exhaust fans (Table 5-26).

Table 5-26 Distribution Parameters Relative to Ventilation Rates, *Case 2*

Ventilation Rate	Average Height	Breathing Zone Concentration	Distance form Source	Dispersion Ratio
Units	[m]	[%]	[m]	[-]
2ACH	1.31	22.3	3.12	0.24
3ACH	1.28	21.7	2.56	0.19
4ACH	1.58	25.6	2.6	0.16
5ACH	1.79	23.8	2.08	0.15

Other distribution parameters such as breathing zone concentrations, and lateral distribution parameters demonstrated a behavior similar to that observed in Case1. However, modifications seemed to have enhanced the removal process. In particular, the distance from the source parameter was somehow amended in higher ventilation rates due to more efficacious ventilation (Figure 5-56). The results suggested that proper ventilation arrangement could better justify the cost of higher ventilation rates in corridors.

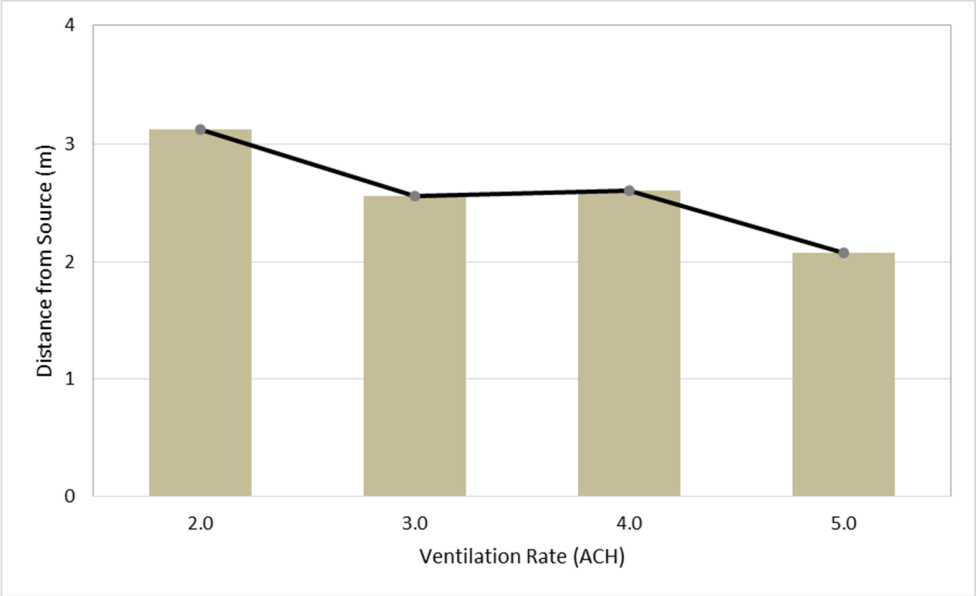

Figure 5-56 Distance from Source Relative to Ventilation Rate, *Case 2*

Table 5-27 Ventilation Costs Relative to Distribution Parameters, *Case 2*

Ventilation Rate	Ventilation Cost	Breathing Zone Concentration	Distance form Source	Dispersion Ratio	Total Cost
Units	[$]	[%]	[-]	[-]	[$]
2ACH	$719	0.223	0.084	0.24	$393
3ACH	$1,078	0.217	0.069	0.19	$513
4ACH	$1,438	0.256	0.070	0.16	$699
5ACH	$1,797	0.238	0.056	0.15	$798

2ACH was still deemed the most cost-effective ventilation rate. However, the ventilation cost for 3ACH in Case 2 was lower than that for 2ACH in Case 1 revealing the positive impact of modifications in the ventilation arrangement.

5.3.2.3 Case 3: Existing Arrangement, Release Inside *(x=14m)*

For 2ACH ventilation rate, particles were found at 1.09m away from the floor (σ= 0.78) (Figure 5-57). Concentrations of particles within the breathing zone was 25.7% suggesting that particles tended to either settle out or be removed.

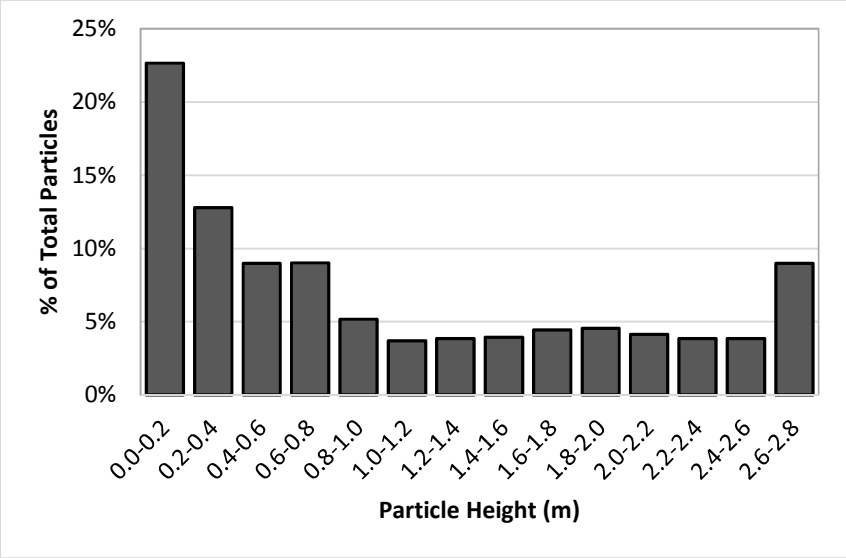

Figure 5-57 Vertical Distribution of Particles under 2ACH, *Case 3*

Next, the lateral distribution parameters were studied. Particles were scattered to the sides of the release point in a nearly symmetric manner. The mean distance from the source was 1.18m (σ= 4.87) (Figure 5-58). Containment was not fully achieved given the relatively moderate dispersion ratio (0.48).This was, perhaps, because of the improper ventilation arrangement and the lack of ventilation rate. The lateral distribution was almost symmetric (g=0.06) under 2ACH and relatively small kurtosis (β=0.56) revealed a mild lateral distribution.

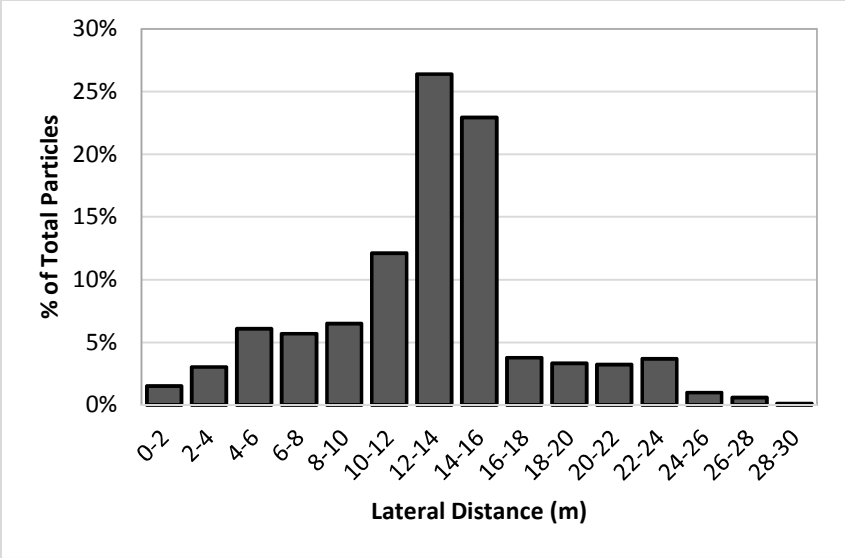

Figure 5-58 Lateral Distribution of Particles under 2ACH, *Case 3*

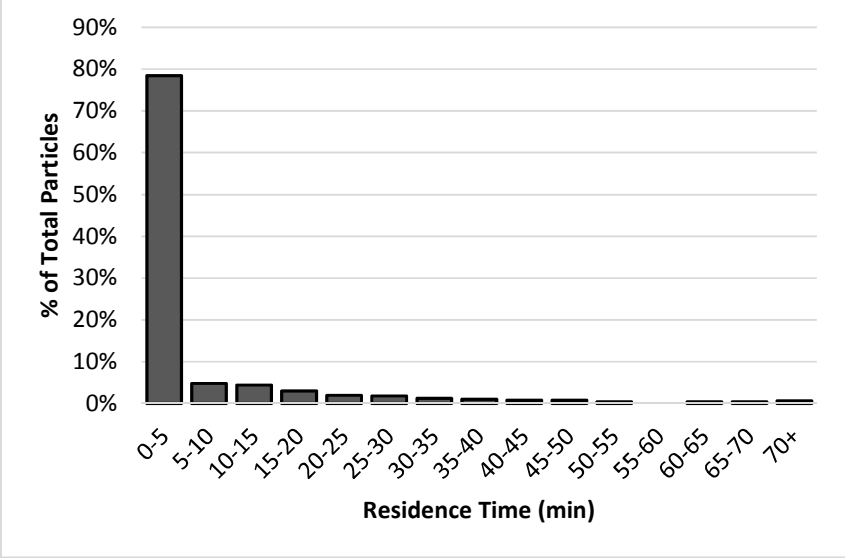

Figure 5-59 Particle Maximum Residence Time Distribution, 2ACH, *Case 3*

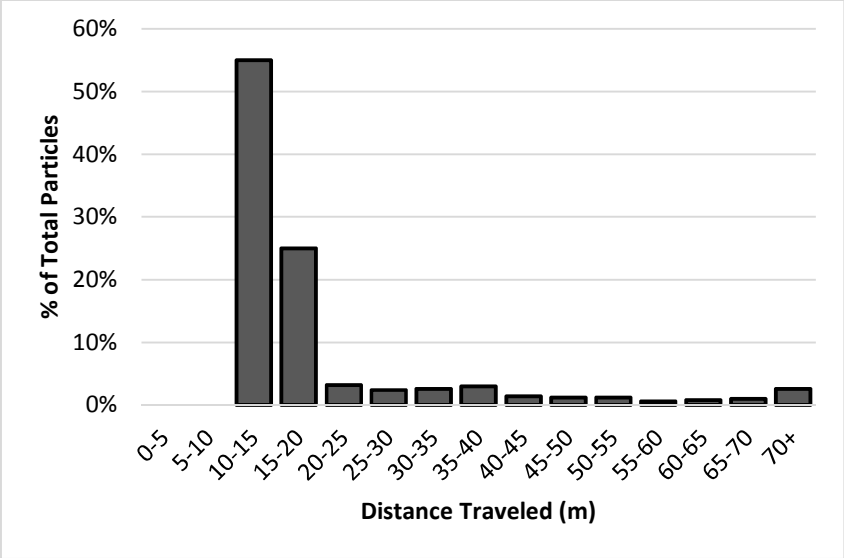

Figure 5-60 Particle Distance Traveled Distribution, 2ACH, Case 3

Particle maximum residence time had a mean of 5.5 minutes (σ= 13.7) (Figure 5-59) and the average distance traveled by particles was 20.9m (σ= 14.8) (Figure 5-60). Only 25% of particles were removed through the ventilation system under 2ACH ventilation rate. This was mainly because of insufficient flowrates at the exhaust fans.

Particle heights were more uniformly distributed under 3ACH (Figure 5-61). In fact, the ventilation rate was not sufficient to drag the particles up towards the exhaust fans. Thus, the breathing zone concentration (32.7%) slightly increased. Particles moved farther from the source under 3ACH (1.9m, σ= 5.80) and the lateral distribution was skewed to the right (g=0.57) where exhaust fans 2 and 3 produced a fairly large suction. Kurtosis was increased compared to 2ACH, but the distribution was still platykurtic (Figure 5-62).

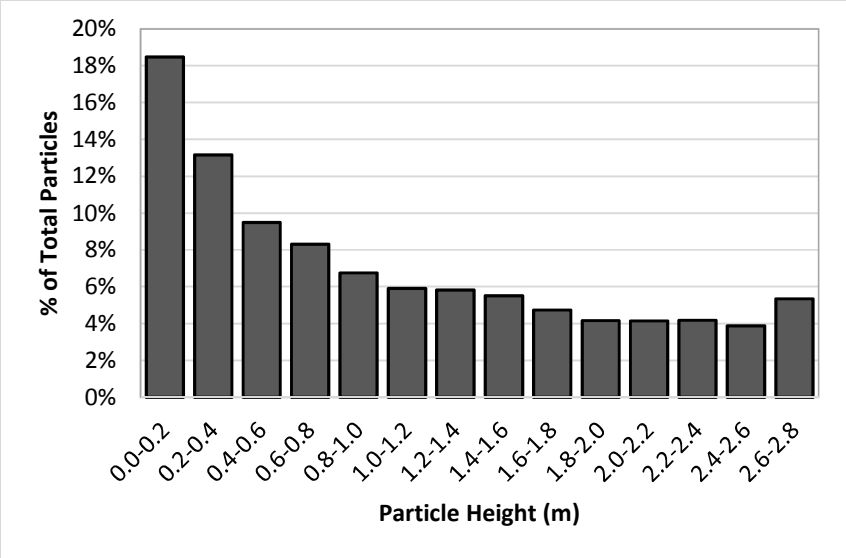

Figure 5-61 Vertical Distribution of Particles under 3ACH, *Case 3*

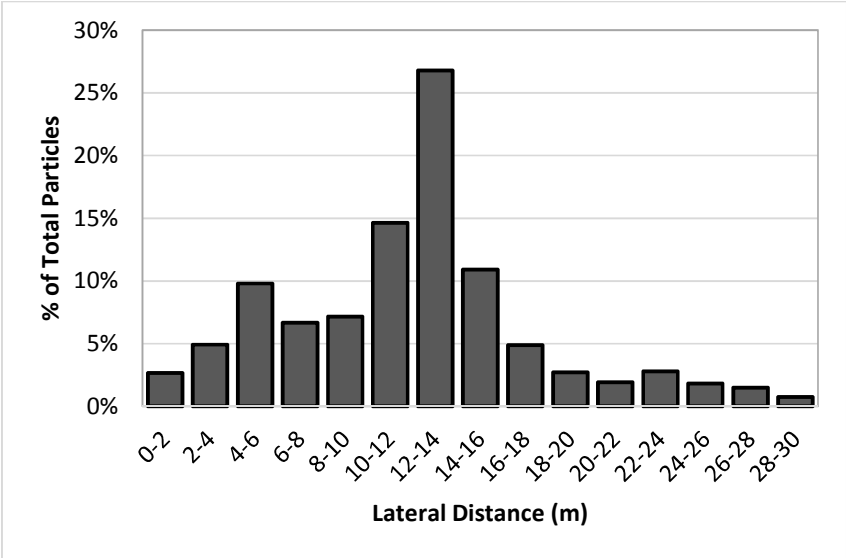

Figure 5-62 Lateral Distribution of Particles under 3ACH, Case 3

Particles remained, on average, 7.8 minutes (σ= 10.5) within the space before their final destiny (i.e. deposition, removal) which was longer than that under 2ACH (Figure 5-63). In addition, particles could travel 28.6m (σ= 21.0) under 3ACH (Figure 5-64).

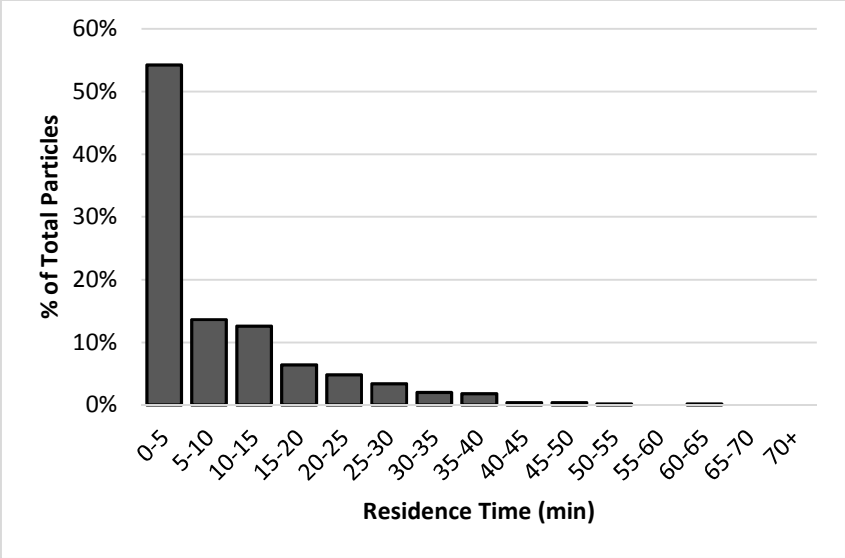

Figure 5-63 Particle Maximum Residence Time Distribution, 3ACH, Case3

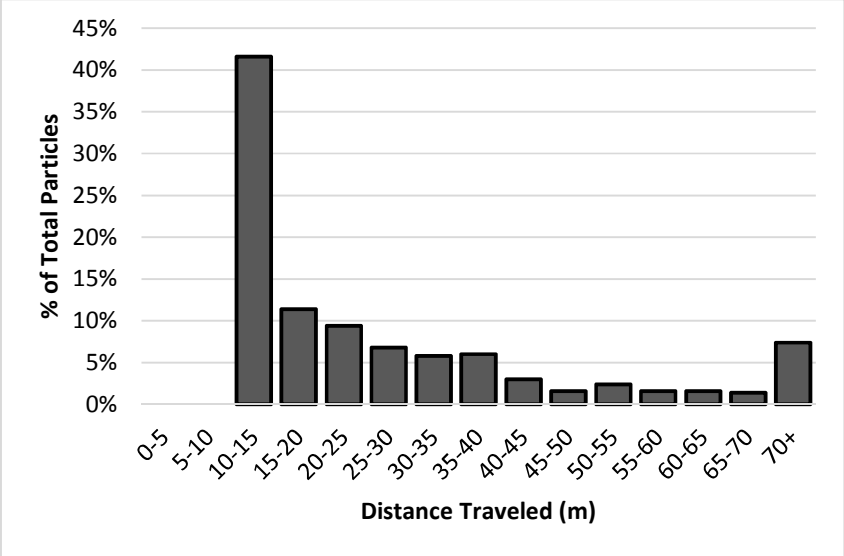

Figure 5-64 Particle Distance Traveled Distribution, 3ACH, Case 3

The ventilation system removed 29% of particles nearly half of which were removed by the exhaust fan at close to the entrance (Fan1) while the rest were removed by Fans 2 and 3.

The average height of particles slightly decreased upon an increase in ventilation rate. Thus for 4ACH the average height was 1.26m (σ= 0.84) reflecting an improvement in the removal process by the ventilation system (Figure 5-65). The breathing zone concentration was 29.5% which was slightly smaller than that for 3ACH.

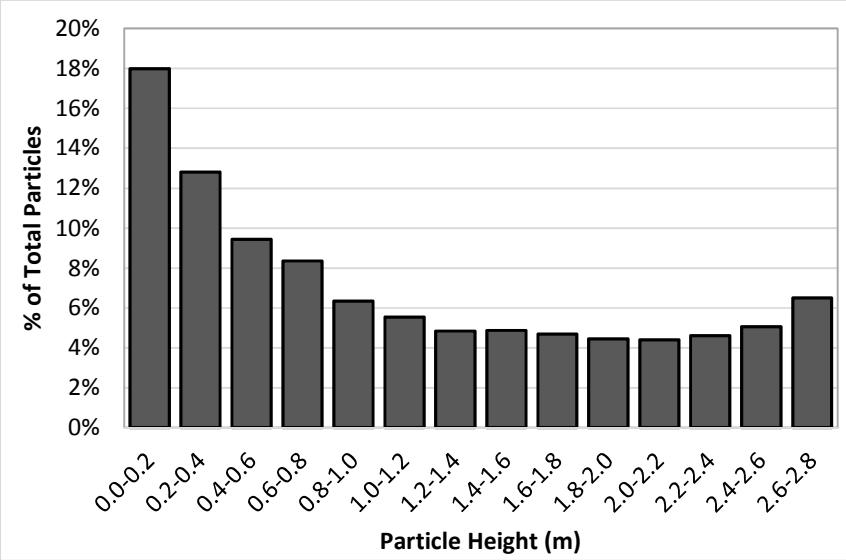

Figure 5-65 Vertical Distribution of Particles under 4ACH, *Case 3*

The lateral distribution of particles was somehow similar to that of 3ACH. However, the distance from source was 1.25m (σ= 5.52) and the distribution was skewed to the right because of the existing arrangement (g=0.6). The kurtosis was 0.91 and the dispersion ratio was 0.56 and particles were more prone to migrate towards the nursing station area (Figure 5-66). The average residence time (Figure 5-67) and distance traveled (Figure 5-68) of particles were 5.7 minutes (σ= 8.1) and 31.3m (σ= 24.1), respectively.

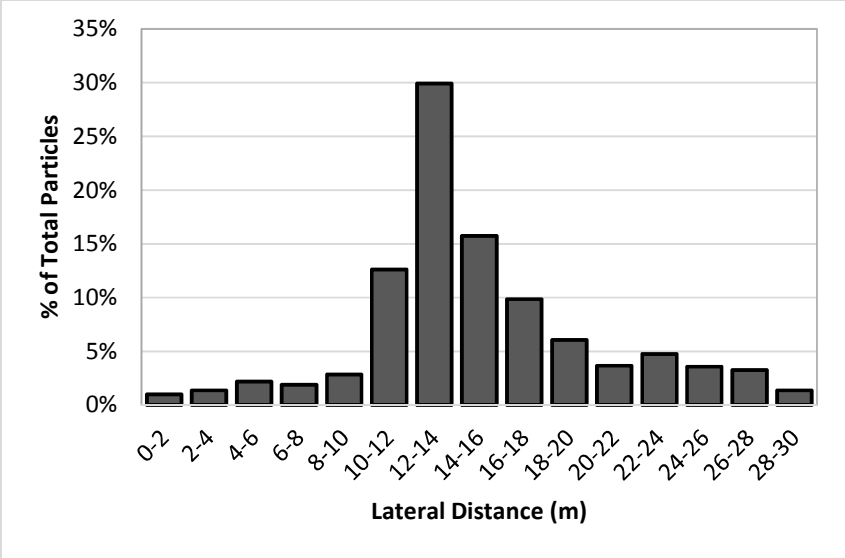

Figure 5-66 Lateral Distribution of Particles under 4ACH, *Case 3*

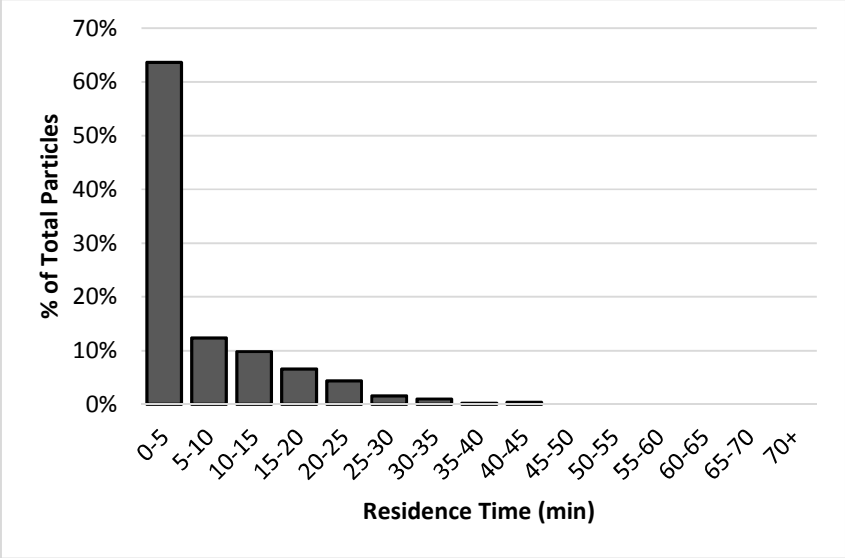

Figure 5-67 Particle Maximum Residence Time Distribution, 4ACH, *Case 3*

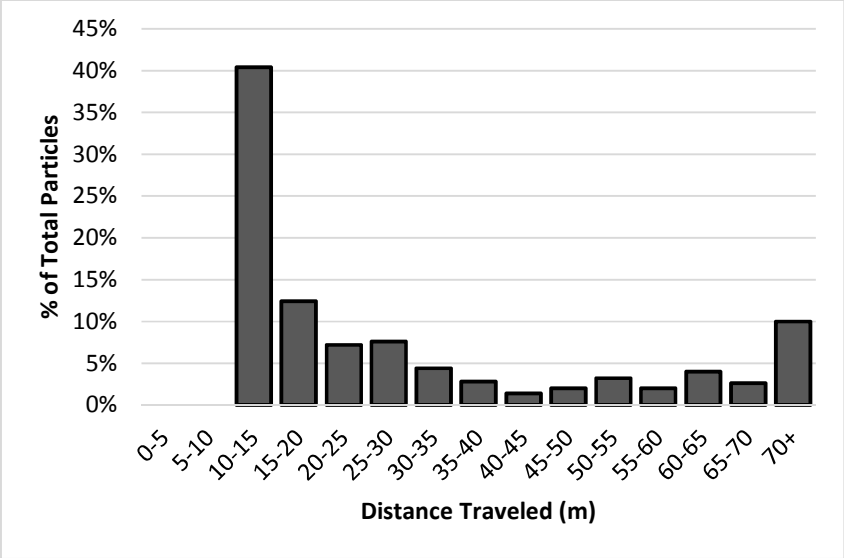

Figure 5-68 Particle Distance Traveled Distribution, 4ACH, *Case 3*

Distributions for 5ACH resembled that of 4ACH. It seemed that the trends in distributions became analogous for higher ventilation rates. A similar phenomenon was found in terms of particle concentrations where concentrations became indifferent to the flowrates upon introducing higher rates. Table 5-28 shows the removal rate and each fan's contribution to the overall removal process relative to ventilation rate. The removal rate increased with ventilation rate, though disproportionately. It should also be noted that particle were drawn to exhaust fans 2 and 3 when the flowrates increased.

Table 5-28 Removal By Ventilation System Relative to Ventilation Rate; *Case 3*

Ventilation Rate	Removal Rate	Fan1	Fan2	Fan3	Fan4	Fan5	Fan6
2ACH	25%	42%	17%	42%	0%	0%	0%
3ACH	29%	50%	34%	16%	0%	0%	0%
4ACH	29%	19%	56%	25%	0%	0%	0%
5ACH	32%	19%	52%	29%	0%	0%	0%

Table 5-29 summarizes the results of Case 3 pertaining to the distribution parameters. Despite the concentration trends, higher ventilation rates resulted in cluttered distributions. This is mainly because of the turbulence effect in higher flowrates. Results also depicted that under higher ventilation rates, the average particle velocity increased, which in turn, increased the risk of infection transmission.

Table 5-29 Distribution Parameters Relative to Ventilation Rate, *Case 3*

Ventilation Alignment	Average Height	Breathing Zone	Lateral Distribution Parameters					Max. Time	Distance Traveled
Units	[m]	[%]	DS[1]	σ	g	β	DR[2]	[min]	[m]
2ACH	1.09	25.7%	1.18	4.87	0.06	0.56	0.48	5.5	20.9
3ACH	1.31	32.7%	1.90	5.86	0.57	0.82	0.54	7.8	28.6
4ACH	1.26	29.8%	1.25	5.52	0.6	0.91	0.56	5.7	31.3
5ACH	1.25	29.3%	0.64	5.22	0.76	1.28	0.51	3.0	26.4

[1] DS = Distance from Source

[2] DR = Dispersion ratio

5.3.2.4 Case 4: Modified Arrangement, Release Inside *(x=14m)*

For this case the ventilation arrangement was modified as described in the method section. This case was essentially designed to examine the effect of ventilation arrangement on the optimum ventilation rate. When air was entrained on a 2ACH rate the average height of particles was 1.29m. Compared to Case 3, more particles were observed at the ceiling height suggesting that the removal process was more effective (Figure 5-69). Accordingly, 23.2% of particles were within the breathing zone range.

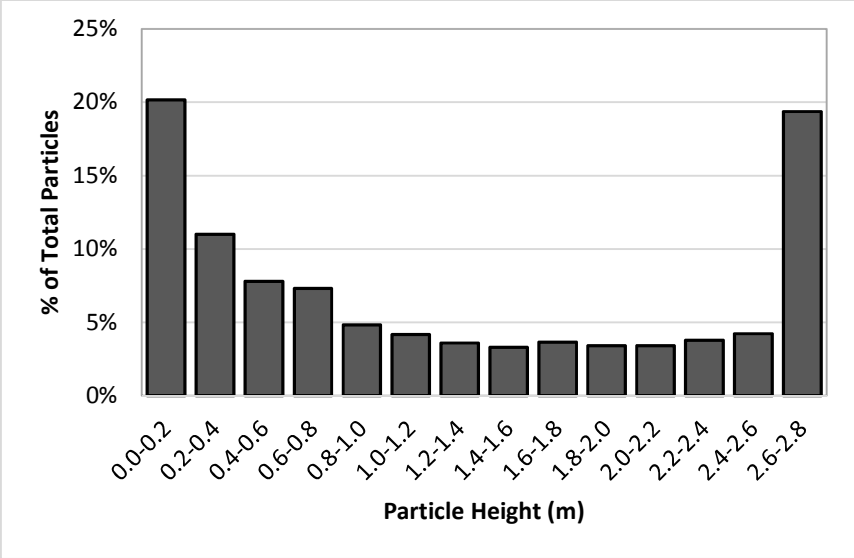

Figure 5-69 Vertical Distribution of Particles under 2ACH, *Case 4*

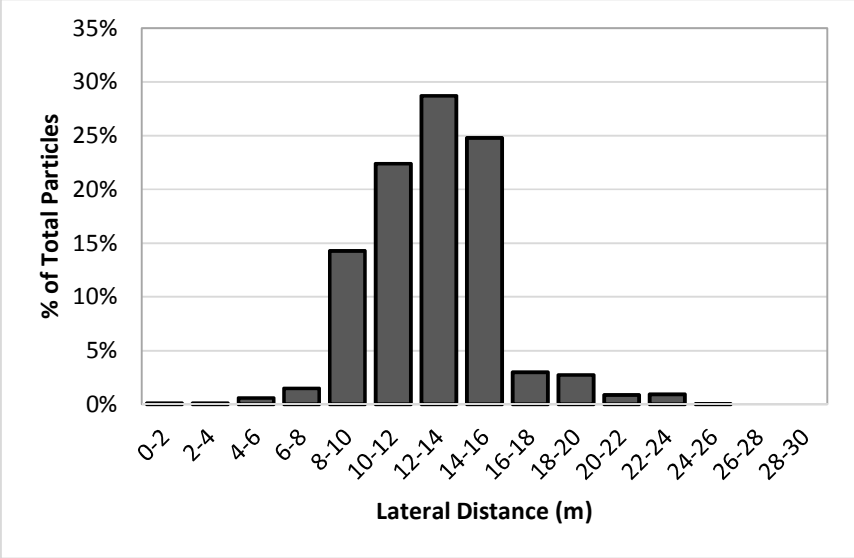

Figure 5-70 Lateral Distribution of Particles under 2ACH, *Case 4*

The lateral distribution of particles was slightly positively skewed (g=0.5) with a relatively high kurtosis (β=1.75) indicating an acceptable distribution compared to the existing arrangement. On the other hand, particles drifted away 1.28m (σ= 2.81) from the

source which brought about a dispersion ratio of 0.21 (Figure 5-70). Considerably improved containment was achieved in comparison with the existing configuration, where the corresponding value of dispersion ratio was 0.48, suggesting that a proper ventilation arrangement weighted more than ventilation rate in this case. Particle maximum residence time had an average of 5.3 minutes (σ= 9.4) (Figure 5-71) and the average distance traveled by particles was 22.7m (σ= 14.3) (Figure 5-72).

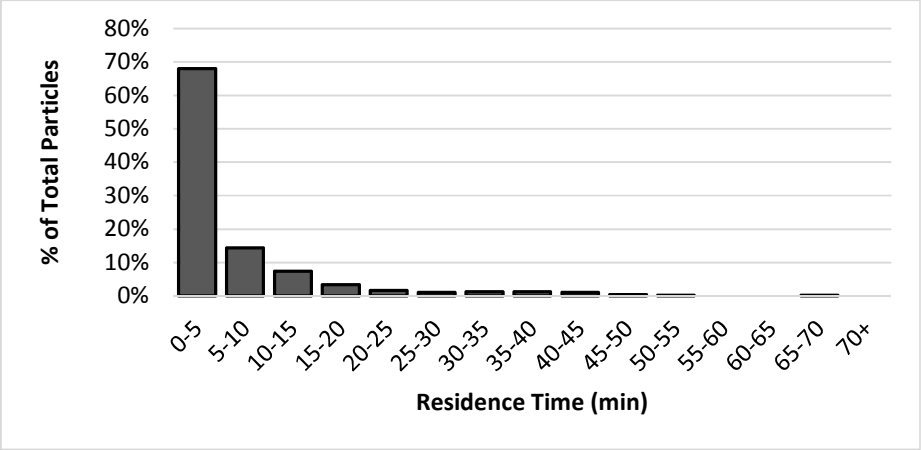

Figure 5-71 Particle Maximum Residence Time Distribution, 2ACH, *Case 4*

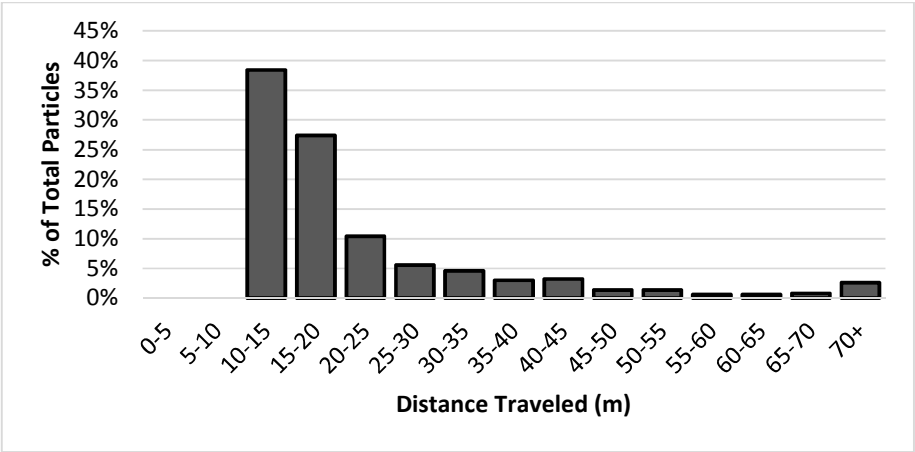

Figure 5-72 Particle Distance Traveled Distribution, 2ACH, *Case 4*

47% of particles were removed through the modified ventilation system under 2ACH ventilation rate. This was nearly twice the corresponding value under the existing arrangement. Indeed, the maximum lateral distance of the source from the closest exhaust fans was reduced from 13m to 5m by the new arrangement. Hence, particles were removed more effectively under the modified arrangement. As a result, more the three-quarters of particles were removed by Fan 7 which was repositioned in the modified arrangement.

Increasing ventilation rate to 3ACH did not result in an increase in the average height of particles. In fact, the average height for 3ACH was 1.17m (σ= 0.91) and only 10% of particles were observed to be within the ceiling height range (Figure 5-73). Moreover, 28.4% of particles were within the breathing zone.

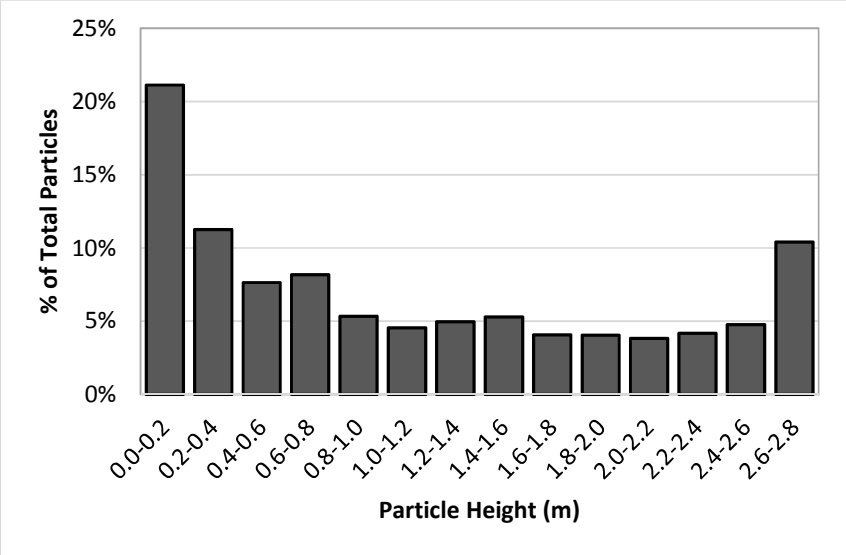

Figure 5-73 Vertical Distribution of Particles under 3ACH, *Case 4*

The average distance from the source was 1.28m (σ= 2.62) for 3ACH which was nearly identical to that for 2ACH. The lateral distribution was skewed to the right (g=0.78) and almost mesokurtic (β=2.83) (Figure 5-74). Dispersion ratio was 0.21 under 3ACH.

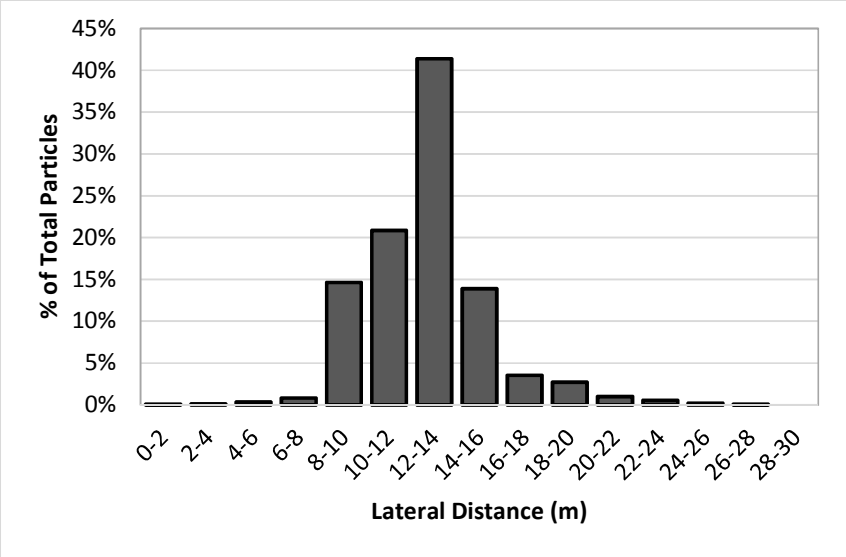

Figure 5-74 Lateral Distribution of Particles under 3ACH, *Case 4*

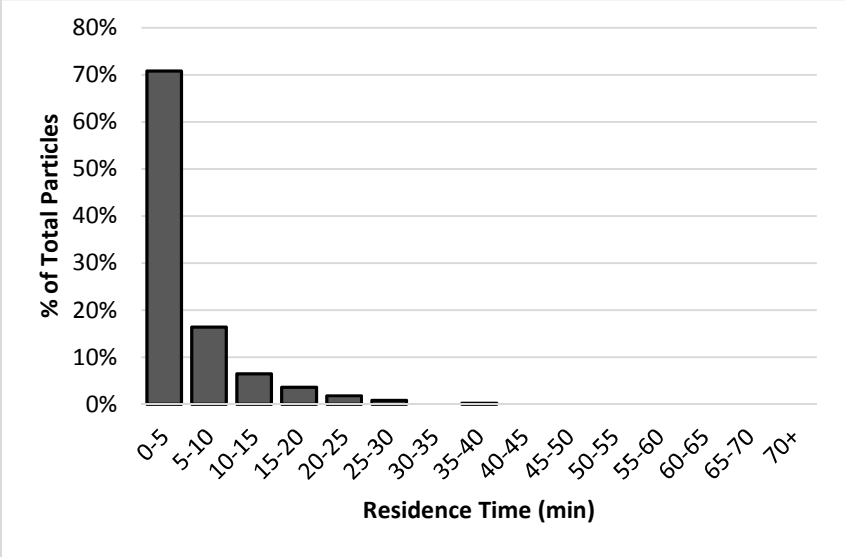

Figure 5-75 Particle Maximum Residence Time Distribution, 3ACH, *Case 4*

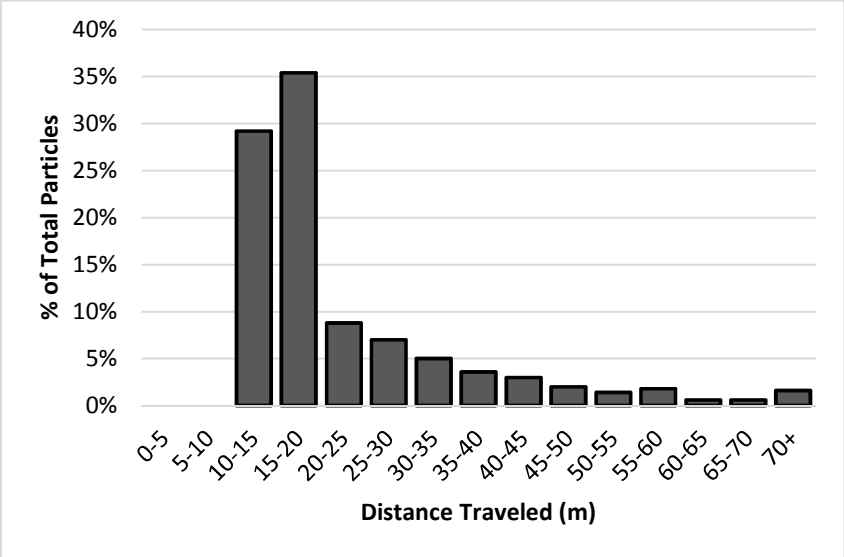

Figure 5-76 Particle Distance Traveled Distribution, 3ACH, *Case 4*

The mean time particles suspended in the space was 4.1 minutes (σ= 5.16) which was over 40% improvement compared to the existing arrangement. Almost 80% of particles were either removed or settled after only 10 minutes (Figure 5-75). Particles, on average, traveled 23.2m (σ= 13.3) before their final destiny. Compared to Case 3, more than 20% improvement was attained. However, particles traveled slightly longer by increasing the flowrates.

50% of particles were removed by the ventilation system. This number was larger than that for 2ACH, though sparingly. Fan 7 played a prominent role in the removal process by acting on 94% of the particles.

Flowrates, when increased to 4ACH, resulted in a more uniform vertical distribution. In fact, higher velocities and turbulence rate hindered the particle settling process such that 34.8% of particles existed within the breathing zone range (Figure 5-77).

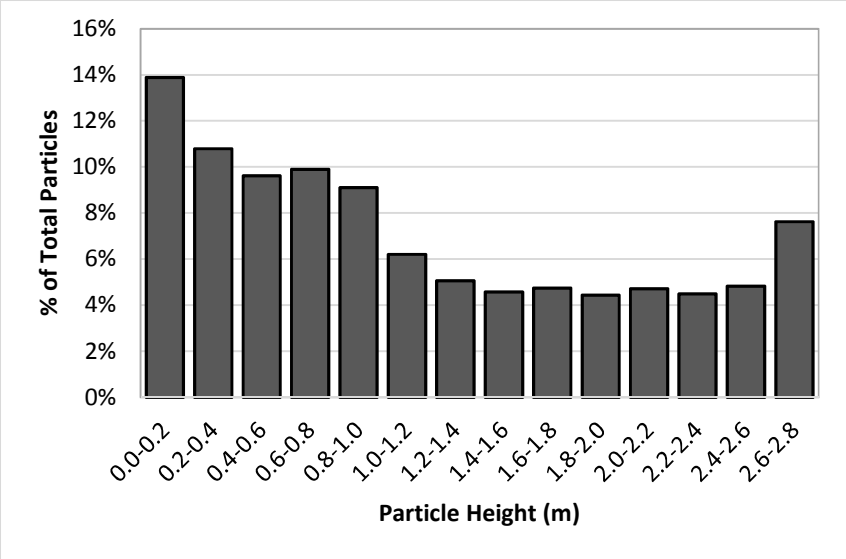

Figure 5-77 Vertical Distribution of Particles under 4ACH, *Case 4*

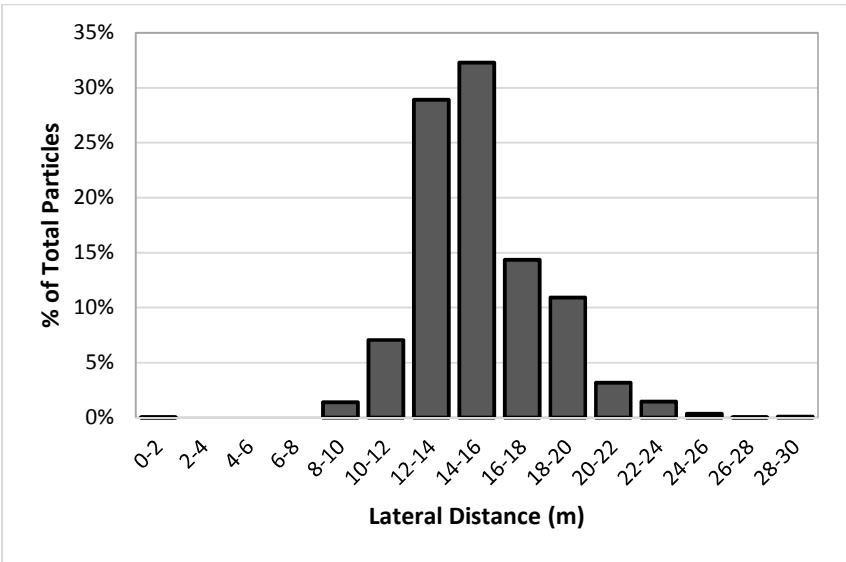

Figure 5-78 Lateral Distribution of Particles under 4ACH, *Case 4*

The lateral distribution of particles were leptokurtic (β=3.18) suggesting that particles tended to remain near the release point. However, the positive skewness (g=1.1) showed a propensity towards the nursing station area (Figure 5-78). The dispersion ratio was 0.34 which was by far the largest value compared to other ventilation rates. Relatively higher dispersion ratio could be attributed to higher air velocities that aggravated the containment and help particles scatter further and faster.

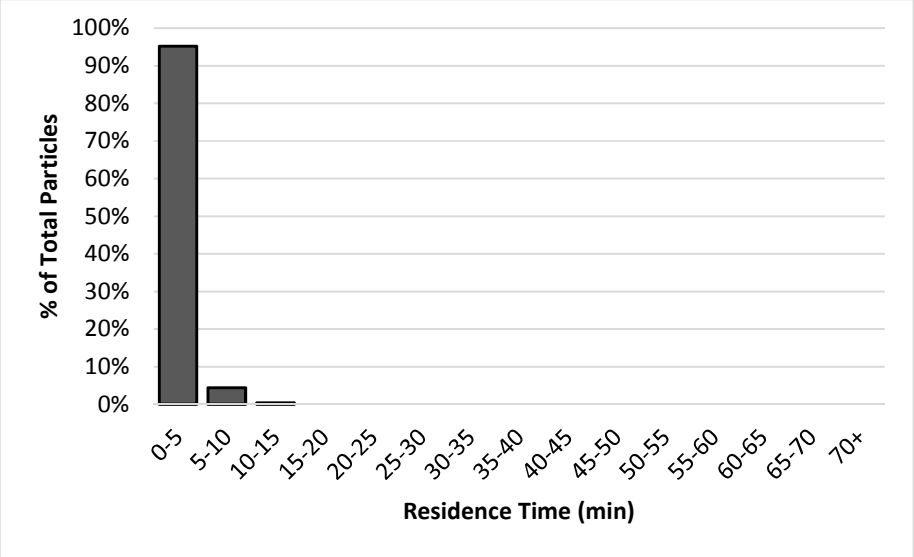

Figure 5-79 Particle Maximum Residence Time Distribution, 4ACH, *Case 4*

The maximum residence time of all particles was within 15 minutes after releasing (Figure 5-79). Given the lower removal rate, it can be concluded that deposition was the dominant destiny. The average distance traveled was 25.6m (σ= 10.15) and none of the particles reached to their final destiny before traveling at least 10.0m (Figure 5-80).

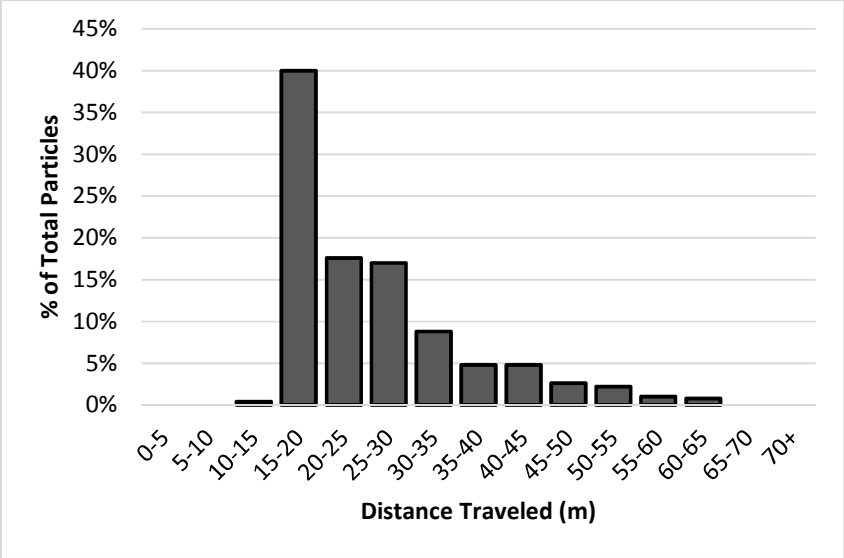

Figure 5-80 Particle Distance Traveled Distribution, 5ACH, *Case 4*

The vertical distribution seemed to aggravate with introducing more ventilation rate. For 5ACH, at least 5% of particles existed within all height ranges resulting in 35.3% dispersion ratio (Figure 5-81).

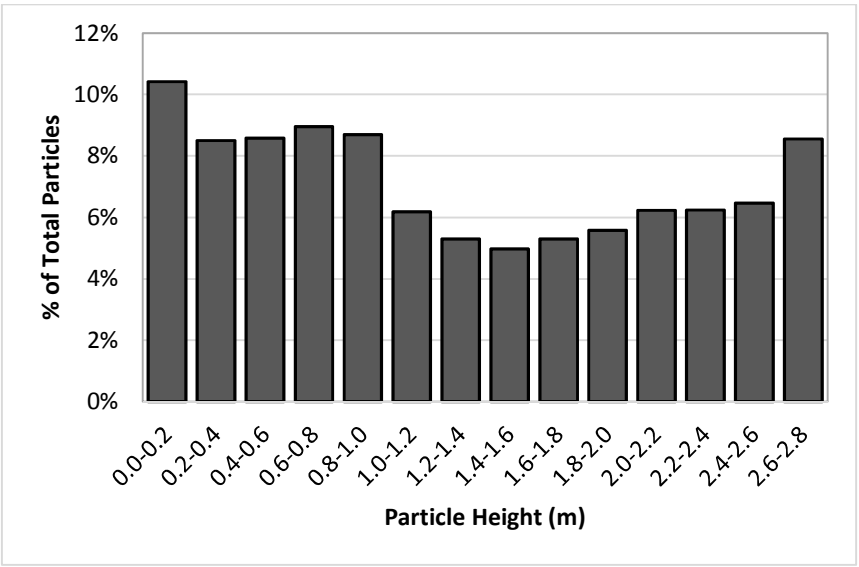

Figure 5-81 Vertical Distribution of Particles under 5ACH, *Case 4*

The lateral distribution was also positively skewed (g= 0.75); however, the kurtosis (β=2.20) was smaller compared to 4ACH mainly because particles were able to migrate further from the source (Figure 5-82). Consequently, the dispersion ratio was 0.27 which was comparable to that of 4ACH. Nevertheless, the dispersion ratio halved compared to the existing arrangement meaning that the modifications were decent and effective.

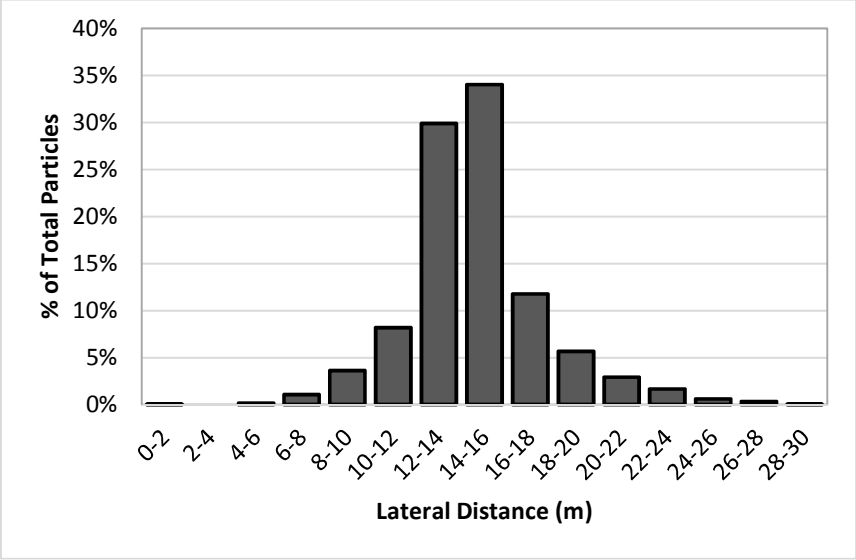

Figure 5-82 Lateral Distribution of Particles under 5ACH, *Case 4*

Ninety nine percent of particles had a maximum residence time less than five minutes (Figure 5-83) and the average distance traveled by particles was 24.0m (σ= 10.09) (Figure 5-84). Data suggested that even though the maximum residence time substantially decreased with the flowrates, the average distance traveled term remained approximately the same, and therefore, particles' average velocity increased with ventilation rate. As alluded to earlier, higher particle velocities *may potentially* lead to a higher risk of infection transmission.

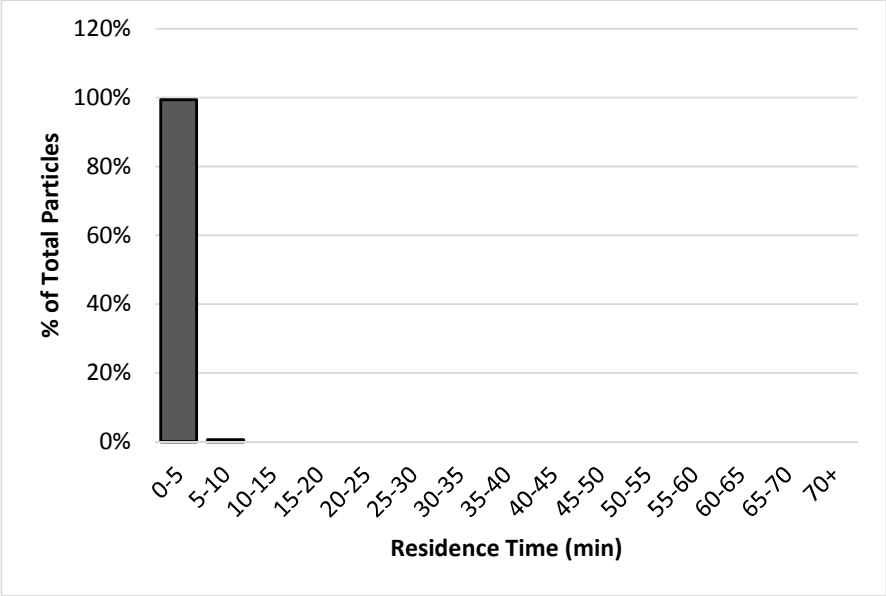

Figure 5-83 Particle Maximum Residence Time Distribution, 5ACH, *Case 4*

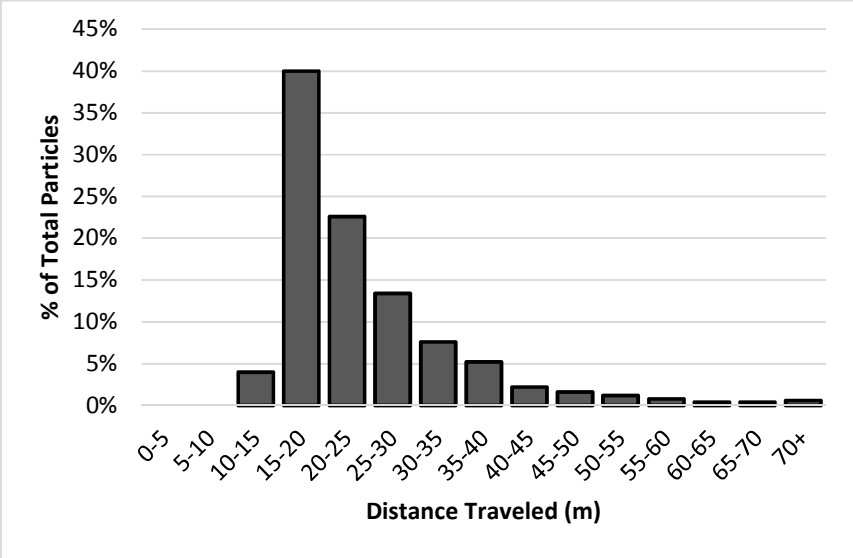

Figure 5-84 Particle Distance Traveled Distribution, 5ACH, *Case 4*

Table 5-30 shows the removal process relative to ventilation rate. Increasing the ventilation rate did not necessarily enhance the removal process mainly because particles with higher velocities were prone to be deposited more easily. In all ventilation rates,

particles were removed by Fans 7, 8, and 3 which were roughly 10.0m apart. Admittedly, by entraining more air, particles migrated further and eventually removed by the farther exhaust fans (i.e. Fans 7 and 3). Thus, the removal rate for Fans 7 and 3 increased for higher ventilation rates (i.e. 4ACH and 5ACH) whereas most of the particles were removed by Fan 8 under lower rates (i.e. 2ACH and 3ACH).

Table 5-30 Removal By Ventilation System Relative to Ventilation Rate; *Case 4*

Ventilation Rate	Removal Rate	Fan7	Fan8	Fan3	Fan4	Fan5	Fan6
2ACH	47%	1%	78%	21%	0%	0%	0%
3ACH	50%	0%	94%	6%	0%	0%	0%
4ACH	35%	8%	54%	38%	0%	0%	0%
5ACH	39%	24%	42%	34%	0%	0%	0%

Table 5-31 summarizes the results of Case 4 pertaining to the distribution parameters. Similar to Case 3 and despite the concentration trends, higher ventilation rates resulted in cluttered distributions. Therefore, as far as the distribution is concerned, an increase in the ventilation rate was neither beneficial nor congruent with the extra ventilation cost.

In addition, comparing Cases 3 and 4 revealed an enormous capacity lied in the root of ventilation arrangement. Not only were the concentrations comparable to those of a higher ventilation rate in the existing arrangement, but the distributions were also appreciably rectified by the proper arrangement.

Table 5-31 Distribution Parameters Relative to Ventilation Rate, *Case 4*

Ventilation Alignment	Average Height	Breathing Zone	Lateral Distribution Parameters					Max. Time	Distance Traveled
Units	[m]	[%]	DS1	σ	g	β	DR2	[min]	[m]
2ACH	1.29	23.2%	1.28	2.81	0.51	1.75	0.21	5.3	22.7
3ACH	1.17	28.5%	1.28	2.62	0.78	2.82	0.21	4.1	23.1
4ACH	1.19	34.0%	1.19	2.79	1.10	3.18	0.29	2.0	25.6
5ACH	1.34	35.3%	0.64	2.96	0.75	2.20	0.27	1.0	24.3

[1] DS = Distance from Source

[2] DR = Dispersion ratio

CHAPTER 6: CONCLUSIONS

6.1 Summary and Conclusions

This work is largely designed to address the issue of airborne infection control in hospital corridors. Specifically, questions are asked about the pressure relationship, ventilation arrangement, and ventilation rates from which the first and last parameters are regulated by current codes. Moreover, nuances on the effect of particle size have been contemplated.

Experimental data suggested that under the neutral ventilation mode, 0.5µm particles remained above background concentrations to a distance of 22.3-25.4m (73.2-83.3ft) in the main corridor of a general patient ward. In contrast, particles 1.0-3.0µm remained above background concentrations roughly half the distance (13.2m, 43.3ft) from the release point and had decay rates three-to-four times higher than 0.5µm particles under the neutral mode. Under the negative ventilation mode, particles 1.0-3.0µm remained above background concentrations more than twice the distance (28.4-31.5m, 93.2-103.3ft) and had deposition rates one-half that of 1.0-3.0µm particles under the neutral mode. Particles 0.5µm remained above background concentrations to a distance of 31.5m (103.3ft) under the negative mode, but had deposition rates nearly the same as 0.5µm particles under the neutral mode. Results also indicate that airflow may have a greater effect on the movement of respiratory aerosols ≥1.0µm (bacteria and fungi) than aerosols <1.0µm (viral droplet nuclei). With comparatively less regard to airflow, <1.0µm particles may readily diffuse into the air and prove more difficult to contain and remove from the healthcare environment. Particles ≥1.0µm may be more effectively contained

and removed by airflow, but may also be more readily dispersed by malfunctioning or improperly designed ventilation systems.

CFD results, by and large, conceded the experimental findings. Particle concentrations and distribution exacerbates upon introducing directional flow (i.e. negative mode). Four cases, defined based on the release point and ventilation arrangement, unanimously corroborate the superiority of a neutral mode in hospital corridors. ASHRAE Standard 170-2013 however, does not require a certain pressure relationship with adjacent spaces. The reason could be sought in the fact that corridors are somehow a common space whose pressure relationship is dictated by the adjoining specialty areas, such as an airborne infectious isolation room. Results of this work, however, illustrate that corridors must be balanced in terms of inlet/outlet flowrates. In other words, the amount of air in and out of a corridor must be equal.

Furthermore, flow direction is not solely dependent on pressurization, but to an extent, it depends on the inlet/outlet arrangement. Accordingly, the results of this study showed that an attentive, premeditated ventilation arrangement may substantially perform better in containment and removal of airborne particles. Specifically, results reveal that a proper arrangement under the negative mode can have analogous performance to that of a poor design under the neutral mode. It is also worthy to note that particular space functions such as isolation rooms, protective environments, and even morgues are required specific grille placements in ASHRAE 170-2013. This study advocates a ventilation arrangement for corridors where an exhaust grille is placed between every two supply diffuser.

Minimum ventilation rates are required in patient corridors by current codes. Both concentrations and distributions of airborne particles are affected by the flowrates at boundaries. Obviously, concentrations of a contaminant decrease when more air is entrained into the space. This however, comes with a price. Therefore, this study attempts to find if the decrease in concentration level is worth the extra ventilation cost. Results suggested that the *cost effective* ventilation rates depends on the source position. If released outside, 2ACH is the optimum rate; whereas, 4ACH seems to be optimum for an internal source. In both cases, the modified arrangements return better results to the extent that the average concentration of particles under 2ACH and modified arrangement was comparable to that of 4ACH under the existing arrangement.

The results pertaining to the distribution of particles are clear-cut. Lower ventilation rates produce less perturbations and cause better containment. By increasing flowrates, and consequently air velocity, particles tend to move farther and faster (**Error! Reference source not found.**). The modified arrangement certainly facilitates the removal process through ventilation system and mitigates particle distributions. Again, the idea of compartmentalization of the corridor can be seen in the results of the modified arrangement (Figure 6-2). Thus, 2ACH demonstrate to have caused more desirable distributions with less risk of airborne infection transmission.

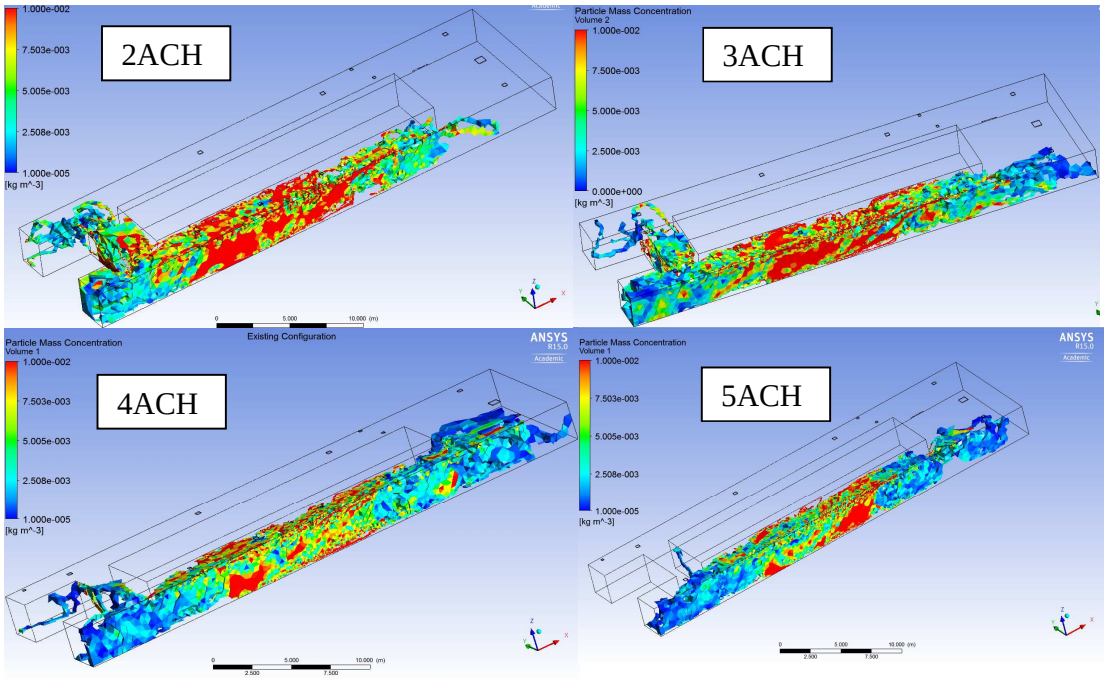

Figure 6-1 Particle Concentration and Distribution versus ventilation rate; Existing Arrangement

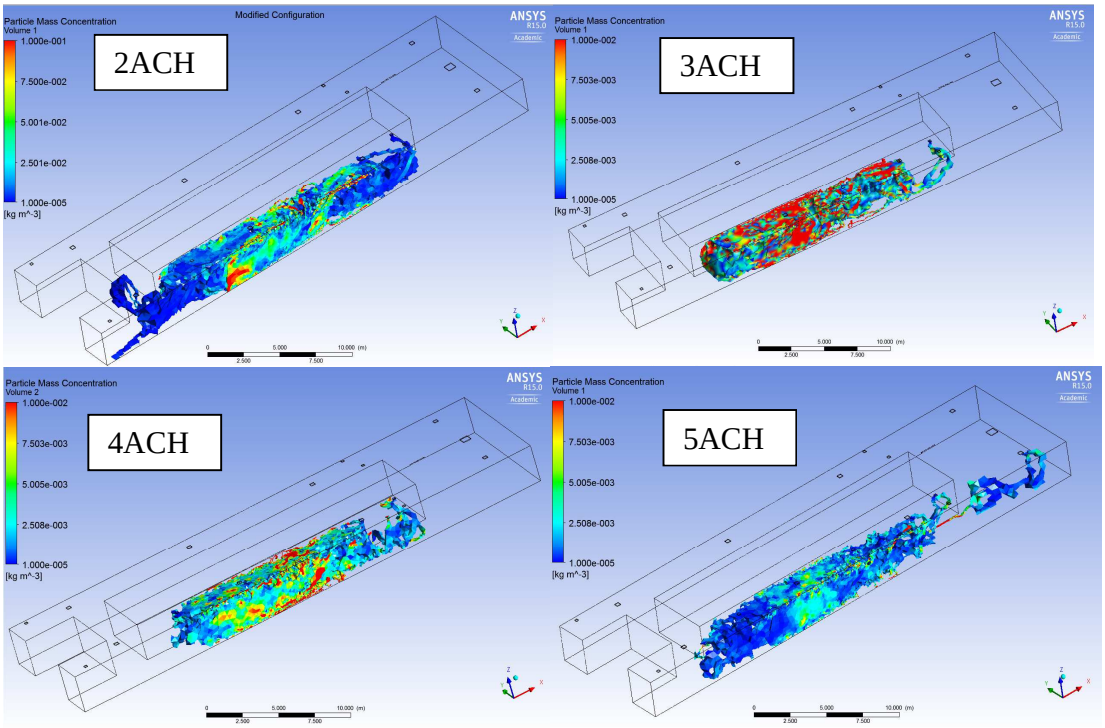

Figure 6-2 Particle Concentration and Distribution versus ventilation rate; *Modified* Arrangement

6.2 Future Work and Limitations

Arising from this work, several lines of research should be followed in the future, which either will improve this work or lead to new findings, and they are discussed below:

- The majority of findings especially those pertaining to ventilation rate emanate from the CFD modeling. Although developing computer models is an excellent and affordable approach for such research, an experimental counterpart could consolidate the findings. Thus, providing a controlled environment where the ventilation rate is adjustable can greatly add to the existing knowledge on this area.
- As stated in the method section, infiltration and exfiltration was neglected for this work due to computational intricacies and uncertainties. Therefore, a real size experimental facility to examine the effect of infiltration and exfiltration of airborne particle transport would be of real interest. This can be also complemented by computer models.
- Supply inlets were assumed to entrain air vertically. This assumption was made due to the type of diffusers used in the actual hospital (Figure 3-14). However, a more common design approach is the horizontal distribution in which better air distribution is achieved. Results of this work may be affected by changing the direction air enters through supply diffusers, and thus, it can be a relevant issue to be experimentally and computationally studied.

- One limitation of this work was the absence of ample information as to heat sources available within corridors of the actual hospital. This could be an indicative of buoyancy force and its consequences on air motion.
- There are several source of uncertainty in hospital corridors of which moving objects are of vigorous importance. In fact, pathogens may be released from a moving object whose direction and velocity influence the transport mechanism of particles. Studying the influence of moving objects on the optimum ventilation rate, pressurization strategy and other standard-level parameters can be a good addition to this research.
- Since not enough sample recorders were available in the experimental procedure, particle concentrations were collected relative to time and distance. In fact, changes in particle concentrations are not readily attributable to spatial or temporal variables. However, since air motion is in the steady-state condition, one could safely assume that after ‘sufficiently long’ time particle concentrations reach to the steady-state condition where no more change is observed in particle concentrations relative to time. Nevertheless, this is an experimental limitation of the current work and may potentially be a decent question for future research.
- Finally, other modifications to ventilation arrangement may be considered for future research. Wall-mounted exhaust fans, or the displacement ventilation system are good examples. Therefore, similar methodology can be adopted to study the effect new modifications on particles, and perhaps, an arrangement may

be discovered that best serves hospital corridors when thermal comfort and indoor air quality are both of concern.

REFERENCES

1. Nicas M, Nazaroff WW, Hubbard A. Toward understanding the risk of secondary airborne infection: emission of respirable pathogens. *J Occup Environ Hyg.* 2005 Mar 17;2(3):143–54.

2. Sehulster L, Chinn RY, Arduino MJ, Carpenter J, Donlan R, Ashford D, et al. Guidelines for environmental infection control in healthcare facilities. *Morb Mortal Wkly Rep Recomm Reports.* 2003;52(10).

3. Wells WF. Airborne Contagion and Air Hygiene: An Ecological Study of Droplet Infections. Harvard University Press; 1955.

4. Rudnick SN, Milton DK. Risk of indoor airborne infection transmission estimated from carbon dioxide concentration. *Indoor Air.* 2003 Sep;13(3):237–245.

5. Graves N. Economics and Preventing Hospital-acquired Infection. *Emerg Infect Dis.* 2004;10(4):561–566.

6. Magill SS, Edwards JR, Bamberg W, Beldavs ZG, Dumyati G, Kainer M a, et al. Multistate point-prevalence survey of health care-associated infections. *N Engl J Med.* 2014 Mar 27;370(13):1198–208.

7. Bischoff WE, Tucker BK, Wallis ML, Reboussin BA, Pfaller MA, Hayden FG, et al. Preventing the airborne spread of Staphylococcus aureus by persons with the common cold: effect of surgical scrubs, gowns, and masks. 2007.

8. Bolister NJ, Johnson HE, Wathes CM. The ability of airborne Klebsiella pneumoniae to colonize mouse lungs. *Epidemiol Infect.* 1992;109(1):121–131.

9. Weber DJ, Sickbert-Bennett EE, Brown V, Rutala WA. Comparison of hospitalwide surveillance and targeted intensive care unit surveillance of healthcare-associated infections. *Infect Control Hosp Epidemiol.* 2007;28(12):1361–1366.

10. ASHRAE. HVAC Design Manual for Hospitals and Clinics. 2nd ed. Atlanta: American Society of Heating, Refrigerating and Air-Conditioning Engineers; 2013.

11. Grosskopf KR, Mousavi ES. Ventilation and Transport Bioaerosols in Health-Care Environments. *ASHRAE J.* 2014;56(8):22–31.

12. ASHRAE. Standard, 170-2008 Ventilation of Health Care Facilities. Atlanta: ASHRAE; 2008.

13. WHO. Infection prevention and control of epidemic-and pandemic-prone acute respiratory diseases in health care: WHO. 2007;

14. AIA. Guidelines for Design and Construction of Health Care Facilities. 2nd ed. Washington DC: The American Institute of Architects; 2006.

15. Wenzel R. Prevention and Control of Nosocomial Infections. Baltimore: Williams & Wilkins; 1987.

16. Memarzadeh F. Literature Review: Room Ventilation and Airborne Disease Transmission. Chicago: The American Society for Healthcare Engineers; 2013.

17. Knibbs LD, Morawska L, Bell SC, Grzybowski P. Room ventilation and the risk of airborne infection transmission in 3 health care settings within a large teaching hospital. *Am J Infect Control.* 2011;39(10):866–872.

18. Li Y, Leung GM, Tang JW, Yang X, Chao CYH, Lin JZ, et al. Role of ventilation in airborne transmission of infectious agents in the built environment - a multidisciplinary systematic review. *Indoor Air.* 2007 Feb;17(1):2–18.

19. Sundell J, Levin H, Nazaroff WW, Cain WS, Fisk WJ, Grimsrud DT, et al. Ventilation rates and health: multidisciplinary review of the scientific literature. *Indoor Air.* 2011 Jun;21(3):191–204.

20. Chiu SS, Chan KH, Chu KW, Kwan SW, Guan Y, Poon LLM, et al. Human coronavirus NL63 infection and other coronavirus infections in children hospitalized with acute respiratory disease in Hong Kong, China. *Clin Infect Dis [Internet]*. 2005 Jun 15 [cited 2015 Jul 10];40(12):1721–9. Available from: http://cid.oxfordjournals.org/content/40/12/1721.short

21. Atkinson J, Chartier Y, Pessoa-silva CL, Jensen P, Li Y, Seto W-H. Natural Ventilation for Infection Control in Health-Care Settings. 2009.

22. Klevens RM, Edwards JR, Richards CL, Horan TC, Gaynes RP, Pollock DA, et al. Estimating health care-associated infections and deaths in U.S. hospitals, 2002. *Public Health Rep.* 122(2):160–6.

23. Guidelines for Environmental Infection Control in Health-Care Facilities. 2003.

24. Ten Berge WF. Mathematical models for estimating occupational exposure to chemicals. AIHA; 2000.

25. Lai ACK. Particle deposition indoors: a review. *Indoor Air.* 2002;12(4):211–214.

26. Papineni RS, Rosenthal FS. The Size Distribution of Droplets in the Exhaled Breath of Healthy Human Subjects. *J Aerosol Med.* 1997 Jan 30;10(2):105–116.

27. Cole EC, Cook CE. Characterization of infectious aerosols in health care facilities: An aid to effective engineering controls and preventive strategies. *Am J Infect Control.* 1998 Aug;26(4):453–464.

28. Xie X, Li Y, Chwang ATY, Ho PL, Seto WH. How far droplets can move in indoor environments--revisiting the Wells evaporation-falling curve. *Indoor Air.* 2007 Jun;17(3):211–25.

29. Yang S, Lee GWM, Chen C-M, Wu C-C, Yu K-P. The size and concentration of droplets generated by coughing in human subjects. *J Aerosol Med.* 2007 Jan 25;20(4):484–94.

30. Weinstein RA, Bridges CB, Kuehnert MJ, Hall CB. Transmission of influenza: implications for control in health care settings. *Clin Infect Dis.* 2003 Oct;37(8):1094–101.

31. Booth TF, Kournikakis B, Bastien N, Ho J, Kobasa D, Stadnyk L, et al. Detection of airborne severe acute respiratory syndrome (SARS) coronavirus and environmental contamination in SARS outbreak units. *J Infect Dis.* 2005;191(9):1472–1477.

32. Tellier R. Review of aerosol transmission of influenza A virus. *Emerg. Infect. Dis.* 2006;12(11):1657–1662.

33. Hui DS, Hall SD, Chan MT V, Chow BK, Ng SS, Gin T, et al. Exhaled air dispersion during oxygen delivery via a simple oxygen mask. *Chest.* 2007;132(2):540–546.

34. Brankston G, Gitterman L, Hirji Z, Lemieux C, Gardam M. Transmission of influenza A in human beings. *Lancet Infect Dis.* 2007 Apr;7(4):257–65.

35. Tellier R. Aerosol transmission of influenza A virus: a review of new studies. *J R Soc Interface.* 2009;6 Suppl 6:S783–S790.

36. Hui DS, Chow BK, Chu L, Ng SS, Lee N, Gin T, et al. Exhaled Air Dispersion during Coughing with and without Wearing a Surgical or N95 Mask. *PLoS One.* 2012;7(12).

37. Fennelly KP, Martyny JW, Fulton KE, Orme IM, Cave DM, Heifets LB. Cough-generated aerosols of Mycobacterium tuberculosis: a new method to study infectiousness. *Am J Respir Crit Care Med.* 2004 Mar 1;169(5):604–9.

38. Kowalski WJ. Air-Treatment Systems for Controlling Hospital-Acquired Infections. *HPAC Eng.* 2007;79(1):28–48.

39. Fennelly KP, Nardell EA. The relative efficacy of respirators and room ventilation in preventing occupational tuberculosis. *Infect Control Hosp Epidemiol.* 1998;19(10):754–759.

40. Noakes CJ, Sleigh PA. Mathematical models for assessing the role of airflow on the risk of airborne infection in hospital wards. *J R Soc Interface.* 2009;6 Suppl 6:S791–S800.

41. Menzies D. Hospital Ventilation and Risk for Tuberculous Infection in Canadian Health Care Workers. *Ann Intern Med.* 2000 Nov 21;133(10):779.

42. Leclair JM, Zaia JA, Levin MJ, Congdon RG, Goldmann DA. Airborne transmission of chickenpox in a hospital. *N Engl J Med.* 1980 Feb;302(8):450–3.

43. Gustafson TL, Lavely GB, Brawner ER, Hutcheson RH, Wright PF, Schaffner W. An outbreak of airborne nosocomial varicella. *Pediatrics.* 1982;70(4):550–556.

44. Anderson JD, Bonner M, Scheifele DW, Schneider BC. Lack of nosocomial spread of Varicella in a pediatric hospital with negative pressure ventilated patient rooms. *Infect Control.* 1985;6(3):120–121.

45. Hutton MD, Stead WW, Cauthen GM, Bloch AB, Ewing WM. Nosocomial transmission of tuberculosis associated with a draining abscess. 1990.

46. Li Y, Huang X, Yu ITS, Wong TW, Qian H. Role of air distribution in SARS transmission during the largest nosocomial outbreak in Hong Kong. *Indoor Air.* 2005 Apr;15(2):83–95.

47. Yu ITS, Wong TW, Chiu YL, Lee N, Li Y. Temporal-spatial analysis of severe acute respiratory syndrome among hospital inpatients. *Clin Infect Dis.* 2005;40(9):1237–1243.

48. Josephson A, Gombert ME. Airborne Transmission of Nosocomial Varicella from Localized Zoster. *J Infect Dis.* 1988;158(1):238–241.

49. Tang JW, Eames I, Li Y, Taha YA, Wilson P, Bellingan G, et al. Door-opening motion can potentially lead to a transient breakdown in negative-pressure isolation

conditions: the importance of vorticity and buoyancy airflows. *J Hosp Infect.* 2005 Dec;61(4):283–6.

50. Eames I, Shoaib D, Klettner C a, Taban V. Movement of airborne contaminants in a hospital isolation room. *J R Soc Interface.* 2009 Dec 6;6 Suppl 6:S757–66.

51. Edlin BR, Tokars JI, Grieco MH, Crawford JT, Williams J, Sordillo EM, et al. An outbreak of multidrug-resistant tuberculosis among hospitalized patients with the acquired immunodeficiency syndrome. *N Engl J Med.* 1992;326(23):1514–1521.

52. Wan MP, Chao CYH, Ng YD, Sze To GN, Yu WC. Dispersion of Expiratory Droplets in a General Hospital Ward with Ceiling Mixing Type Mechanical Ventilation System. *Aerosol Sci Technol.* 2007 Apr;41(3):244–258.

53. Richmond-Bryant J. Transport of exhaled particulate matter in airborne infection isolation rooms. *Build Environ.* 2009 Jan;44(1):44–55.

54. Liu J, Wang H, Wen W. Numerical simulation on a horizontal airflow for airborne particles control in hospital operating room. *Build Environ.* 2009 Nov;44(11):2284–2289.

55. Méndez C, San José JF, Villafruela JM, Castro F. Optimization of a hospital room by means of CFD for more efficient ventilation. *Energy Build.* 2008 Jan;40(5):849–854.

56. Hyttinen M, Rautio A, Pasanen P, Reponen T, Earnest GS, Streifel A, et al. Airborne Infection Isolation Rooms - A Review of Experimental Studies. *Indoor Built Environ.* 2011 Jul 18;20(6):584–594.

57. Bonakdari H, Larrarte F, Lassabatere L, Joannis C. Turbulent velocity profile in fully-developed open channel flows. *Environ Fluid Mech.* 2008;8(1):1–17.

58. Young DF, Munson BR, Okiishi TH, Huebsch WW. A Brief Introduction To Fluid Mechanics. New York: John Wiley & Sons, Inc.; 2011.

59. Kim J, Moin P, Moser R. Turbulence statistics in fully developed channel flow at low Reynolds number. *J Fluid Mech [Internet]*. 1987;177:133–166. Available from: citeulike-article-id:592293\nciteulike-article-id:1260716\nhttp://adsabs.harvard.edu/cgi-bin/nph-bib_query?bibcode=1987JFM...177..133K

60. Piomelli U. Large-eddy simulation: achievements and challenges. *Prog Aerosp Sci.* 1999;35(4):335–362.

61. Sagaut P. Large Eddy Simulation for Incompressible Flows. 3rd ed. Berlin: Springer; 2006.

62. Lesieur M. New Trends in Large-Eddy Simulations of Turbulence. *Annu. Rev. Fluid Mech.* 1996;28(1):45–82.

63. Lai ACK, Nazaroff WW. Modeling indoor particle deposition from turbulent flow onto smooth surfaces. *J Aerosol Sci.* 2000;31(4):463–476.

64. Apte SV, Mahesh K, Lundgren T. A Eulerian-Lagrangian model to simulate two-phase / particulate flows. *Cent Turbul Res Annu Res Briefs.* 2003;161–171.

65. Zhang Z, Chen Q. Prediction of particle deposition onto indoor surfaces by CFD with a modified Lagrangian method. *Atmos Environ.* 2009;43(2):319–328.

66. Hinds WC. Aerosol Technology Properties, Behavior, and Measurement of Airborne Particles. 2nd ed. New York: John Wiley & Sons, Inc.; 1999.

67. Chao CYH, Wan MP, Sze To GN. Transport and Removal of Expiratory Droplets in Hospital Ward Environment. *Aerosol Sci Technol.* 2008 Mar 31;42(5):377–394.

68. ASHRAE. ANSI/ASHRAE 52.2-2007 Method of Testing General Ventilation Air-Cleaning Devices for Removal Efficiency by Particle Size. *Ashrae Stand.* 2007;30.

69. ASME. Standard AG-1-2009: Code on Nuclear Air and Gas Treatment. 2009.

70. White FM. VISCOUS FLUID FLOW. *New York.* 2000;Second:413.

71. Yakhot V, Orszag SA, Thangam S, Gatski TB, Speziale CG. Development of turbulence models for shear flows by a double expansion technique. *Phys Fluids A Fluid Dyn.* 1992 Jul 1;4(7):1510.

72. Chen C, Zhao B. Some questions on dispersion of human exhaled droplets in ventilation room: answers from numerical investigation. *Indoor Air.* 2010 Apr;20(2):95–111.

73. Novoselac A, Srebric J. A critical review on the performance and design of combined cooled ceiling and displacement ventilation systems. *Energy Build.* 2002 Jun;34(5):497–509.

74. Patankar S., Spalding D. A calculation procedure for heat, mass and momentum transfer in three-dimensional parabolic flows. *Int J Heat Mass Transf.* 1972 Oct;15(10):1787–1806.

75. Moser R. The Message of Annex 20: Air Flow Patterns within Buildings. In: 12th AIVC Conference. 1991.

76. Zhang JS, Christianson LL, Wu GJ, Zhang RH. An experimental evaluation of a numerical simulation model for predicting room air motion. In: Jacques Cartier Conference. 1992.

77. Vogel P, Richter E, Rosler M. The effect of various inlet conditions on the flow pattern in ventilated rooms - measurements and computations. In: 14th AIVC Conference. 1993.

78. Regard M, Carrie FR, Voeltzel A, Richalet V. Measurement and CFD modeling of IAQ indices. In: 16th AIVC Conference. 1995.

79. Jacobsen TV, Nielsen PV. Numerical modeling of thermal environment in a displacement-ventilated room. In: Indoor air Conference. 1993.

80. Chen Q, Moser A. Simulation of a multiple-nozzle diffuser. In: 12th AIVC Conference. 1991. p. 1–14.

81. Skovgaard M, Nielsen PV. Modelling complex inlet geometries in CFD - Applied to air flow in ventilated rooms,. In: 12th AIVC Conference. 1991.

82. Nielson PV. Representation of boundary conditions at supply openings,. In: IEA, Annex 20, Research Item 1.11. 1989.

83. Nielson PV. The Box Method: a Practical Procedure for Introduction of an Air Terminal Device in CFD Calculation. 1997.

84. Huo Y, Zhang J, Shaw C, Haghighat F. A new method to describe the diffuser boundary conditions in CFD simulation. In: Proc. of ROOMVENT. 1996. p. 233–240.

85. Srebric J, Chen Q. Simplified Numerical Models for Complex Air Supply Diffusers. *HVAC&R Res.* 2002;8(3):277–294.

86. Lau J, Chen Q. Floor-supply displacement ventilation for workshops. *Build Environ.* 2007;42(4):1718–1730.

87. Joubert P, Sandu A, Beghein C, Allard F. Numerical study of the influence of inlet boundary conditions on the air movement in a ventilated room. In: Proc. of ROOMVENT. 1996. p. 235–242.

88. Lau J. The Performance of Floor-supply Displacement Ventilation in Workshop Configurations with Measurements and Simulation Studies. 2005;

89. Azad RS. Turbulent flow in a conical diffuser: A review. *Exp Therm Fluid Sci.* 1996 Nov;13(4):318–337.

90. Zhao B, Zhang Y, Li X, Yang X, Huang D. Comparison of indoor aerosol particle concentration and deposition in different ventilated rooms by numerical method. *Build Environ.* 2004 Jan;39(1):1–8.

91. Gorenflo R, Mainardi F, Moretti D, Pagnini G, Paradisi P. Discrete random walk models for space–time fractional diffusion. *Chem Phys.* 2002 Nov;284(1-2):521–541.

92. Hathway E a., Noakes CJ, Sleigh P a., Fletcher L a. CFD simulation of airborne pathogen transport due to human activities. *Build Environ.* 2011 Dec;46(12):2500–2511.

93. Gao NP, Niu JL. Modeling particle dispersion and deposition in indoor environments. *Atmos Environ.* 2007 Jun;41(18):3862–3876.

94. Glass G V, Peckham PD, Sanders JR. Consequences of Failure to Meet Assumptions Underlying the Fixed Effects Analyses of Variance and Covariance. *Rev. Educ. Res.* 1972;42(3):237–288.

95. Nazaroff WW. Indoor particle dynamics. *Indoor Air.* 2004 Jan;14 Suppl 7:175–83.

96. Fryar CD, Gu Q, Ogden CL. Anthropometric reference data for children and adults: United States, 2007-2010. 2012.

97. Forbes C, Evans M, Hastings N, Peacock. B. Statistical Distributions. John Wiley & Sons, Inc.; 2011.